5-2014

# Functional Study of the Suppressor of Hairy-wing Insulator Protein in Drosophila melanogaster

Shih-Jui Hsu
*University of Tennessee - Knoxville*, shsu2@utk.edu

To the Graduate Council:

I am submitting herewith a dissertation written by Shih-Jui Hsu entitled "Functional Study of the Suppressor of Hairy-wing Insulator Protein in Drosophila melanogaster." I have examined the final electronic copy of this dissertation for form and content and recommend that it be accepted in partial fulfillment of the requirements for the degree of Doctor of Philosophy, with a major in Biochemistry and Cellular and Molecular Biology.

Mariano Labrador, Major Professor

We have read this dissertation and recommend its acceptance:

Bruce McKee, Albrecht von Arnim, Ranjan Ganguly, David Brian

Accepted for the Council:

Carolyn R. Hodges

Vice Provost and Dean of the Graduate School

(Original signatures are on file with official student records.)

# Functional Study of the Suppressor of Hairy-wing Insulator Protein in *Drosophila melanogaster*

**A Dissertation Presented for the**

**Doctor of Philosophy**

**Degree**

**The University of Tennessee, Knoxville**

**Shih-Jui Hsu**

**May 2014**

# ACKNOWLEDGEMENTS

Without many people's support over the years, I would not be able to accomplish this work. I would like to thank Dr. Mariano Labrador, my PhD advisor, for giving me the opportunity to join his laboratory and complete my graduate studies. His patience and encouragement helped me through my PhD. His passion and endurance for science taught me to never give up because of negative results. I am also very grateful for the support of my committee members Drs. Bruce McKee, Albrecht von Arnim, Ranjan Ganguly and David Brian who have provided fruitful discussions and critical evaluations of my work.

Also, I would like to express my thanks to my former and present labmates. I especially appreciate Dr. Heather Wallace for being my good friend and coach at work. She is a great resource for professional discussion, and her advice helped me through my PhD. Also, Drs. Hyuck-Joon Kang, Shaofei Zhang and Todd Schoborg served as great teachers and I am grateful for their support. I would also like to thank Dr. Srilalitha Kuruganti, Piedad Plata, Ran An and Saghi Asgarifar for their collaboration and discussion.

I would like to thank my friends Sudershana Nair and Kai Sha in Dr. Jae Park's lab for scientific discussion and levity.

Last but not least, I would like to express my gratitude to my friends and dear family in Taiwan for their constant support. I owe my grandparents and parents a special debt of

gratitude, and I would not be here and be who I am without them. My grandmother has had an especially important impact on my life, and I owe her my success. Without her support, this work would have been impossible. Finally, I would also like to thank my family in the U.S for sharing my ups and downs during my time here. I would like to express my deepest thanks to my husband Tim Wesley who has been my greatest support during my PhD as he always encourages me to pursue my career.

# ABSTRACT

Eukaryotic chromatin insulators play an essential role in regulating gene expression and modifying nuclear architecture by organizing the higher-order chromatin structure in response to cellular and developmental cues. The details on how insulators function in this capacity are not completely understood.

Five different types of insulators have been identified in *Drosophila*. Each functional insulator consists of an insulator DNA response element bound by an insulator protein, which recognizes specific DNA sequences. Each type of insulator functions individually as well as collaboratively. Except for the Su(Hw) insulator protein, the other insulator proteins are necessary for viability considering loss of Su(Hw) only interrupts insulator function and causes female sterility. It has been suggested that Su(Hw) may play a separate role in these two functions. To gain a better understanding of Su(Hw), its functions were studied using female germline development as a model system, and the mechanisms of its regulation were studied using an *in vitro* cell culture system.

This study examined the critical function of Su(Hw) in both gene regulation and genome organization during oogenesis. Chapter one describes a remarkable ring canal developmental defect phenotype first identified and characterized in *su(Hw)* mutants, and this phenotype may contribute to female infertility. Chapter two details a newly discovered role of Su(Hw) in maintaining the genome integrity of germline cells. Loss of Su(Hw) causes accumulation of double strand breaks (DSBs), further triggering DNA

damage signaling. Genome instability causes developmental defects resulting in incomplete oogenesis and consequent female sterility.

To understand insulator function regulatory mechanisms, *Drosophila* Schneider 2 cells (S2 cells), were used as the system for investigation. Chapter three demonstrates that Su(Hw) was identified at a novel sub-cellular location within the midbody during mitotic telophase, and SUMOylation and phosphorylation may play a role in the functional regulation and sub-cellular localization of Su(Hw).

Our work proposes that in spite of regulating gene expression, the Su(Hw) insulator also plays a critical role in maintaining genome stability by directing higher-order organization of the chromatin structure. Moreover, the protein-protein interactions and sub-cellular localization of Su(Hw) may regulate its function, and this functionality control may be fine-tuned by post-translational modifications.

# TABLE OF CONTENTS

# LIST OF TABLES

# LIST OF FIGURES

# INTRODUCTION

## Chromatin organization and gene expression in eukaryotes

In eukaryotes, DNA is packed with histone octamers called nucleosomes, a basic unit of chromatin structure containing two copies of the histone proteins H2A, H2B, H3 and H4 wrapped with approximately 146 base-pairs of supercoiled DNA (KORNBERG and LORCH 1999). This primary packing structure physically accommodates of DNA into the nucleus and plays a dynamic role in altering DNA accessibility in response to various cellular events, such as transcription, DNA replication, recombination and repair (MISTELI 2007). Nucleosomes combine with chromatin-associated RNA and proteins to form chromatin, a structure regulated by post-translational modification of histones through acetylation, methylation or phosphorylation. These modifications not only alter chromatin structure but also affect interaction between chromatin and its binding proteins such as transcriptional regulators in order to control gene expression. For example, methylated histone H3 lysine 9 recruits heterochomatin protein 1 (HP1) which is involved in heterochromatin formation that can spread along the chromatin fiber and silence expression of nearby genes (BLACK and WHETSTINE 2011; ZENTNER and HENIKOFF 2013).

Gene expression is highly regulated in eukaryotes. In addition to chromatin structure, gene expression is also controlled by regulatory sequences such as enhancers and silencers. Within eukaryotic genomes, enhancers frequently act over

tens of kilobases of DNA to activate cognate promoters that in turn activate the target gene expression. Considering enhancers can act upon promoters in a manner independent of distance or orientation, a mechanism must exist to prevent inappropriate activation of intervening promoters. Communication between promoters and distal enhancers can be prevented when insulators are positioned inbetween, thereby altering gene expression. Furthermore, insulators function as boundaries protecting genes against heterochromatin-mediated silencing. By blocking enhancer-promoter interactions and serving as boundary barriers, insulators serve their primary role as gene expression regulators. Genome-wide distribution of insulators indicates that insulators may have effects spanning both local and global levels of chromatin organization. Beyond their primary role in regulating gene expression, studies have proposed that insulators may be able to organize chromatin into independent domains in order to ensure proper temporal and spatial gene expression (BRASSET and VAURY 2005; GASZNER and FELSENFELD 2006; WEST *et al.* 2002).

Accumulated evidence suggests that a remote enhancer may activate distant genes via chromatin loop formation. The chromatin-looping model proposes chromatin is divided into functional domains regulating interactions between promoters and enhancers. Insulators facilitate the chromatin looping at the local level, indicating the entire genome may be divided into functional domain clusters of co-regulated genes sharing similar expression profiles. (LABRADOR and CORCES 2002; WALLACE *et al.* 2010). By way of rapidly developing genomic technologies, insulators have been characterized as mediators of long range intra- and/or inter-chromatin interactions, organizers of

chromatin loop formation within the nucleus, and modifiers of nuclear architecture - three roles which further control particular gene expression patterning during development (GURUDATTA and CORCES 2009; LEE and IYER 2012; PHILLIPS-CREMINS and CORCES 2013; VAN BORTLE and CORCES 2012a).

**Eukaryotic insulators and their associated proteins**

With in a variety of organisms, insulators have been identified from yeast to humans as performing a conserved function requiring insulator DNA elements to recruit their associated insulator binding proteins. To date, six insulators have been identified, including suppressor of hairy wing [Su(Hw)], GAGA factor, boundary element-associated factor (BEAF-32), Zeste-white 5 protein (Zw5), transcription factor IIIC (TFIIIC) and CCCTC-binding factor (CTCF) (GURUDATTA and CORCES 2009; VAN BORTLE and CORCES 2012a). Amongst all, CTCF is a highly conserved insulator protein within invertebrates and vertebrates (MOON *et al.* 2005), with the vertebrate CTCF having been studied for decades.

The primary mammalian insulator protein CTCF has been reported as a classical transcription factor and a tumor suppressor. CTCF is an eleven zinc-finger nuclear protein (KLENOVA *et al.* 1993) with a wide distribution of approximately 66,800 sites in the human genome, and it targets diverse DNA sequences using different combinations of its zinc fingers (WANG *et al.* 2012). As a tumor suppressor, CTCF is involved in regulating numerous oncogenes and tumor suppressor genes. Deregulation of CTCF may cause epigenetic silencing of growth suppressor genes, leading to an epigenetic

imbalance which causes cancer (BANIAHMAD *et al.* 1990; FILIPPOVA *et al.* 1996; LOBANENKOV *et al.* 1990). Moreover, CTCF was initially found interacting with insulator DNA elements and blocking promoter-enhancer communication in both the β-globin locus and the *Igf2/ H19* imprinting control region (ICR) (BELL and FELSENFELD 2000; BELL *et al.* 1999; FILIPPOVA 2008; FILIPPOVA *et al.* 2001).

The multiple functions of CTCF may be determined by its target DNA sequences, post-translational modifications, and protein-protein interactions (OHLSSON *et al.* 2010). CTCF associated proteins are important regulators of CTCF function, and their discovery has provided a more detailed picture of CTCF's insulator function. Genome-wide analysis reveals that CTCF overlaps with cohesin-binding sites in the mammalian genome. Cohesin together with CTCF contributes to stabilization of long-range chromosome interactions and establishes chromatin loops (GAUSE *et al.* 2008; GONDOR and OHLSSON 2008; PARELHO *et al.* 2008; RUBIO *et al.* 2008; WENDT *et al.* 2008). Also, CTCF recruits its binding partner RNA polymerase II (RNAPII) to certain CTCF/cohesin target sequences in the genome for further regulation of gene expression at those loci (CHERNUKHIN *et al.* 2007; FAY *et al.* 2011; LEE and IYER 2012; SHUKLA *et al.* 2011).

Although CTCF has not been identified in fungi, yeast or plants, other insulator proteins may function in these organisms. Highly conserved tRNA genes associated with TFIIIC (transcription factor III C) were first identified functioning as insulators in yeast (*Saccharomyces cerevisiae*) (DONZE *et al.* 1999) and were recently characterized in humans as well (RAAB *et al.* 2012). Genome-wide mapping of the location of TFIIIC

reveals its association with CTCF that suggests these two insulator proteins may have a joint regulatory function in genome organization (CARRIERE *et al.* 2012; MOQTADERI *et al.* 2010). Additionally, TFIIIC binding sites in mice are also associated with cohesin, suggesting TFIIIC shares the same accessory protein, cohesin, with CTCF and may function similarly to CTCF in organizing nuclear structure and regulating gene expression in mammalian genomes (VAN BORTLE and CORCES 2012b).

**Different types of insulators in Drosophila**

Five different types of insulators have been identified in *Drosophila* and defined by their associated insulator proteins (Figure I-1), wheras only two types of insulators have been discovered in mammals so far. The diversity of fly insulator types may offer an opportunity to discern different aspects of insulator function. Although mammalian CTCF has been studied for decades, *Drosophila* CTCF (dCTCF) has only been identified relatively recently (MOHAN *et al.* 2007). Except for dCTCF, the other four types of insulators have not been discovered within vertebrates. In *Drosophila,* the insulators *scs* and *scs'* were first found close to the junction between the decondensed 87A7 locus and the flanking condensed chromatin. These insulators also contain binding sites for Zw5 and BEAF (GASZNER *et al.* 1999; KELLUM and SCHEDL 1991; UDVARDY *et al.* 1985; ZHAO *et al.* 1995). In addition to *scs* and *scs'*, the Fab-7 element is another type of insulator recruiting the GAGA factor, a DNA binding protein, for insulator activity (OHTSUKI and LEVINE 1998). The *gypsy* insulator is the most well known insulator and is found in the *gypsy* retrotransposon, which recruits Su(Hw) and two accessory proteins, Modifier of mdg4 [Mod(mdg4)-67.2] and Centrosomal Protein 190 (CP190), for

insulation function (GERASIMOVA and CORCES 2001; PAI *et al.* 2004; WALLACE and FELSENFELD 2007).

**The gypsy insulator**

The *gypsy* insulator represents a well-characterized model for insulator studies. The insertion of the *gypsy* retrotransposon within gene regulatory regions, such as *yellow* and *cut*, causes tissue specific phenotypes. Phenotypes resulting from the insertion of *gypsy* retrotransposons can be reversed by mutations in *su(Hw),* indicating functional Su(Hw) is required for the *gypsy* mutagenic effect in flies (MODOLELL *et al.* 1983). Su(Hw), a zinc finger protein, recognizes the twelve repeated copies of a short sequence motif in the 5' untranslated region of the *gypsy* retrotransposon, and a leucine zipper domain of Su(Hw) mediates its repressive effect on enhancer function. Kim et al., suggested that the amino (N) and carboxyl (C) terminal domains of Su(Hw) are not absolutely required for its insulator function (HARRISON *et al.* 1993; KIM *et al.* 1996); however, the leucine zipper and adjacent regions of the Su(Hw) protein are important for its enhancer-blocking function (HARRISON *et al.* 1993), which is performed through interaction with the C-terminal acidic domain of Mod(mdg4)-67.2 (GHOSH *et al.* 2001). Mod(mdg4)-67.2 is a BTB (broad complex, tramtrack, bric-a-brac)/POZ (poxvirus and zinc finger) domain protein, which is a large family of proteins in organisms ranging from yeast to humans. The BTB domain is involved in facilitating protein-protein interactions via the formation of BTB dimers, which are required for insulator function (GOLOVNIN *et al.* 2007). The third component of the *gypsy* insulator complex, CP190, was identified in a genetic screen for dominant enhancers of the *mod(mdg4)* mutant phenotype. CP190

co-localizes with both Su(Hw) and Mod(Mdg4) onto polytene chromosomes, and it is essential for formation of insulator bodies. In yeast-two hybrid and immunoprecipitation assays, CP190 interacts with Mod(mdg4) through the N-terminal BTB domain and binds to Su(Hw) (PAI *et al.* 2004). Hundreds of Su(Hw) binding sites in the genome can be visualized on polytene chromosomes and are thought to correspond to endogenous *gypsy* insulators. Some of these endogenous *gypsy* insulators have been shown to have a regulatory function by inhibiting promoter-enhancer interactions, and insulator strength has been shown to depend on the location and number of endogenous Su(Hw) binding sites (RAMOS *et al.* 2006).

**Alteration of nuclear organization through association of different Drosophila sub-classes of insulators**

CP190 co-localizes in the genome with three different insulators, BEAF32, Su(Hw) and dCTCF, and each of these represents an insulator subclass with differential genome occupancy. These insulator proteins may play different roles in organizing chromatin in order to establish cell-type-specific gene expression profiles via sharing of CP190 (BUSHEY *et al.* 2009b; GERASIMOVA *et al.* 2007; PAI *et al.* 2004). Genome wide analyses showed over eighty percent of binding sites of BEAF and dCTCF are located at the 5' end, close to transcription start sites (TSS) of highly expressed genes; however, Su(Hw) is often found associated with genes expressed at low levels or located in relatively gene poor regions in the genome. Differential insulator distribution in the genome is also relevant to specific cellular processes. Gene function analysis indicates that genes containing dCTCF binding sites upstream of TSS are involved in

developmental processes while genes associated with BEAF are related to metabolic pathways. Remarkably, both dCTCF and BEAF display high enrichment binding sites in cell cycle related genes. On the other hand, the distribution of Su(Hw) does not significantly show its relevance to biological functions (BUSHEY *et al.* 2009a; EMBERLY *et al.* 2008b; JIANG *et al.* 2009). Regardless, of all the insulator proteins, Su(Hw) is the only one to show a significant occupancy at the borders of and at particular positions in lamina-associated domains (LADs) of the genome (VAN BEMMEL *et al.* 2010). Such a distribution may reveal a role of Su(Hw) in fine-tuning the interaction between the genome and the nuclear periphery. By anchoring to the nuclear lamina at the nuclear periphery, different types of insulators may organize chromatin fibers through collaboration with each other as they share accessory proteins, forming a higher-order chromatin rosette-like structure (Figure I-2).

**Post-translational modification of insulator proteins**

In addition to the collaboration of different insulator proteins in order to specify functionality, post-translational modifications of insulator proteins also play an important role in regulating insulator function. In mammals, transcriptional properties and insulator function of CTCF have each been found to be regulated by different post-translational modifications, including phosphorylation, small ubiquitin-like Modifier conjugation (SUMOylation) and poly-(ADP-ribosyl)ated (PARylation) (DELGADO *et al.* 1999; MACPHERSON *et al.* 2009b; YU *et al.* 2004). These same modifications influence *Drosophila* insulator function. Remarkably, PARylation is required for insulator function in *Drosophila,* and PARylation of CP190 plays a central role in mediating interaction

between different genome sites in order to direct the intra- and inter-chromatin loop formations (ONG *et al.* 2013). Besides, SUMOylation is a known modification that controls *gypsy* insulator protein complex formation but is not necessary for insulator function (GOLOVNIN *et al.* 2012). A contradictory conclusion suggested SUMOylation negatively regulates insulator function (CAPELSON and CORCES 2006). The two studies used different systems and techniques to test their hypotheses; hence, further studies are required to draw a clear conclusion. On the other hand, dTopors, an E3 ubiquitin ligase, interacts with the *gypsy* insulator complex and plays a role in stabilizing the *gypsy* insulator chromatin domain formation (CAPELSON and CORCES 2005; CAPELSON and CORCES 2006). A growing body of evidence shows that the influence of post-translational modifications during insulator-protein complex formation ultimately affects chromatin organization. These studies shed light on the clockwork nature of the regulation mechanism controlling nuclear chromatin organization as it employs different combinations of insulators as well as various post-translational modifications of insulator proteins in response to different cellular and developmental cues.

### *Gypsy* insulator function in developmental processes

During *Drosophila* development, the *gypsy* insulator plays an important role in regulating gene expression, and null mutations of either *CP190* or *mod(mdg4)* gene are lethal (GERASIMOVA *et al.* 1995; PAI *et al.* 2004); however, *su(Hw)* null mutants show a less severe developmental defect: female sterility. The *su(Hw)* mutation was first discovered and identified as a recessive mutation in 1923 by C. B. Bridges. It was named so because of the suppression of the mutant phenotype of a sex-linked gene,

Hairy-wing (BRIDGES and BREHME 1944). The ovarian phenotype of the *su(Hw)* mutant was first characterized in 1968, and an ovary transplantation experiment showed the ovarian pathology in mutants resulted from the genotype of the ovarian cells (KLUG *et al.* 1968).

### *Drosophila* oogenesis

The body axes of many animals are defined during embryogenesis; however, in *Drosophila*, axis formation begins during oogenesis, long before egg fertilization. Serial symmetry-breaking events during the mid-stage of oogenesis establish both *Drosophila* anterior-posterior (AP) and dorsal-ventral (DV) axes. The two key steps of symmetry-breaking are oocyte selection and oocyte posterior positioning.

In *Drosophila*, each female contains one pair of ovaries, with each ovary composed of sixteen to twenty functional units named ovarioles, which are independent strings of egg chambers. The ovariole has two sections: the germarium, a specialized structure where the egg chamber initially forms and harbors stem and somatic cells, and the vitellarium, where the egg chamber matures. Fourteen stages comprise egg chamber development, and these stages are based on morphological changes during oogenesis. Oogenesis starts with the first asymmetric cell division of a germline stem cell located at the far anterior-tip within the germarium. A daughter stem cell and a cystoblast are generated from this asymmetric division, and the cystoblast continuously divides four times to produce sixteen cystocytes. Eventually, one of these cells adopts the oocyte cell fate, and the remaining fifteen cells become nurse cells containing polypoid chromosomes producing specific cytoplasmic markers such as mRNA and

proteins. These markers are then transported to the oocyte through inter-connected cytoplasmic bridge structures inbetween these sixteen cells called ring canals to support oocyte development (BASTOCK and ST JOHNSTON 2008; HUYNH and ST JOHNSTON 2004).

**Step one of symmetry breaking: selection of the oocyte**

The initial signal that determines which of the sixteen cells becomes the oocyte relates to the distribution of the fusome, a continuous branching structure which grows within and connects the cells by winding through the ring canals, ultimately making a cluster of the sixteen cells. Each cell division produces another banch of the fusome which connects the new cell to the existing cluster, and this process continues until all sixteen cells are formed. By the end of fourth division, only two of the sixteen cystocytes will contain four ring canals and the largest portions of the fusome. These two cells are called “pro-oocytes,” and only one will become the oocyte though an unknown mechanism (GRIEDER *et al.* 2000; LIN *et al.* 1994; LIN and SPRADLING 1995). During oocyte determination, two unique characteristics of the oocyte become evident: specific localization of cytoplasmic markers and meiotic arrest. The first unique characteristic relates to organization of the polarized microtubule (MT) network by the fusome in order to facilitate transport of mRNA and proteins produced by polyploidy nurse cells towards the microtubule organizing center (MTOC) within the oocyte (POKRYWKA and STEPHENSON 1995). The second unique characteristic relates to meiotic arrest during meiosis I as DNA condenses (Bastock and St Johnston 2008; Roth and Lynch 2009).

**Step two of symmetry breaking: posterior positioning of the oocyte**

Three key mRNAs determine body axes patterning: *gurken, bicoid* and *oskar (*BERLETH *et al. 1988; KIM-HA et al. 1991;* NEUMANSILBERBERG *and* SCHUPBACH *1993)*. Between stages six and ten, Grk (a TGF-$\alpha$ homologue) provides signals at two different times that participate in oocyte polarization. The first signal occurs during stage six when Grk induces terminal follicle cells surrounding the oocyte to adopt the posterior fate, after which the posterior follicle cells send an unknown response signal back to the oocyte. This response signal is necessary for the microtubule repolarization that facilitates oocyte nucleus migration to the anterior-lateral corner during stage nine (GONZALEZREYES *et al.* 1995; ROTH *et al.* 1995; SCHUPBACH 1987). The second Grk signal triggers the follicle cells closest to the oocyte nucleus to adopt the dorsal fate, and Grk restricts the expression of *pipe* in the ventral follicle cells in order to control D/V axis formation during stage ten (RIECHMANN and EPHRUSSI 2001; TECHNAU *et al.* 2012).

On the other hand, localization and translation of bicoid (bcd) and oskar mRNA determine the anterior-posterior polarity of the oocyte. bcd mRNA is MT-dependent and is coupled with the minus-end-directed motor dynein in the nurse cells prior to its transport to the oocyte. The Bicoid protein gradient is required for regulation of zygotic gap genes and formation of anterior structures. Another key player in AP polarity determination is *oskar* mRNA, which associates with the plus-end directed motor kinesin and is transported along MT to the posterior pole of the oocyte (CHA *et al.* 2001; CHA *et al.* 2002; SCHNORRER *et al.* 2000). Several critical molecules involved in the patterning of the embryo are recruited to the posterior pole by the Oskar protein, such

as *nanos* mRNA, which is an abdominal determinant of the embryo (EPHRUSSI *et al.* 1991). A Nanos protein gradient produced from the posterior of the embryo inhibits translation of *hunchback* mRNA, allowing posterior zygotic gap gene expression and abdominal patterning progression (HULSKAMP *et al.* 1990; IRISH *et al.* 1989).


**Figure I1. Five different types of insulators in *Drosophila.***

Each functional insulator unit contains a DNA binding protein that recognizes and binds to the sequence-specific insulator DNA element. The accessory proteins, such as Mod(mdg4) and CP190 are recruited to the insulators and facilitate collaboration between different subclasses of insulators. This figure was modified from the reference (VAN BORTLE and CORCES 2012b).

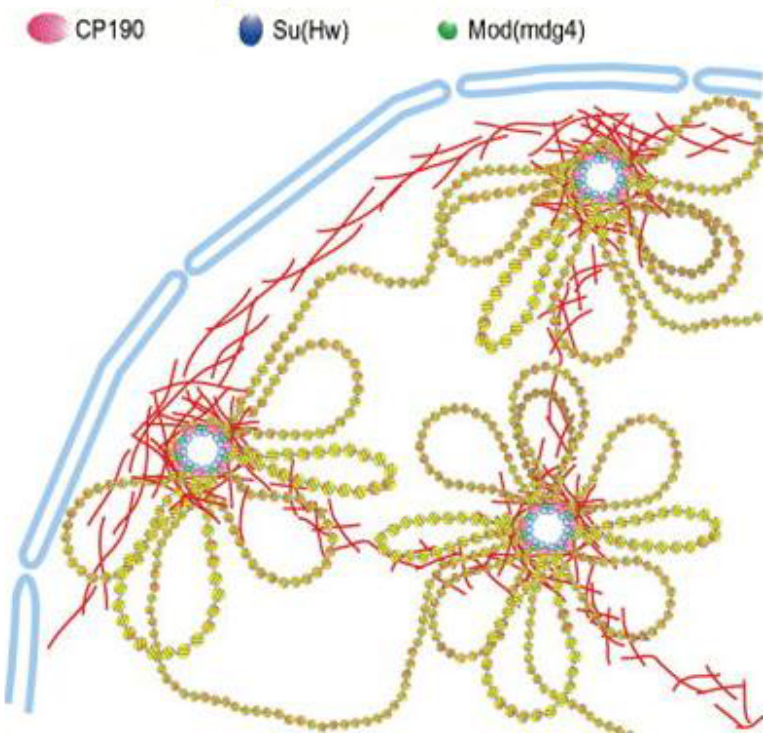


**Figure I2. Insulators facilitate the formation of higher-order chromatin rosette-like structures.**

It has been suggested that insulators separate the chromatin fiber into domains. The domains of open chromatin (yellow nucleosomes) are flanked by insulator associating proteins (pink, blue and green ovals), which anchor the whole complex to the nuclear periphery by interacting with the nuclear lamina (red lines). This figure was modified from the reference (LABRADOR and CORCES 2002).

# CHAPTER I.

# Abnormal Development of Ring Canals Contributes to Female Sterility in *Suppressor of Hairy wing* Mutant Females.

Shih-Jui Hsu, Maria P. Plata, Ben Ernest and Mariano Labrador

This paper will be sumbitted to Developmental Biology.

1). Shih-Jui Hsu: Conceiving and designing experiments, performing experiments, analyzing data, making figures and writing the manuscript.
2). Maria P. Plata: Designed and performed microarray experiment.
3). Ben Ernest: analyzed microarray data.
4). Mariano Labrador: Conceiving and designing experiments, analyzing data, and writing the manuscript.

## ***Abstract***

Chromatin insulators organize eukaryotic genomes into chromatin domains, orchestrating gene transcription by stabilizing interactions between distant genome sites. Mutations in genes encoding insulator proteins generally are lethal; however, in *Drosophila*, mutations in the gene encoding the Suppressor of Hairy-wing insulator protein [Su(Hw)] have no noticeable phenotype except female sterility, suggesting this protein specifically plays an important role during oogenesis. Whereas previous reports have indicated the role of Su(Hw) in oogenesis is independent of its insulator activity, the function of Su(Hw) in *Drosophila* oogenesis remains unclear. We show here that mutations in *su(Hw)* result in smaller ring canal lumens and smaller outer ring diameters, particularly in stage eight egg chambers, which likely impede molecular and vesicle passage from nurse cells to the oocyte. Fluorescence microscopy reveals mutations in *su(Hw)* lead to excess accumulation of Kelch (Kel) and Filament-actin (F-actin) proteins in the ring canal structures of developing egg chambers. Furthermore, we found down-regulation of the *Src* oncogene at *64B* (*Src64B*) is important for ring canal development as microarray analysis and real-time RT-PCR revealed there is a three-fold decrease in *Src64B* expression in *su(Hw)* mutant ovaries. Restoration of *Src64B* expression in *su(Hw)* mutant female germ cells rescued the ring phenotype but did not restore fertility. We conclude that loss of Su(Hw) affects expression of many oogenesis related genes and down-regulates *Src64B*, causing ring canal development defects potentially

contributing to obstruction of molecular flow and eventual failure of egg chamber organization.

## ***Introduction***

While DNA provides the blueprint for eukaryotic cell structure and function, chromatin structure is critical for regulating gene expression considering post-translational modifications of histones have positive or negative effects on the binding of transcriptional machinery to target DNA sequences. Target sequences, such as enhancers, may act over tens of kilobases of DNA in conjunction with cognate promoters in order to activate the expression of a target gene (MARSMAN and HORSFIELD 2012; ONG and CORCES 2011), and insulators have the ability to block this communication when placed between enhancers and promoters. In addition, insulators may function as boundaries protecting genes from heterochromatin mediated silencing (BRASSET and VAURY 2005; GASZNER and FELSENFELD 2006; YANG and CORCES 2012). These two properties of insulators suggest they organize chromatin into independent gene expression domains that ensure proper temporal and spatial gene expression during development and cell differentiation (LABRADOR and CORCES 2002; WALLACE and FELSENFELD 2007).

Chromatin insulators have been discovered in a variety of organisms ranging from yeast to humans (GURUDATTA and CORCES 2009; SCHOBORG and LABRADOR 2010). One of the best-characterized insulators is the *Drosophila gypsy* insulator which is composed of three major proteins: Su(Hw), which directly binds the insulator DNA, Modifier of mdg4 protein [Mod(mdg4)-67.2], and Centrosomal protein 190 (CP190). These three *gypsy* insulator components

engage via protein-protein interactions, thus allowing chromatin insulator function (GERASIMOVA *et al.* 1995; GHOSH *et al.* 2001; PAI *et al.* 2004). Although the two binding partners of Su(Hw), Mod(mdg4)-67.2 and CP190 proteins, are required for chromatin insulator activity, only Su(Hw) is essential for oogenesis (BAXLEY *et al.* 2011).

In *Drosophila*, oogenesis begins at the first asymmetric division of one germline stem cell located at the far anterior-tip of the germarium. This asymmetric cell division gives rise to a daughter stem cell and a cystoblast, which will later form an egg chamber by generating sixteen cells following four incomplete mitotic divisions. In each developing egg-chamber, only one cell adopts the oocyte cell fate while the remaining fifteen cells become nurse cells, which will produce essential nutrients that provide support for the oocyte and later embryo development (RIECHMANN and EPHRUSSI 2001).

In the germarium, each mitotic division ends with incomplete cytokinesis generating cytoplasmic bridge structures called ring canals that eventually interconnect all germline cells within the egg chamber. Within the germarium, a germline-specific organelle called the fusome (encoded by *Hu-li tai shao* gene, *hts*) grows within the cystocytes as a continuous branching structure that winds through and plugs the ring canals. Each cell division produces another branch of the fusome, connecting the new cell to the cluster of previously formed cells. This process continues until all sixteen cells form, but eventually, the plugs break

down when the cystocytes leave the germarium. The ring canals remain, functioning as channels facilitating transport of cytoplasmic constituents including mRNAs, proteins, macro-molecules, organelles and vesicles that ultimately travel to the developing oocyte (DE CUEVAS and SPRADLING 1998; LIN *et al.* 1994).

The molecular flow towards the oocyte occurs in two phases: the early slow phase, a process releasing specific and selected molecules from nurse cells to the oocyte, and a later fast phase, a rapid process beginning at stage 10B when nurse cells dump the entirety of their cytoplasmic contents into the oocyte (BATE and MARTINEZ ARIAS 1993a; BUSZCZAK and COOLEY 2000; HAGLUND *et al.* 2011). A phenotype described as “dumpless” (i.e. defective yolk deposit phenotype) commonly arises from mutations in genes encoding components of protein complexes involved in cytoskeleton organization pathways or ring canal formation, such as the mutations *hts, kelch*, and *Src64B (DODSON et al. 1998; XUE and COOLEY 1993; YUE and SPRADLING 1992)*.

Su(Hw) is detected in the nucleus of both somatic follicle cells and germline cells in ovaries, and loss of Su(Hw) results in female sterility. Early studies noticed that *su(Hw)* mutations suppressed yolk deposition and sequentially arrested ovary development at mid-oogenesis, thereby causing sterility (BAXLEY *et al.* 2011; HARRISON *et al.* 1993; KLUG *et al.* 1968; KLUG *et al.* 1970). The *su(Hw)* mutant allele $su(Hw)^{f}$ encodes a protein contaning a defective Zinc-finger 10 that eliminates insulator activity even though germline

development remains normal (HARRISON *et al.* 1993). Analyzing the global role of Su(Hw) during oogenic transcription, Baxley et al. (2011) concluded that the effect of Su(Hw) in germline development is independent of its function of demarcating transcriptional domains, suggesting that the functions of Su(Hw) in regulating insulator activity and female germline development are seperable (BAXLEY *et al.* 2011). Additionally, a recent report suggests that Su(Hw) may function as a classic transcriptional regulator during oogenesis and that a major effect of the absence of Su(Hw) during oogenesis is failure to repress RNA-binding protein 9 (*Rbp9*). In fact, reducing *Rbp9* expression by half within ovaries largely rescued *su(Hw)* mutant oogenesis defects, although fertility was not completely restored given that eggs produced by rescued females contained patterning defects and did not produce viable offspring (SOSHNEV *et al.* 2013; SOSHNEV *et al.* 2012).

This study used a cell type and stage specific Gal4-UAS binary system to examine spatial and temporal expression of Su(Hw) and also determine its precise role in different stages of oogenesis and ovary development. We show that germline specific expression of Su(Hw) driven by Gal4 in *su(Hw)* mutant ovaries is necessary for yolk-deposition and normal oocyte development. At the same time, Gal4 driven expression of Su(Hw) in somatic follicle cells is not sufficient for oogenesis. Interestingly, we found intracellular transport is blocked prior to stage eight in *su(Hw)* mutants, and this blockage may result from defective ring canal development during oogenesis. Ring canals in *su(Hw)*

mutant ovaries show abnormal morphology with excess accumulation of F-actin and Kelch, yielding a smaller lumen similar to those of unrelated ring canal mutations preventing molecular passage. Furthermore, microarray data showed eighty-five misregulated genes in *su(Hw)* mutants participate in oogenesis, and among these genes Src64B is significantly down-regulated. Overexpression of Src64B in *su(Hw)* mutants rescues the ring canal phenotype but cannot completely restore intracellular transport within egg chambers, suggesting Su(Hw) is required for other components of egg chamber organization necessary for proper transport and development in addition to ring canal formation.

## ***Materials and methods***

### Fly stocks and culture conditions

All fly stocks were cultured using cornmeal-agar food and yeast in a 25°C incubator. Fly stocks used in this study included *su(Hw)* mutant lines: $w^{1118}$; *PBac(LALL)su(Hw)* $^{e04061}$*/TM6B* (BDSC: 18224), $y^2wct^6$*; su(Hw)* $^{v}$*/TM6B* and *su(Hw)e1*, gifts from Victor Corces (Emory University). Expression of Su(Hw)::eGFP [*yw; P{suHw::eGFP,w*$^+$*}*] was driven by various Gal4 drivers including *w*; P{en*$^{2.4}$*-Gal4}*$^{e22C}$ (BDSC: 1973); *w*;P{GAL4-nos.NGT40}* (BDSC: 4442); w*; *P{nos-Gal4::VP16}*, w*; *P{matalpha4-GAL-VP16}V37* (BDSC:7063), gifts from Bruce McKee (University of Tennessee) and *yw; P{Tj-Gal4},* a gift from Dr. Steven DiNardo (University of Pennsylvania). For the Src64B restoration experiment, we used *w*$^*$*;* P{UAS-Src64B.C}2 (BDSC: 8477).

### Egg chamber staining and image processing

Three to five-day-old female flies were collected and their ovaries were dissected for ovary whole mount immunostaining following standard protocols (PAGE and HAWLEY 2001). Briefly, tissues were fixed in heptane (Sigma) with 4% para-formaldehyde and washed with PBST. Fixed tissues were incubated with blocking solution. Multiple primary antibodies were used for staining and dilution: 1:100 rabbit anti-GFP antibody (Invitrogen), 1:200 mouse anti-Orb antibody, 1:200 mouse anti-Kel antibody, 1:200 mouse anti-Hts F antibody, 1:200 mouse anti-Hts RC antibody and 1:200 Lamin Dm0 antibody (Developmental studies hybridoma bank). Secondary antibodies: FITC-conjugated anti-rabbit IgG,

TexRed-conjugated anti-rabbit IgG and FITC-conjugated anti-mouse IgG (The Jackson Laboratory) were used with a 1:200 dilution. F-actin staining was performed using TexRed-phallodin (Life Technologies). DNA was stained with 4′, 6-diamidino-2-phenylindole (DAPI, 0.5 µg/ml) and all samples were mounted in Vectashield mounting medium (Vector Laboratories).

Slides were analyzed using a Lecia DM6000B wide-field fluorescence microscope equipped with a Hamamatsu ORCA-ER CCD camera and a HC PL FLUOTAR 20x /0.50NA objective. Image acquisition was performed using Simple PCI v6.6 (Hamamatsu Photonics). Images were processed using the AutoQuant's 3D Deconvolution Algorithm utilizing an adaptive (blind) PSF implemented into Lecia Deblur (v2.3.2) software. All wild-type and mutant samples were processed and imaged under identical immunostaining conditions and microscope, camera and software settings. Egg chambers were measured using Image J software and specific stages were determined based on size (SULLIVAN *et al.* 2000).

**Microarray and data analysis**

Fifteen three-day-old wild-type (Oregon R) and homologous mutant [$su(Hw)^{e1}$] female flies were collected for ovary dissection. Ovarian mRNA was extracted and used for microarray hybridization through Affymetrix Drosophila 2.0 arrays (Cat. #900532) that were performed by the microarray facility at the University of Tennessee, Knoxville. Three biological repeats of each genotype were analyzed.

Microarray analysis was performed using R version 3.0.2 (R Core Team (2013)). Raw expression data were normalized using the gcrma package (Wu *et al.* 2004). The mas5 calls function from the affy package (Gautier et al. 2004) was used to identify each expression value as present, absent, or marginal. Genes present in all replicates of at least one treatment group were kept for further analysis, ultimately giving 7324 genes. The limma package (Smyth 2005) was used to compare gene expression between mutants and wild-type flies, and the p-values were adjusted by the FDR method to control the false discovery rate. Affymetrix probe IDs were matched with FlyBase IDs and gene symbols using the Ensembl BioMart tool. Based on gene ontology at FlyBase, 962 probe IDs were matched to oogenesis-related genes. Heatmaps were constructed with hierarchical clustering (heatmap.2 function in R gplots package (Warnes 2013)) to determine the difference of transcriptional profiles between mutants and wild-type ovaries.

**Real-time RT-PCR**

Three to five-day-old female flies were collected for ovary dissection, and late-stage egg chambers after stage nine were removed. Ovarian total RNA was purified using TRIzol reagent (Invitrogen) and was then reverse-transcribed to cDNA using the SuperScript First-strand cDNA synthesis kit (Invitrogen). For each genotype sample, two independent biological RNA samples were prepared. Real-time PCR was performed using specific primers of targeted genes and iQ SYBR Green Supermix (Biorad) while the reactions were set up on a BioRad iQ5

Multicolor Real-Time PCR Detection System. For each gene amplification, three independent technical repeats were prepared. Each amplification condition was optimized, and primer specificity was determined using the melting curve. The expression level of each gene was normalized to the internal control rp49 (ΔCt value), and the relative abundance of target gene transcripts among each genotype was determined using the relative quantitative method (ΔΔCt value). Primers used in this study were listed in Table A.1 in the appendix.

**Fertility assay**

Wild-type and rescued virgin female flies were collected and mated with male flies (*yw*). Rescue female flies carrying either the *su(Hw):eGFP* or *Src64B* transgenes were driven by the Gal4 drivers. Eggs were collected for three days using grape juice agar plates containing wet yeast paste (SULLIVAN *et al.* 2000). The fertility rescue ratio was calculated using the total number of eggs laid by rescued females divided by the total number laid by wild-type females.

## ***Results***

### Oocyte development is defective in *su(Hw)$^{e04061/v}$* mutants

*su(Hw)* mutant females are sterile as a result of incomplete oogenesis, and mutant egg chambers ultimately undergo apoptosis following arrested development at mid-oogenesis (BAXLEY *et al.* 2011; HARRISON *et al.* 1993; HARRISON *et al.* 1992; KLUG *et al.* 1968; KLUG *et al.* 1970). In order to further characterize the role of Su(Hw) in oogenesis, we used the *su(Hw)$^{e04061}$* mutant, created by an insertion of a piggy-bac transposon at the 5' end of the second exon, as well as the *su(Hw)$^{v}$* mutant, which carries a deletion of the *su(Hw)* promoter (HARRISON *et al.* 1992). Both homozygous *su(Hw)$^{e04061/e04061}$* and trans-heterozygous *su(Hw)$^{e04061/v}$* mutant flies show a loss of insulator activity as well as female fertility (Figure A1, in Appendix ) (BAXLEY *et al.* 2011; SCHOBORG *et al.* 2013). The oogenesis phenotype of both mutant genotypes is practically undistinguishable, and to avoid genetic interference from second site mutations, we used a trans-heterozygous *su(Hw)$^{e04061/v}$* mutant for phenotype characterization.

We began by analyzing the structures of egg chambers throughout oogenesis using TexRed-phalloidin staining as a filamentous actin probe and verified that *su(Hw)* mutant oocytes cease growing after stage eight of oogenesis (Figure 1.1). At stage nine, the volume of wild-type oocytes reaches more than one-third of the overall egg chamber size; however, the mutant oocyte does not expand dramatically from stage eight to nine as it does in wild-type (Figure 1.1 D-

E and I-J). Some mutant egg chambers continued growing beyond stage nine, yet the size of these oocytes never expanded and instead showed a shrunken nuclear lamina in the oocyte and nurse cells, an early indication that these cells were undergoing apoptosis (PRITCHETT *et al.* 2009), which consequently leads to degeneration of the entire egg chamber (Figure A2). Since oocyte development depends on yolk deposition and transport of essential factors from nurse cells to the oocyte through the ring canals, our result suggests this process is impaired in *su(Hw)* mutant ovaries, yielding defective oocyte development.

**Continuous spatial and temporal expression of Su(Hw) is critical for normal ovary development**

Loss of *su(Hw)* results in oocyte developmental defects that may be derived from failed communication between nurse cells and developing oocytes. Su(Hw) is detected in somatic follicle cells and post-mitotic nurse cells in egg chambers (BAXLEY *et al.* 2011), and introducing exogenous *su(Hw)* expression in both types of cells rescues the *su(Hw)* mutant phenotype (HARRISON *et al.* 1993). To determine which cell type and stage of Su(Hw) expression is necessary for oogenesis, we took advantage of the Gal4-UAS binary system to express a *su(Hw)::eGFP* transgene in $su(Hw)^{e04061/v}$ mutant flies (SCHOBORG *et al.* 2013). We used *traffic jam* (*tj*-Gal4) to drive gene expression in all somatic follicle cells throughout oogenesis and *en2.4*-Gal4 to drive expression of Su(Hw)::eGFP in follicle stem cells specifically (LEATHERMAN and DINARDO 2010; SOKOL and COOLEY 2003). We used three different Gal4 drivers to control Su(Hw)::eGFP

expression in germline cells at different stages of oogenesis: *met$\alpha$*-Gal4 which expresses Gal4 under the *alphaTub67C* promoter starting at stage four of oogenesis, and *nanos*-Gal4 as well as *nos*-Gal4 which both express Gal4 throughout oogenesis, though *nanos*-gal4 gives specific expression peaks during the germarium stage and later in stage nine egg chambers (RORTH 1998; VAN DOREN *et al.* 1998). Expression of Su(Hw)::eGFP with each driver was confirmed by immunofluorescence staining using anti-GFP specific antibodies (Figure 3A).

Rescued virgin females with Su(Hw)::eGFP expression driven under different Gal drivers were collected and crossed with male flies (*yw*). We quantified the number of eggs laid by each rescued line within three days to determine the fertility rescue rate. Mutant flies expressing Su(Hw)::eGFP driven by *tj*-Gal4 and *en2.4*-Gal4 in follicle cells were infertile and manifested the same incomplete oogenesis as mutant flies not overexpressing Su(Hw)::eGFP (Table 1). On the other hand, introducing Su(Hw)::eGFP expression in germline cells restored mutant fertility to different degrees depending upon the specific driver. All three overexpression lines showed less than a 50% fertility rescue rate (Table 1), and only mutant females with *nanos*-Gal4 driven Su(Hw)::eGFP expression were able to lay a small number of wild-type eggs (41.4%) that hatched successfully. Furthermore, mutant flies rescued by Su(Hw)::eGFP expression driven by *met$\alpha$*-Gal4 and *nos*-Gal4 laid significantly less eggs, indicating that fewer egg chambers were able to complete oogenesis, likely a result of an inappropriate amount of Su(Hw) expression. In addition, all embryos produced by

*met*$\alpha$-Gal4 and *nos*-Gal4 females displayed axis defects (Hsu et al. unpublished data), revealing the possibility Su(Hw) affects axis determination. In summary, the expression of Su(Hw) only in follicle cells is not sufficient for completing oogenesis, and reveals that the Su(Hw) expression in germline cells is necessary. These results suggest that normal oocyte differentiation requires precise temporal and spatial expression of Su(Hw).

**Intercellular transport between nurse cells and the oocyte is partially blocked in *su(Hw)* mutant ovaries**

The transport of cytoplasm from nurse cells to the oocyte is divided into two phases: the slow phase, which is longer and takes place from early stages to stage ten of oogenesis, and the fast dumping phase, which takes place from stage 10B to 11 while the oocyte doubles in volume. After observing a marked lack of volume expansion in mutant oocytes from stage eight to nine, we speculate that loss of Su(Hw) may affect nurse cell dumping. An indicator of nurse cell preparation for the fast dumping phase is the formation of actin filament cables, called actin bundles, that are derived from the cortex extending toward the nucleus at stage ten (GUILD *et al.* 1997; GUTZEIT 1986). Since *su(Hw)* mutant egg chambers never reach stage 10B, no fast dumping occurs in mutants. To understand whether Su(Hw) is required for fast dumping to take place, we used TexRed-phallodin staining to detect actin bundle formation in egg chambers. We found that the oocyte enlargement at stage 10B as well as the actin bundles appeared normal in egg chambers with overexpression of Su(Hw)

using the *nos*-Gal4 driver (Figure A4). These data suggest the failed fast dumping process is at least partially a consequence of a lack of Su(Hw) expression in female mutant germline cells.

In addition to nutrients released during the fast dumping phase, the slow phase also releases maternal morphogens, which will be later required for proper determination of the embryo dorsal-ventral patterning during development (BATE and MARTINEZ ARIAS 1993a). To determine whether these slow phase molecules can also travel from nurse cells to the oocyte in the earlier stages of oogenesis in *su(Hw)* mutant ovaries, we used the oo18 RNA binding protein Orb (POKRYWKA and STEPHENSON 1995) as a marker to evaluate molecular flow efficiency in wild-type and mutant ovary egg chambers. As expected, Orb translocated from nurse cells to the oocyte and specifically accumulated posteriorly in the wild-type oocyte (Figure 1.2-A). In mutant egg chambers, Orb localization appeared normal in most early stage chambers (Figure 1.2-C), indicating that lack of Su(Hw) does not cause major problems with oocyte determination or molecular transport during early stages of oogenesis. In both heterozygous and trans-heterozygous mutants, we detected an abnormal accumulation of Orb in the cytoplasm of nurse cells and a striking reduction of Orb in stages seven and eight of the oocytes (Figure 1.2-B and C). These data suggest that an inefficient translocation of essential maternal morphogens from the nurse cells to the oocyte in *su(Hw)* mutant egg chambers may be the cause of severe developmental defects.

**Genes involved in nurse cell-oocyte transport are misexpressed in *su(Hw)* mutant ovaries**

To understand whether the defective transport phenotype in the *su(Hw)* mutant results from misregulation of the genes involved in molecular transport, microarray analysis was performed using wild-type (OR) and $su(Hw)^{e1}$ homozygous mutant ovarian mRNA. $su(Hw)^{e1}$ is a loss of function allele resulting from a point mutation that causes the splice junction alteration (HARRISON *et al.* 1993).

The microarray data show significant changes in the expression of eighty-five genes ($P<0.001$) known to have a role in oogenesis (Figure 1.3-A). The relative amount of change for a select group of these genes is shown in Figure 1.3-B. In spite of a forty-three fold decrease of *su(Hw)* expression in $su(Hw)^{e1}$ mutants, a few genes were up-regulated. Among these, *rbp9* was increased almost thirty-two fold, a finding consistent with results obtained by Soshnev et al., suggesting Su(Hw) can indeed function as a transcriptional repressor in *Drosophila* ovaries (SOSHNEV *et al.* 2013). On the other hand, seventy-five out of eighty-five genes appeared to be down-regulated. In particular, *Src64B* (down-regulated) and *hts* (up-regulated) have a role directly related to the structure and function of ring canals.

**Loss of Su(Hw) causes structural defects in ring canals during oogenesis**

Considering the discovery of misexpression of *hts and Src64B,* immunofluorescence experiments were performed to determine whether *su(Hw)* mutant ring canals show defects related to inefficient molecular transport. Comparison of *su(Hw)* mutant and wild-type ring canal sizes using F-actin fluorescence staining revealed a remarkable difference (Figure 1.1). We further confirmed this observation through immunostaining experiments in mutant and wild-type ovaries using antibodies specific to Kelch, a structural component of ring canals that functions in cross-linking F-actin within the ring (KELSO *et al.* 2002; ROBINSON and COOLEY 1997). Results showed that amounts of cytoplasmic Kelch distributed in the nurse cell cytoplasm of mutant egg chambers were above normal (Figure 1.4-A and B) and that ring canals appeared thicker (Figure 1.4-C and D) and longer (Figure 1.4-E and F) as a consequence of excessive accumulation of F-actin in the ring structure (Figure 1.4-G and H).

Loss of *hts* causes female sterility (DING *et al.* 1993; YUE and SPRADLING 1992), and the *hts* gene encodes a polyprotein Ovhts in ovaries that undergoes cleavage to produce two different proteins, Ovhts-Fus and Ovhts-RC. Ovhts-Fus localizes at the fusome in mitotic cells within the early germarium, whereas Ovhts-RC serves as a ring canal structure protein in later oogenesis (PETRELLA *et al.* 2007). Except for F-actin and Kelch, we used an antibody against Ovhts-RC to determine the detailed structure of ring canals using immunostaining. Interestingly, the mutant rings at stage six were not only thinker but also had

smaller inner diameters due to accumulation of the structural proteins, Kelch and Ovhts-RC (Figure 1.5). These thicker rings created smaller lumens that may have caused obstruction of molecular passage.

**The ring canal developmental defect is observed in the *su(Hw)* mutant**

To monitor ring growth differences between wild-type and mutant egg chambers during development, we measured ring canal outer diameters from stages four to eight (Figure 1.6-A). Given that ring sizes vary in each egg chamber depending upon ring age such that older rings formed earlier during mitosis within the germarium appear larger, we used fluorescence microscopy to measure all fifteen rings in each egg chamber, recording data only from images clearly displaying all fifteen rings. The ring size distribution of stages five and eight in mutant and wild-type egg chambers is shown within histograms in Figures 1.6-B and C. The average ring size at stage five was 3.2 μm in wild-type and 2.9 μm in mutants, revealing no significant difference (Figure A5). Additionally, ring sizes at stages six and seven did not show a significant difference; however, wild-type rings at stage eight expanded to 5.7 μm (N=120, standard deviation=0.9), while mutant rings expanded only to 4.8 μm (N=90, standard deviation=0.8), showing mutant ring canals are significantly smaller (Student's t-Test, $p<0.0001$) (Figure 1.6-B and C). In addition to the significantly delayed outer ring diameter expansion at stage eight in *su(Hw)* mutants, inner ring diameters were abnormally small during earlier stages. These data suggest

that the smaller rings at stage eight may be an accumulative effect of abnormal ring development from earlier stages.

The *hts* gene misexpression together with the observation of abnormal rings at different stages in *su(Hw)* mutants (Figure 1.5) leads us to ask whether fusome development during the germarium stage is affected. We used an anti-Hts F monoclonal antibody to perform immunostaining in the wild-type and the mutant germarium. These experiments revealed a seemingly normal fusome in *su(Hw)* mutants, plugging ring canals during initial mitotic divisions and forming branched structures in the germarium that disappeared at stage one, consistent with observations in wild-type ovaries (Figure 1.7-A). We concluded fluorescence microscopy could not detect significant fusome organization defects in *su(Hw)* mutant ovaries (Figure 1.7-B). Consequently, these results suggest defects in ring canals do not originate from *hts* overexpression in the germarium stage, and that *hts* overexpression does not cause major defects in the formation and structure of the fusome.

**Misexpression of *Src64B* in *su(Hw)* mutant ovaries causes structural defects in ring canals**

While *hts* was up-regulated, *Src64* was down-regulated in the *su(Hw)* mutant (Figure 1.3). Src64B is a protein tyrosine kinase playing an important role in regulating ring canal growth and morphogenesis during *Drosophila* oogenesis, and *su(Hw)* mutants and *Src64B* mutants have the same phenotype of retained

Orb in nurse cells (DJAGAEVA *et al.* 2005). *Src64B* mutants produce abnormally small eggs due to unsuccessful nurse cell dumping, caused in part by defects of fusome development, ring canal growth and morphogenesis (COOLEY 1998; DJAGAEVA *et al.* 2005; DODSON *et al.* 1998).

The actin binding protein Kelch functions in cross-linking actin monomers during ring canal formation, consequently stabilizing F-actin by protecting it from depolymerization (ROBINSON *et al.* 1994). F-actin polymerization and depolymerzation are dynamic processes during ring canal development. At stage six for example, the ring canal expands rapidly in preparation for nurse cell dumping during subsequent stages. When the outer ring canal diameter rapidly expands to increase the lumen, F-actin must depolymerize in the inner ring rim to prepare for ring size expansion. *kel* null mutants show disorganized actin filaments starting at stage four and present a completely disrupted organization at stage six when ring expansion is necessary for nurse cell dumping (ROBINSON and COOLEY 1997; XUE and COOLEY 1993). Src64B kinase activity regulates Kel function through phosphorylation, and both a mutation of tyrosine 627 in *kelch* and a null mutation of *Src64B* cause a dramatic reduction in actin monomer turnover resulting in thicker rings with small lumens, a phenotype similar to the ring phenotype described in *su(Hw)* mutant egg chambers (Figure 1.4 and 1.5) (DODSON *et al.* 1998; KELSO *et al.* 2002; ROBINSON and COOLEY 1997; XUE and COOLEY 1993).

These observations suggest not only that abnormal ring canal structure in *su(Hw)* mutants may impact molecular transport within the egg chamber, thereby causing oogenesis failure and sterility, but also that this phenotype is partially due to *Src64B* misexpression. To exclude the possibility that decreased expression of *Src64B* observed in microarray experiments stems from a developmental factor, we performed real-time RT-PCR to compare *Src64B* expression in wild-type and *su(Hw)* mutants by manually removing egg chambers older than stage nine. Results showed *Src64B* expression is suppressed by more than 70% in *su(Hw)* mutant ovaries compared to wild-type, a result consistent with the microarray data (Figure 1.3-C). As we detected an abnormal accumulation of F-actin in ring canals and found that *Src64B* is under-expressed in *su(Hw)* mutants, we hypothesized the thick ring phenotype resulted from lack of *Src64B* expression. To test this hypothesis, we used *nos*-Gal4 to drive *Src64B* expression in *su(Hw)* mutants and then observed ring canal morphology in Src64B rescued females. Ovary immunostaining in Src64B rescued females showed that Kelch and F-actin accumulation within rings was eliminated, a finding similar to wild-type rings (Figure 1.8). These data suggest abnormal ring canal morphology in *su(Hw)* mutants was caused by *Src64B* misregulation. Nevertheless, fertility of these Src64B rescued females was not recovered, indicating other factors may be critical to cause oogenesis failure in addition to *Src64B* misregulation.

## ***Discussion***

Loss of *su(Hw)* causes female sterility as a result of incomplete oocyte development as well as egg chamber degeneration beginning at mid-oogenesis (BAXLEY *et al.* 2011; HARRISON *et al.* 1993; KLUG *et al.* 1968; KLUG *et al.* 1970). To further understand causes of mutant sterility, we investigated egg chamber structure and molecular flow while searching for corresponding misregulated genes. Ultimately, we found *Src64B* down-regulation causes abnormal ring canal development, thereby disrupting Kelch functionality of actin organization.

### Oocyte development depends upon Su(Hw) expression in germline cells

We first found mutant oocyte cytoplasm ceases enlarging at stage nine (Figure 1.1), indicating absence of nurse cell rapid dumping. Also, in earlier stages, Orb remained in the nurse cell cytoplasm, revealing an impact on molecular transport between nurse cells and the oocyte (Figure 1.2). Specific morphogens traveling into the oocyte are important for oocyte maturation and embryo development, and loss or mislocation of these morphogens causes oogenesis failure or abnormal embryo production. Moreover, restoration of Su(Hw) expression using germline specific Gal4 drivers rescues nurse cell dumping, oocyte development, and female fertility (Table 1 and Figure A4). The fact the fertility rescue rate was increased from 1.6% (*met$\alpha$*-Gal4) to 6.1% (*nos*-Gal4) indicates that Su(Hw) expression in germline cells is necessary in early oogenesis before stage four. In addition, the fertility rescue rate is also

dependent on the appropriate amount of Su(Hw) expression at particular stages. The flies with Su(Hw) expression under *nanos*-Gal4 showed the highest rescue rate (41.4%) compared to the flies with expression under the stronger *nos*-Gal4 driver (6.1%). Overall, these data show Su(Hw) expression in germline cells is required for proper oocyte development. Although Su(Hw) expression in germline cells is necessary for female fertility, production of abnormal embryos suggests Su(Hw) expression in somatic follicle cells may be necessary for embryo development.

**Actin organization is misregulated in *su(Hw)* mutants**

Ring canal position and orientation corresponds to neighboring nurse cell arrangements within egg chambers, and mutant ring positioning is atypical (Figure 1.1), indicating the fifteen nurse cells are arranged differently within the egg chamber. This unusual organization may contribute to inefficient molecular transport. Excessive F-actin accumulation in rings suggests actin organization is misregulated upon loss of *su(Hw)* expression; hence, this misregulation may contribute to the difficulty of molecular transport in egg chambers.

**Su(Hw) affects the expression of ring canal related genes**

In this study, microarray analysis was performed using the mature female ovaries of a loss of function mutant, $su(Hw)^{e1}$. In addition, we also compared the transcriptional changes in response to the *su(Hw)* mutation using array data

generated from young virgin female ovaries including, wild-type, *su(Hw)*$^{2/e04061}$, *su(Hw)*$^{2/v}$ and *su(Hw)*$^{f}$ (SOSHNEV *et al.* 2013). Given the developmental differences between our data and Soshnev's, we reasoned that gene sets that have a similar transcriptional response to the *su(Hw)* mutation in both are likely to be highly influenced by this gene. Hierarchical clustering based on oogenesis-related genes and most other gene sets showed that our samples clustered separately from Soshnev's samples, indicating that there were large differences between our samples and theirs due to the different developmental stages. When the samples were clustered based on genes in “eggshell chorion assembly” (GO:0007306), “structural constituent of chorion” (GO:0005213) and “multicellular organism development” (GO:0007275), all of which contain mostly chorion-related genes, the *su(Hw)* mutants from both data sets and the wild types clustered tightly together. This may indicate that these chorion-related genes are tightly regulated by Su(Hw) since they exhibited a similar response in our samples and Soshnev's samples despite the large differences in gene expression due to different developmental stages (Figure A6).

Consistently, *Rbp9* is highly up-regulated in *su(Hw)*$^{e1}$ mutants and in other *su(Hw)* mutants. This gene encodes a RNA-binding protein belonging to the ELVA/Hu gene family that participates in regulating gene expression by influencing mRNA splicing and translation (HILGERS *et al.* 2012; SOLLER *et al.* 2010). *Drosophila* Rbp9 interacts with U-rich mRNA and regulates the turnover of its target mRNAs (KIM and BAKER 1993; PARK *et al.* 1998). In *su(Hw)* mutants,

*Rbp9* is de-suppressed, and decreased expression of *Rbp9* partially rescued fertility (SOSHNEV *et al.* 2013).

A decreased binding affinity of Su(Hw) at the *Rbp9* promoter region in *su(Hw)*$^{f/v}$ was shown in the ChIP-seq analysis; however, suppression of *Rbp9* remained (SOSHNEV *et al.* 2013). This data indicates either that the Su(Hw) regulation of *Rbp9* may not be sensitive to Su(Hw) binding affinity or that other critical factors contribute to *Rbp9* regulation. Additionally, overexpression of *Rbp9* driven by *nos*-Gal4 causes apoptosis of stage ten egg chambers; yet, the enlargement of oocytes at stage ten was still observed (JEONG and KIM-HA 2003). This indicates oocyte development in *Rbp9* overexpression egg chambers advanced beyond the stages when *su(Hw)* mutant oocytes terminated. This comparison also suggests that other important factors may contribute to failed oocytes development and egg chamber degeneration before stage ten in *su(Hw)* mutants. Altogether, we reasoned that *Rbp9* may not be the only target gene of Su(Hw) that contributes to female sterility upon loss of Su(Hw).

Two ring canal related genes, *hts* and *Src64B*, were found to be misregulated according to our microarray analysis using the *su(Hw)*$^{e1}$ mutant. We also compared expression patterns of those two genes using publicly available data of other *su(Hw)* mutants, including *su(Hw)*$^{e04061/2}$ and *su(Hw)*$^{v/2}$ (SOSHNEV *et al.* 2013), and both genes showed a similar expression pattern among the different mutants. In addition, qRT-PCR confirmed the microarray results by

revealing a three-fold down-regulation of *Src64B* in *su(Hw)*$^{v/e04061}$ mutants (Figure 1.3). These results suggest that the misregulation of ring canal related genes is a general effect in the *su(Hw)* mutant. In order to understand how those two genes are regulated by Su(Hw), we analyzed the location of Su(Hw) using ChIP on chip data in ovary tissues at the UCSC genome browser (SOSHNEV *et al.* 2012). The results showed neither Su(Hw) binding sites in the *hts* gene coding region nor the regulatory region; yet, they showed a strong Su(Hw) binding site approximately 4 Kb upstream of the *Src64B* gene and two other binding sites at the intron sequences of *Src64B*. This analysis suggests a possible direct regulatory role of Su(Hw) in *Src64B* gene expression through RNA splicing or promoter regulation.

**Abnormal ring canal development in *su(Hw)* mutants results from *Src64B* down-regulation**

The abnormally thick ring structure appears throughout oogenesis from stage four to stage eight in *su(Hw)* mutant egg chambers (Figures 1.4 and 1.5). To rule out the possibility egg chamber degeneration delays ring expansion, we examined rings in egg chambers older than stage eight, noting the outer diameter of rings continuously increased instead of shrinking.

Misexpression of Src64B may cause ring canal actin disorganization due to dysfunctional Kelch, which normally maintains rapid turnover of the actin cytoskeleton. Restoration of Src64B expression in *su(Hw)* mutants recovers ring canal morphology but not female fertility (Figure 1.8). Altogether, we

demonstrated a novel *su(Hw)* mutant ring canal phenotype resulting from significant *Src64B* down-regulation during oogenesis. Although *Src64B* down-regulation is not the only factor leading to infertility, mutation of *su(Hw)* may have a pleiotropic effect in oogenesis. More studies are needed to characterize other critical factors causing oogenesis failure in the *su(Hw)* mutant.

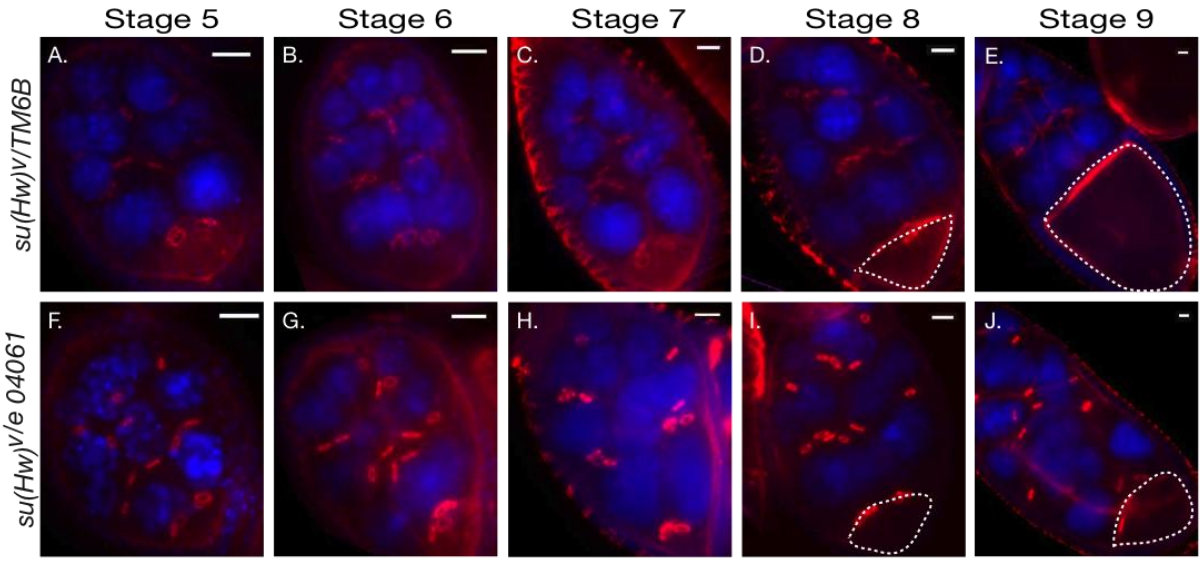


**Figure 1.1. Oocyte developmental defects are observed in *su(Hw)* mutants.**

F-actin staining on wild-type and *su(Hw)* mutant ovaries appears red and DAPI staining of DNA appears blue. The oocyte was observed at different stages of each genotype and the scale bar is 50 μm in each image. The dashed lines highlight the regions of oocytes at stage eight and nine.

**Table 1.1. Spatial and temporal expression of Su(Hw) is critical for ovary development.**

| Gal4 Driver | Cell Types | Stages | Fertility Rescue % |
|---|---|---|---|
| nanos-Gal4 | Germline Cells | From G throughout oogenesis | 41.4 % (235/567) |
| nos-Gal4 | Germline Cells | From G throughout oogenesis | 6.1 % (33/539) |
| metα-Gal4 | Germline Cells | From stage four throughout oogenesis | 1.6 % (2/128) |
| en2.4-Gal4 | Somatic germline cells | From G to stage one | 0 % |
| tj-Gal4 | Somatic cells | From G throughout oogenesis | 0 % |

Different Gal4 drivers were used in *su(Hw)* mutants to control *su(Hw)::eGFP* expression within specific cell types and ovary developmental stages (G: germarium) as listed in the table. The sterility rescue rate of each line was determined by counting eggs.

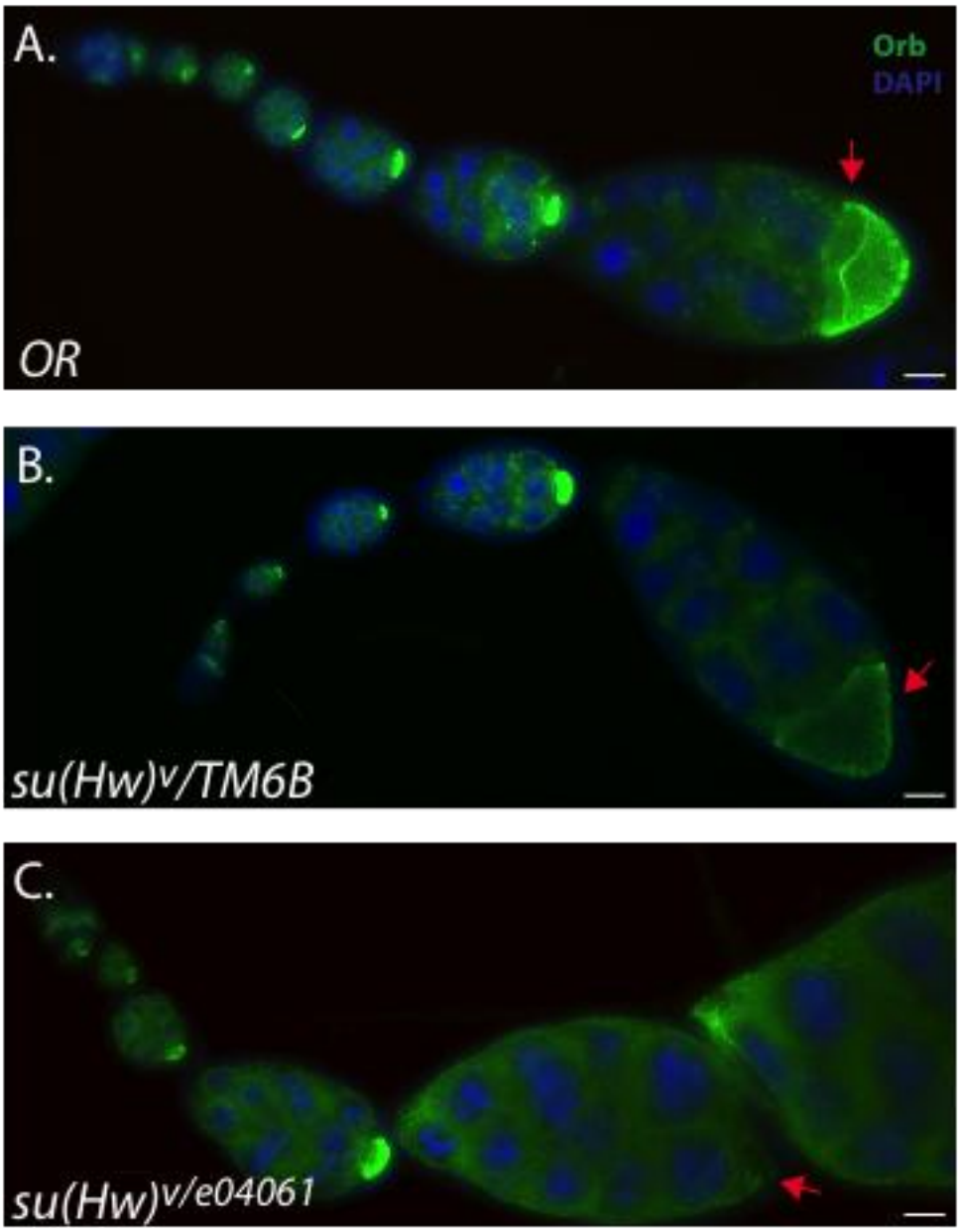


**Figure 1.2. Orb is mislocated in *su(Hw)* mutant egg chambers.**

Wild-type (A), *su(Hw)* heterozygous (B), and trans-heterozygous (C) egg chambers were stained with an Orb antibody in green and DAPI in blue. The scale bar is 50 μm.

**Figure 1.3. Su(Hw) regulates many genes involved in oogenesis.**

Eighty-five genes related to ovary development having a significant change in expression greater than three-fold were shown in the heatmap with up-regulation shown in red and down-regulation in blue. The color key is shown at the bottom of (A). The table showed the selected genes and their corresponding change in expression (B). Gene expression of *Src64B* in ovaries was confirmed with qRT-PCR (C).

A.

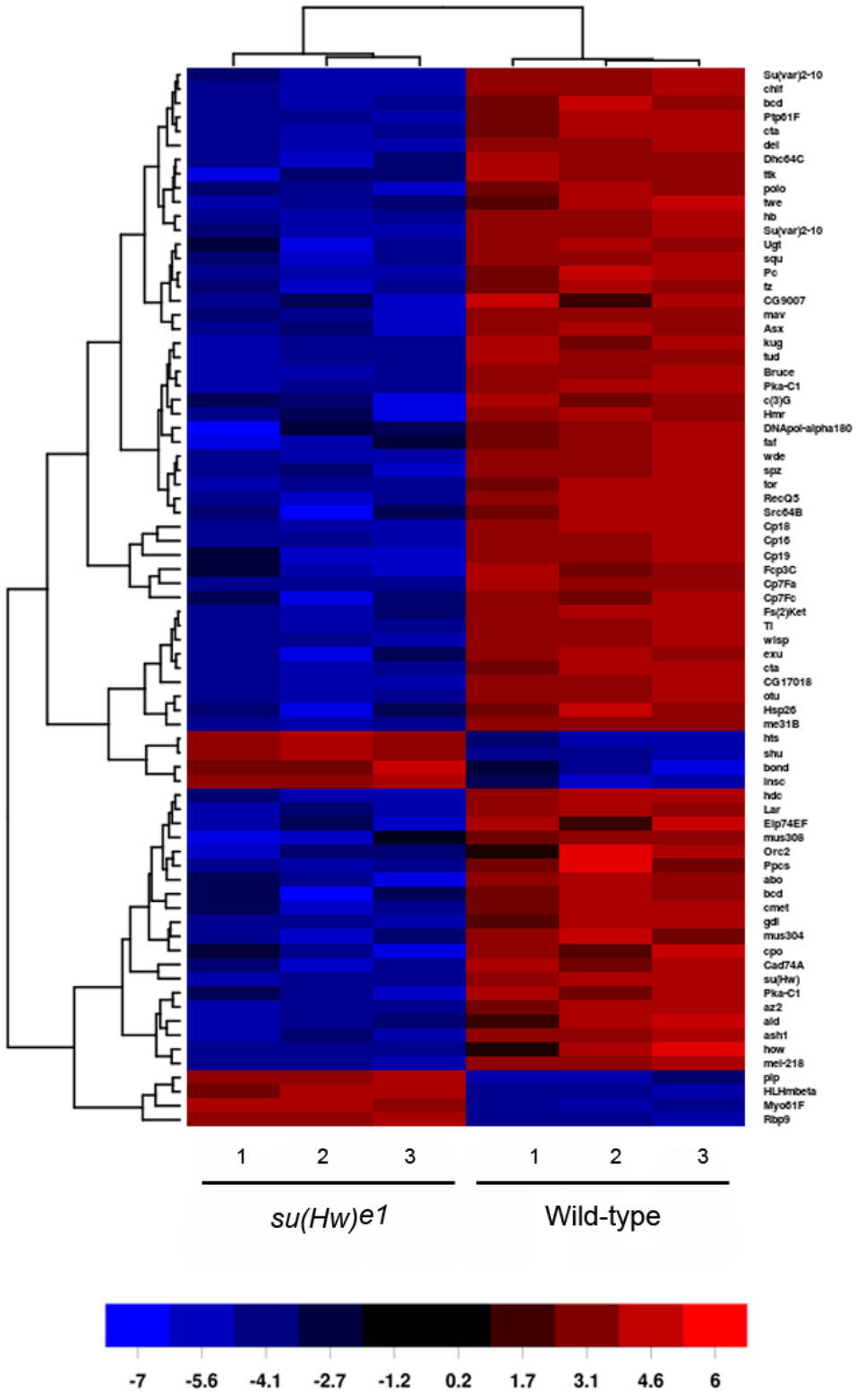
Su(var)2-10
chif
bcd
Ptp61F
cta
del
Dhc64C
ttk
polo
twe
hb
Su(var)2-10
Ugt
squ
Pc
tz
CG9007
mav
Asx
kug
tud
Bruce
Pka-C1
c(3)G
Hmr
DNApol-alpha180
taf
wde
spz
tor
RecQ5
Src64B
Cp18
Cp16
Cp19
Fcp3C
Cp7Fa
Cp7Fc
Fs(2)Ket
Tl
wisp
exu
cta
CG17018
otu
Hsp26
me31B
hts
shu
bond
insc
hdc
Lar
Elp74EF
mus308
Orc2
Ppcs
albo
bcd
cmet
gdl
mus304
cpo
Cad74A
su(Hw)
Pka-C1
az2
ald
ash1
how
mei-218
plp
HLHmbeta
Myo61F
Rbp9
1
2
3
1
2
3
su(Hw)e1
Wild-type
-7
-5.6
-4.1
-2.7
-1.2
0.2
1.7
3.1
4.6
6

B.

| Gene symbol | Gene name | Fold change |
|---|---|---|
| Up-regulated gene | | |
| *Rbp9* | RNA-binding protein 9 | 31.9 |
| *Pip* | Pipe | 4.33 |
| *Hts* | Hu-li tia shao | 1.42 |
| | | |
| Down-regulated gene | | |
| *Cp18* | Chorion protein 18 | 1120 |
| *su(Hw)* | suppressor of Hairy wing | 46.73 |
| *Del* | deadlock | 7.54 |
| *Cort* | Cortex | 5.45 |
| *Chif* | Chiffon | 5 |
| *Src64B* | Src oncogene at 64B | 3.52 |
| *Squ* | Squash | 3.49 |
| | | |

C.

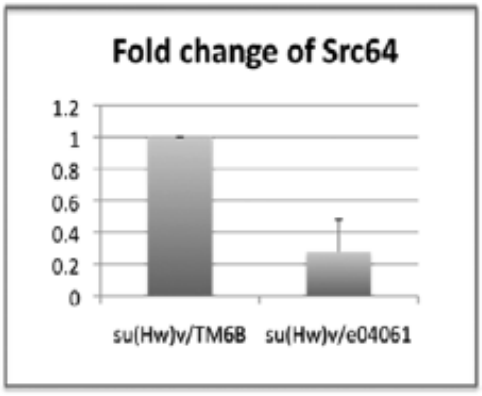


**Figure 1.3. Continued.**

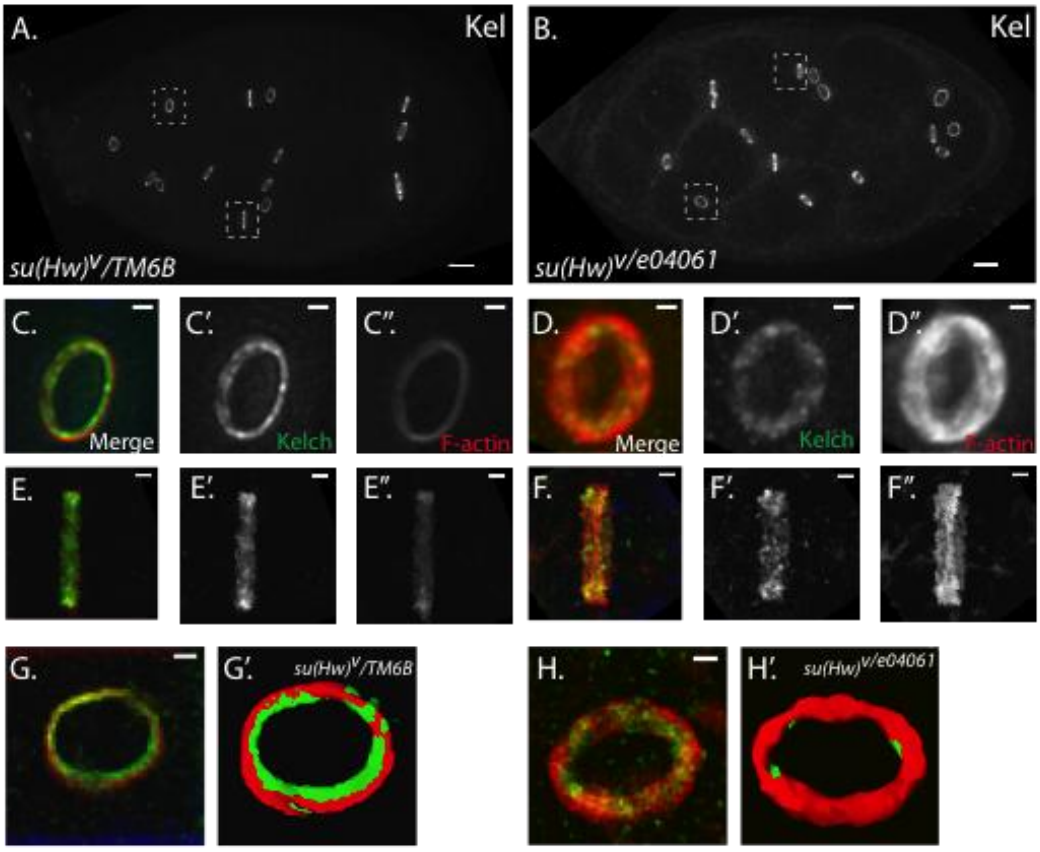


**Figure 1.4. Ring canal morphological differences are identified in *su(Hw)* mutants.**

Ring canals in wild-type and mutant egg chambers were stained with Kelch antibody in green and Phalloidin in red. A and B show Kelch staining throughout the whole egg chamber at stage eight and individual rings in wild-type (C and E) and mutants (D and F). The isosurface images of rings (G and H) were generated using Leica Deblur software. The cartoon ring image showed the accumulation of actin in rings. The scale bars in whole egg chamber images represent 10 μm, and those in individual ring images are 1μm.

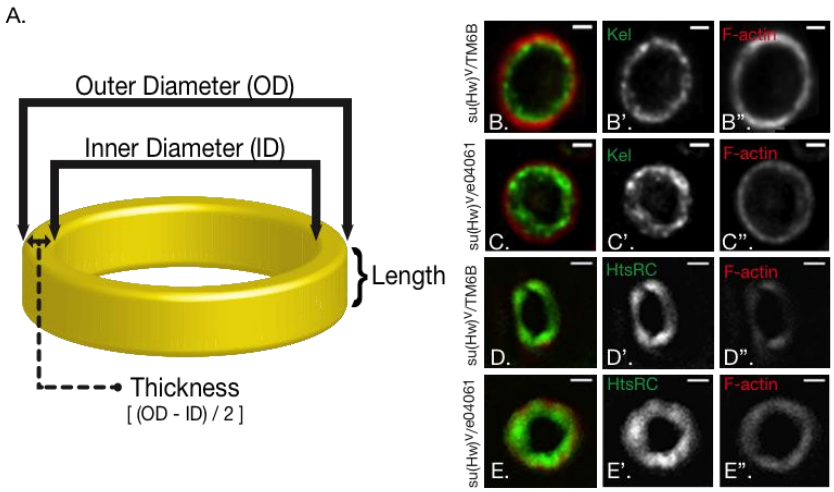


**Figure 1.5. Accumulation of structural proteins in the ring canal was detected in su(Hw) mutants.**

The cartoon ring image illustrates the ring structure (A). Staining for different structural proteins is shown in (B-E). Both Kelch and Ovhts-RC show accumulation at the inner rim in mutants (C and E) but not wild-type (B and F).

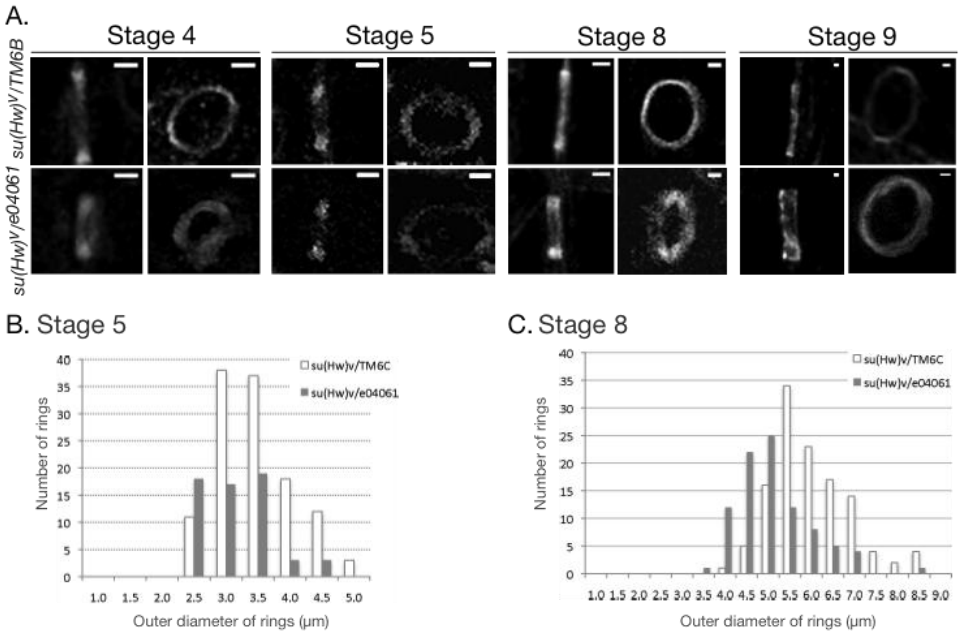


**Figure 1.6. Ring canal development is defective in *su(Hw)* mutants.**

From stage four to eight, the rings were detected using F-actin staining (A) and the size of rings at each stage were quantified using the measurement tool in image J. The measurements of ring outer diameters in each genotype at stage five and eight are shown in histograms (B and C) (wild-type: white bar, mutant: grey bar).

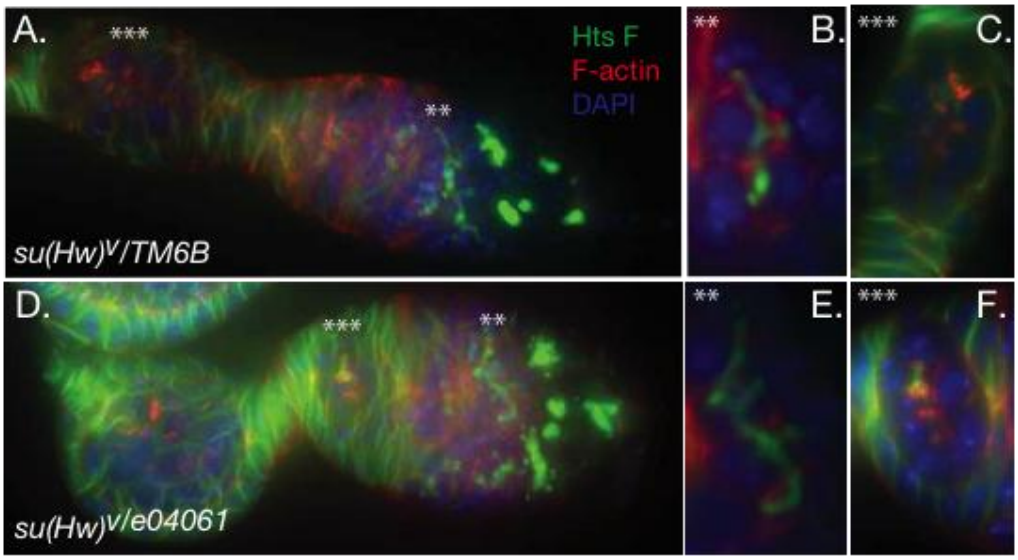


**Figure 1.7. Fusome development in *su(Hw)* mutants.**

Ovary staining was performed using Hts F antibody for fusomes showing in green, F-actin in red and DAPI in blue. Early germarium stage egg chambers in wild-type (A-C) and *su(Hw)* mutants (D-F) are shown. Region 3 (stage one egg chambers) was labeled with three white asterisks and region 2 was labeled with two. The labeled region images were cropped, and the magnified images of these are shown in B and C for wild-type and E and F for mutants.

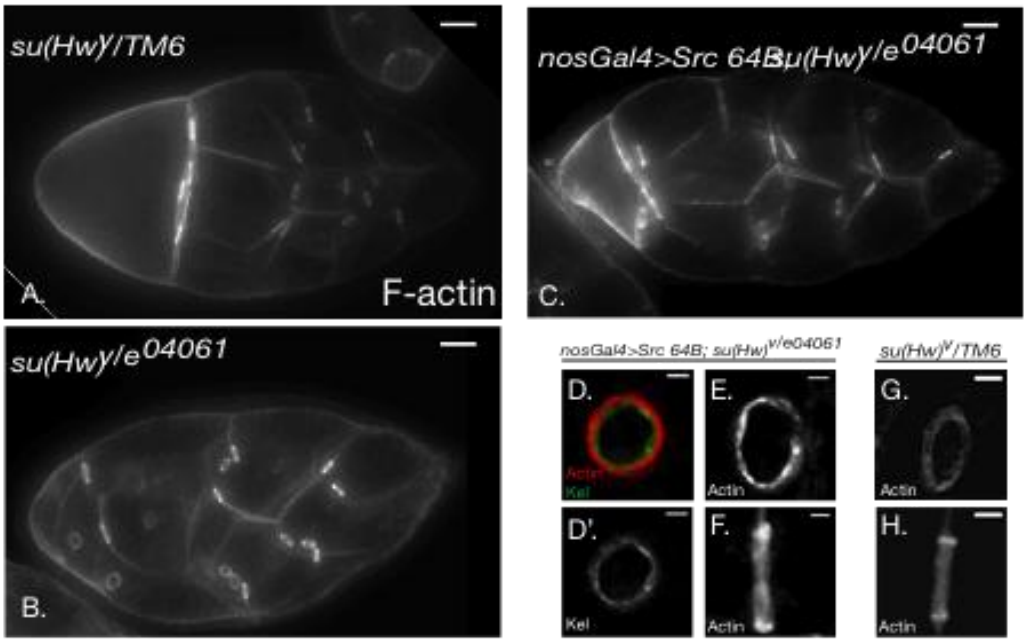


**Figure 1.8. Restoration of Src64B rescues ring phenotype in *su(Hw)* mutants.**

The ring morphology was detected using F-actin staining in wild-type (A), *su(Hw)* mutant (B), and *nos*Gal4>>*Src64B* rescued *su(Hw)* mutant egg chambers (C). Also, the individual rings from rescued and wild-type egg chambers stained with F-actin in red and Kel in green were cropped and shown in D to H.

# CHAPTER II.

## The Chromatin Insulator Protein Suppressor of Hairy Wing Maintains Genome Integrity During *Drosophila* Female Germline Development

Shih-Jui Hsu, Heather Ann Wallace, and Mariano Labrador

Author contributions:

1). Shih-Jui Hsu: Conceiving and designing experiments, performing experiments, analyzing data, making figures and writing the manuscript.
2). Heather A. Wallace: designed and performed experiments and analyzed data related to detection of transposon activity.
3). Mariano Labrador: Conceiving and designing experiments, analyzing data, making figures and writing the manuscript.

## ***Abstract***

Chromatin insulator proteins mediate the formation of stable interactions between distant insulator sites along chromatin fibers. Lack of insulator function is generally lethal, since these long-range contacts orchestrate communications between regulatory sequences and gene promoters throughout the genome, allowing accurate gene transcription regulation during embryo development and cell differentiation. Conversely, the *Drosophila* insulator protein Suppressor of Hairy wing [Su(Hw)] is not required for viability, and has been identified as playing a crucial role in female oogenesis. Insulator proteins act by facilitating protein-protein interactions that stabilize distant chromatin contacts, but the mechanisms by which these contacts enable insulator function remain unclear. To gain insight into the functional properties of chromatin insulators, we further characterized the oogenesis phenotypes of *su(Hw)* mutant females. We found that mutant egg chambers frequently display an irregular number of nurse cells, have poorly formed microtubule organization centers (MTOC) in the germarium, and have mislocalized Gurken (Grk) in later stages of oogenesis. Furthermore, embryos from partially rescued females exhibited unequivocal dorsal-ventral patterning defects that are identical to defects found in spindle mutants or in piRNA pathway mutants. Analysis using antibodies against phosphorylated H2Av (γH2Av) revealed an excess of DNA double strand breaks (DSBs) which trigger activation of the ATR mediated DNA-damage response. Our data also revealed that these DSBs do not result from faulty suppression of transposable elements, altogether suggesting that Su(Hw) plays a critical role in maintaining genome

integrity during germline development in *Drosophila* females by a mechanism unrelated to transposable elements activity.

## ***Introduction***

Higher-order chromatin organization in the nucleus is facilitated by chromatin insulators, which stabilize interactions between distant sites in the chromatin fiber. These long-range contacts help orchestrate interactions between regulatory sequences and gene promoters in order to accommodate the complex genomic networks of gene transcription required to promote cell and tissue differentiation during embryo development (LABRADOR and CORCES 2002; YANG and CORCES 2012).

Although not well understood in plants and only understood to have limited activity in yeasts, insulators conserve function throughout eukayotes (GURUDATTA and CORCES 2009; VAN BORTLE and CORCES 2012b). Insulator properties have been characterized in two ways: preventing communication between distal enhancers and promoters when positioned in between, and acting as boundaries to protect genes against heterochromatin-mediated silencing (BRASSET and VAURY 2005; GASZNER and FELSENFELD 2006; WEST *et al.* 2002). These properties are facilitated by insulator proteins, which bind the insulator DNA and mediate protein-protein interactions (PHILLIPS-CREMINS and CORCES 2013; VAN BORTLE and CORCES 2012a).

One of the earliest characterized insulators is found in the *Drosophila gypsy* retrotransposon. *Gypsy* can integrate into the regulatory region of genes, thereby disrupting communication between enhancers and promoters and causing mutations that can be suppressed by a second site mutation in the *suppressor of Hairy wing* gene [*su(Hw)*] (MODOLELL *et al.* 1983; PARKHURST and

CORCES 1986; SPANA *et al.* 1988). In addition to Su(Hw), which directly binds to the insulator DNA, two other major proteins have been identified that are required for *gypsy* insulator function: Modifier of mdg4 [Mod(mdg4)-67.2] and Centrosomal Protein 190 (CP190), which both directly interact with Su(Hw) (GEORGIEV and KOZYCINA 1996; GEORGIEV and GERASIMOVA 1989; GERASIMOVA *et al.* 1995; GHOSH *et al.* 2001; PAI *et al.* 2004). Unlike other insulator proteins in *Drosophila* such as dCTCF, CP190, BEAF or GAGA factor, the function of both Su(Hw) and its binding partner Mod(mdg4)-67.2 are dispensable for viability (BUTCHER *et al.* 2004; GERASIMOVA *et al.* 1995; KATOKHIN *et al.* 2001; KLUG *et al.* 1968; MOHAN *et al.* 2007; ROY *et al.* 2007). CP190, the other binding partner, has insulator activity that is independent from Su(Hw) and forms insulators in the genome in association with other insulator proteins (BUSHEY *et al.* 2009a; MOHAN *et al.* 2007; MOSHKOVICH *et al.* 2011). Homozygous Su(Hw) loss-of-function mutations are viable with no evident phenotype, except that females are sterile (KLUG *et al.* 1968; KLUG *et al.* 1970). Although the two binding partners of Su(Hw), Mod(mdg4)-67.2 and CP190, are required for *gypsy* insulator activity, only Su(Hw) is essential for oogenesis. In ovaries, Su(Hw) is detected in the nucleus of both somatic follicle cells and germ cells (BAXLEY *et al.* 2011). Loss of Su(Hw) leads to suppression of yolk deposition in the oocyte and oocyte development arrests at mid-oogenesis (HARRISON *et al.* 1993; KLUG *et al.* 1968; KLUG *et al.* 1970), but the mechanisms causing these oogenesis defects remain poorly understood, and a thorough analysis of *su(Hw)* mutant phenotypes could

be instrumental for further understanding the role of Su(Hw) in oogenesis as well as insulator protein function in general.

In *Drosophila*, oogenesis begins with an asymmetric cell division of a germline stem cell at germarium stage, which gives rise to a daughter stem cell and a cystoblast. The cystoblast will undergo four incomplete mitotic divisions, forming an egg chamber containing sixteen germ cells that remain interconnected by ring canals and are enclosed by an epithelium of follicle cells. Each egg chamber undergoes a developmental process fourteen stages long that culminates with the formation of a mature oocyte. As oogenesis progresses, the endopolyploidy nuclei of the fifteen nurse cells undergo a dramatic change from a condensed five-blobs configuration to a decondensed morphology at stage six (BATE and MARTINEZ ARIAS 1993b). Before the mid-oogenesis arrest, the only visible chromatin-configuration defect in *su(Hw)* mutant egg chambers is a delayed chromatin dispersal of nurse cell polytene chromosomes occurring at stage seven or eight, and mid-oogenesis arrest eliminates the prolonged development of defective egg chambers resulting in egg chamber degeneration around stage nine or ten (BAXLEY *et al.* 2011; HARRISON *et al.* 1993; KLUG *et al.* 1968). This defective nurse-cell chromatin dispersal phenotype is common among a large number of unrelated mutants carrying mutant allele genes, such as *prp22*, encoding a spliceosome component, and *rhino*, encoding a piwi-interacting RNA (piRNA) related protein (KLATTENHOFF *et al.* 2009; VOLPE *et al.*

2001); however, this phenotype makes it difficult to understand the activity of Su(Hw) in ovaries.

In addition to defects resulting from mutations of genes encoding proteins that perform specific tasks during oogenesis, uncontrolled transposon activity may also cause severe disruption of development. Numerous studies have characterized piRNAs, which are the critical molecules involved in suppression of transposon activity. These RNA sequences were originally called repeat-associated siRNAs (rasi-RNAs) as they are derived from retrotransposons and repetitive sequences in the genome (ARAVIN *et al.* 2003; BRENNECKE *et al.* 2007; FESCHOTTE 2008; YIN and LIN 2007). Mutations in genes involved in piRNA production such as *aubergine* (*aub*), *spindle-E* (*spnE*) and *maelstom* (*mael*) result in transposable element overexpression and mobilization that create double strand breaks (DSBs) in the host genome (COOK *et al.* 2004; KLATTENHOFF *et al.* 2007; SIENSKI *et al.* 2012). The unleashed retrotransposon activation triggers the DNA damage response, thereby causing defects in polarity formation of the microtubule organization center (MTOC) in early oogenesis and further disrupting Gurken signaling in later stages that are essential to dorsal-ventral determination during embryonic development (KHURANA and THEURKAUF 2010; KLATTENHOFF *et al.* 2007). This consequent DNA damage response utilizes the same pathway triggered by unrepaired DSBs in mutants of spindle class genes encoding meiotic DNA damage repair enzymes. These unrepaired DSBs activate meiotic checkpoints mediated by *mei-41* (ataxia telangiectasia-related,

ATR orthologue) and *mnk* (checkpoint kinase 2 ortholog) (ABDU *et al.* 2002; GHABRIAL and SCHUPBACH 1999; LAROCQUE *et al.* 2007).

Recent insights into the role of Su(Hw) during oogenesis came from genome-wide studies of the transcriptional activity of genes which suggested that the function of Su(Hw) in oogenesis could be independent of its function as a chromatin insulator, and that Su(Hw) functions as a transcriptional regulator rather than as a chromatin insulator demarcating transcriptional domains (BAXLEY *et al.* 2011; HARRISON *et al.* 1993; SOSHNEV *et al.* 2013; SOSHNEV *et al.* 2012). In this study, we demonstrated that the loss of Su(Hw) created massive non-meiotic DSBs that accumulated in germline cells of ovaries, thereby activating the DNA damage checkpoints which result in oogenesis failure. We found the cause of DSBs was not from over-activation of transposable elements, but rather may stem from misregulation of DNA repair or DNA replication.

## ***Materials and methods***

### Fly genetics

All fly stocks were cultured on cornmeal-agar food with yeast at 25°C. The fly stocks used in this study are: *$y^2 wct^6$; su(Hw)$^v$/TM6B*, a gift from Victor Corces (Emory University); w*;P{GAL4-nos.NGT40} (BDSC: 4442) and *mei-41 $^{D5}$*, gifts from Laura Lee (Vanderbilt University); P{naos-Gal4::VP16} and spn$D^2$, gifts from Bruce McKee (University of Tennessee); mnk$^{6006}$, a gift from Bill Theurkauff (University of Massachusetts, Worcester). Other fly stocks were from the Bloomington stock center.

### Immuno-fluorescence staining of ovaries

Three- to five-day-old female ovaries were collected for ovary whole mount immunostaining as described (PAGE and HAWLEY 2001). Briefly, tissues were fixed in heptane (Sigma) with 4% para-formaldehyde and washed with PBST. Fixed tissues were incubated with blocking solution. Primary antibodies used for staining are as follows: anti-rabbit eGFP (Invitrogen, 1:100), anti-rabbit γH2Av (Rockland, 1:5000), anti-mouse Orb and anti-mouse Grk (Developmental Studies Hybridoma Bank, 1:200). The following secondary antibodies were used at 1:200 dilution: FITC-conjugated anti-rabbit IgG, Texas Red-conjugated anti-rabbit IgG and FITC-conjugated anti-mouse IgG (The Jackson Laboratory). F-actin staining was performed using Texas Red-X phallodin (Life Technologies). Ovaries were stained with 4′, 6-diamidino-2-phenylindole (DAPI, 0.5 μg/ml) and were mounted in Vectashield mounting medium (Vector Laboratories). Slides

were analyzed under a Leica DM6000B wide-field fluorescence microscope equipped with a Hamamatsu ORCA-ER CCD camera and a HC PL FLUOTAR 20x /0.50NA objective. Image acquisition was performed using Simple PCI v6.6 (Hamamatsu Photonics). Images were processed using the AutoQuant's 3D Deconvolution Algorithm utilizing an adaptive (blind) PSF implemented into Lecia Deblur (v2.3.2) software. Wild-type and mutant samples were prepared and imaged under identical immunostaining conditions and microscope, camera and software settings. Egg chamber stage was determined based on the size (SULLIVAN *et al.* 2000) measured in Image J.

**Documentation of embryo phenotype**

Two to three-day-old *su(Hw)* mutant virgin females carrying the *su(Hw):eGFP* transgenes driven by nano-Gal4 driver were crossed with *yw* male flies. Eggs were collected for three days using grape juice agar plates containing wet yeast paste (SULLIVAN *et al.* 2000). The embryo morphology was observed under the Leica MZ16FQ stereomicroscope.

**Western blot**

Three- to five-day-old female ovaries were dissected and then homogenized in RIPA lysis buffer with protease inhibitor and phosphatase inhibitors (Roche). Lysates were resolved on a 15% acrylamide gel, wet transferred overnight at 4°C, and then probed with both anti-rabbit monomethylated H4K20 (Abcam, 1:1000) and anti-mouse LaminDm0 (Developmental Studies Hybridoma Bank,

1:1000).

**Real-time RT-PCR**

Real-time PCR quantification of TE expression was carried out with ABGene (Rockford, IL) SYBR green PCR master mix. PCR conditions for each primer pair were tested to determine the efficiency of amplification and to ensure amplification was in the linear range. PCR products for each primer pair were amplified from cDNA using the BioRad iQ5 Multicolor Real-Time PCR detection system (Primers listed in Table A1). cDNA was reverse transcribed from at least three different RNA samples. Ct values were normalized to the Ct values of the housekeeping gene *rp49*. Change in expression level was calculated using the ΔΔCt method based on the threshold cycle (Ct) value for each PCR reaction (BioRad real time PCR application guide). Results are presented as fold-change in mutant relative to wild-type. The statistical significance of the results was calculated using the Student's t-test.

## ***Results***

### Egg chamber formation is abnormal in *su(Hw)* mutants

Loss of Su(Hw) causes female sterility from incomplete oocyte development which then induces egg chamber degeneration at mid-oogenesis (BAXLEY *et al.* 2011; HARRISON *et al.* 1993; KLUG *et al.* 1968; KLUG *et al.* 1970). In addition to this, earlier observations identified a different phenotype found in $su(Hw)^{v}$ homozygous mutants and $su(Hw)^{e04061/2}$ trans-heterozygous mutants that has an increased number of nurse cells in a fraction of egg chambers. The increased number of nurse cells was detected only in egg chambers of certain *su(Hw)* mutants; therefore, this phenotype was disregarded and not considered as common (BAXLEY *et al.* 2011; HARRISON *et al.* 1993). To further examine the function of Su(Hw), we decided to perform a comprehensive analysis of the causes of female sterility in *su(Hw)* mutants including abnormal nurse cell number. We used the mutant alleles $su(Hw)^{e04061}$ and $su(Hw)^{v}$, the former containing an insertion of a piggyBac transposon in the 5' end of the second exon (BAXLEY *et al.* 2011) and the latter carrying a deletion of the *su(Hw)* promoter (HARRISON *et al.* 1992). Consistent with the previous findings, we also observed an abnormal number of nurse cells in mutant egg chambers from $su(Hw)^{e04061/e04061}$ homozygotes (Figure 2.1 D) and $su(Hw)^{e04061/v}$ trans-heterozygotes (Figure 2.1 A-C). As our observations also showed an increased number of nurse cells in mutant egg chambers, we decided to perform a quantitative analysis of the number of nurse cells within each individual egg chamber of $su(Hw)^{e04061/v}$ trans-heterozygous mutants using an antibody against

nuclear lamin to stain the nuclear periphery of nurse cells for cell counts. Mutant and wild-type stained ovaries were selected randomly, and egg chambers were analyzed using maximum projections of twenty Z-stack images that were collected with increments of 2 μm. Maximum projection images contain all the information required for reliable counts of nurse cells nucleus in each egg chamber. Results show that in addition to an increased number, a reduced number of nurse cells was also observed in *su(Hw)*$^{e04061/v}$ trans-heterozygous egg chambers. Overall, 7.48 % of the *su(Hw)*$^{e04061/v}$ mutant population of egg chambers had an irregular number of nurse cells, either with less or more than the fifteen cells normally found in egg chambers from wild-type ovaries. Approximately 2% of egg chambers had more than fifteen nurse cells (Figure 2.1 E). This phenotype may arise from defective development of follicle cells, leading to fused egg chambers (MATA *et al.* 2000), yet this might result from an additional mitotic division of cystoblasts in the early germarium. On the other hand, 5.61% of egg chambers had a reduced number of nurse cells. Fewer nurse cells in mutant egg chambers may indicate incomplete mitotic divisions during the germarium stage. Taken together, these observations suggest that an irregular number of nurse cells, whether greater or fewer, is a mutant phenotype generated upon loss of *su(Hw)* indicating that phenotypic defects of these mutants already manifest in the germarium at the early stages of oogenesis.

**Microtubules are misorganized in *su(Hw)* mutant egg chambers**

Another similar phenotype with abnormal nurse cell numbers in egg chambers was also observed in the mutants which have a loss of function in

piRNA related pathways, including *rihno*, *fmr1* and *maelstrom* (*mael*) mutants (EPSTEIN *et al.* 2009; SATO *et al.* 2011b; VOLPE *et al.* 2001). Maelstrom is a $\gamma$-tubulin associated protein involved in proper positioning of the microtubule organization center (MTOC), which is required to determine oocyte polarity and the precise localization of specific mRNAs within the *Drosophila* oocyte (CLEGG *et al.* 2001; CLEGG *et al.* 1997; SATO *et al.* 2011a; SATO *et al.* 2011b).

Microtubule organization is critical at various stages of oogenesis. In stage one, formation of the MTOC, a structure with concentrated $\alpha$-tubulin at the posterior of the oocytes, is required for oocyte differentiation. In stages three through six, a microtubule array is extended from the MTOC through ring canals to the neighboring nurse cells. This polarized network of microtubules is required for intercellular transport from nurse cells to the oocyte. During stage seven, the microtubule network is reorganized, causing a shift in the polarity of the MTOC from posterior to anterior, and the growing microtubule network pushes the oocyte nucleus to the anterior corner (STEINHAUER and KALDERON 2006; THEURKAUF *et al.* 1992). To address whether the irregular number of nurse cells in *su(Hw)* mutants correlated to microtubule disorganization, we used an $\alpha$-tubulin antibody to detect microtubule networks in the ovaries. We found that the wild-type MTOC forms properly, exhibiting a concentrated signal at the posterior of the oocyte in the germarium (Figure 2.2 A and A'); however, in *su(Hw)* mutants, the $\alpha$-tubulin signal is weaker and more diffused within the egg chamber and is not as highly concentrated at the MTOC as it is in wild-type (Figure 2.2 B

and B'). This phenotype was specific to *su(Hw)* mutants, as we did not observe the same phenotype in the *mod(mdg4)*$^{u1}$ mutant (Figure 2.2 C and C').

Next, to determine whether the disorganization of the MTOC is a phenotype caused by loss of Su(Hw), we asked whether the MTOC phenotype could be rescued by ectopic expression of *su(Hw)::eGFP* driven by the *nanos*-Gal4 driver. We have previously shown that *su(Hw)::eGFP* completely rescues insulator activity in *su(Hw)* mutants (SCHOBORG *et al.* 2013) and that the fertility of these mutants can also be partially rescued by introducing exogenous *su(Hw)::eGFP* expression under a *nanos*-Gal4 driver in germline cells (Hsu et. al submitted). The *nanos*-Gal4 driver directs the expression of Gal4 throughout all the stages of oogenesis (RORTH 1998; VAN DOREN *et al.* 1998). Expression of Su(Hw)::eGFP with this driver was confirmed using immunofluorescence staining with anti-GFP antibodies (Hsu et. al submitted). Here, our results show that expression of *su(Hw)::eGFP* driven by *nanos*-GAL4 also rescues the defective MTOC phenotype in the germarium of *su(Hw)* mutant ovarioles (Figure 2.2 D). All together, these data suggest that loss of Su(Hw) impairs proper formation of the MTOC and imply that this microtubule network is disorganized and may not efficiently function to facilitate egg chamber development.

**Gurken is mislocalized in the oocyte of *su(Hw)* mutant egg chambers**

We have shown that Su(Hw)::eGFP expression driven by *nanos*-Gal4 rescues the MTOC in egg chambers and restores fertility in mutant flies.

However, *nanos*-Gal4 driven Su(Hw)::eGFP rescued females laid a small number of eggs, and approximately 75% of the embryos produced by these females revealed a dorsal-ventral axis defect phenotype (Figure 2.3 A). We categorized these phenotypes as described in Ghabrial et al.: type I with two wild-type appendages, type II with two abnormal appendages, type III with a single appendage, and type IV with no appendages (GHABRIAL *et al.* 1998). The number of each type of embryo was quantified and shown in the stacked column graph (Figure 2.3 B). Type I embryos are viable and have no noticeable developmental defects through the adult stage. These results show that ectopically driven expression of Su(Hw) by *nanos*-Gal4 is not sufficient to completely rescue Su(Hw) function in mutant ovaries but partially recovers the fertility because rescued females laid a small number of viable eggs (41%) compared to wild-type (Hsu et al., submitted); besides, these data also reveal that Su(Hw) expression in germline cells is also required for specification of dorsal-ventral patterning during oogenesis.

Embryo dorsal-ventral patterning is determined by the key axis-determining mRNAs of *gurken* (*grk*), *oskar* (*osk*) and *bicoid* (*bcd*), which are transported along microtubules to specific locations in the oocytes (KUGLER and LASKO 2009). In order to understand whether defective microtubule organization in *su(Hw)* mutants affects axis determination, we used anti-Gurken antibodies to detect the localization of Gurken, a *Drosophila* transforming growth factor $\alpha$ (TGF $\alpha$) protein, which is important for dorsal-ventral determination of embryos

(NEUMAN-SILBERBERG and SCHUPBACH 1993). In wild-type egg chambers, *grk* mRNA requires transportation to the oocyte prior to subsequent translation. Gurken protein specifically localizes at the anterior of the oocyte during stage six (Figure 2.4 A and C) and later, as the oocyte relocates to the anterior-dorsal corner, Gurken gradually moves to the corner and forms a crescent shape around the oocyte nucleus at stage nine (Figure 2.4 B). Our data shows that in *su(Hw)* mutants, Gurken fails to translocate to the anterior-dorsal corner of the oocyte in 95% (N=20) of the egg chambers at stage nine (Figure 2.4 E). Likely, mislocalization of Gurken causes oocyte failure to signal follicle cells to determine dorsal fate, consequently interrupting the axis plan of the developing egg chamber. Summarizing, our data suggest that lack of Su(Hw) expression causes defective formation of the microtubule network in developing egg chambers, thereby impeding Gurken localization which causes specification failure of dorsal-ventral patterning in embryos.

**Loss of *su(Hw)* activates DNA damage checkpoints during oogenesis**

Disorganized microtubules, mislocalized Gurken and disrupted axis specification in eggs are phenotypes frequently observed in mutants of *spindle* class genes and piRNA pathway related genes, such as *spnE, armi and maelstrom* (KLATTENHOFF *et al.* 2007; SATO *et al.* 2011b). In these mutants, cells lose the ability to repair DNA damage or repress retrotransposon activity, generating an excess of DSBs to the point unrepaired DSBs accumulate and turn

on the ATR/Chk2 dependent DNA-damage signaling pathway in the female germline (KHURANA and THEURKAUF 2010).

As *su(Hw)* mutants have a similar phenotype to spindle class and piRNA mutants, we suspected developmental failure of female germline in *su(Hw)* mutant flies is caused by activation of the DNA damage checkpoints. We first asked whether the DNA-damage signaling pathway is activated, preventing further development of *su(Hw)* mutant egg chambers. To address this question, we examined the possible restoration of both oocyte development and female fertility using *su(Hw)* and *mei-41*$^{D5}$ (*Drosophila ATR)* double mutant flies (BRODSKY *et al.* 2004). Results showed that although double mutant females remained sterile, they contained more stage nine egg chambers with correct positioning of Gurken around the oocyte nucleus (54% recovery, N=24) (Figure 2.5 A-C) and had proper enlargement of the developing oocyte at stage nine and ten (Figure 2.5 B and D). These results show that loss of ATR partially recovers oocyte development in the *su(Hw)* mutant and suggest that loss of Su(Hw) function triggers a DNA-damage response, possibly through the ATR-dependent pathway.

To understand whether loss of Su(Hw) activates the ATR/Chk2 mediated DNA-damage pathway in the same manner as mutants related to the piRNA pathway, we generated a double mutant with *su(Hw)* and *chk2* (*mnk*$^{6006}$ allele) (BRODSKY *et al.* 2004) mutations, as Chk2 is a downstream kinase of ATR. We

tested whether a *chk2* mutation is able to rescue the female sterile phenotype in the *su(Hw)* mutant. The results showed neither the fertility nor the Gurken localization was recovered in the double mutants (Figure A7). These results suggest that spindle phenotypes caused by loss of Su(Hw) may be Chk2 independent and that there may be a Chk2 alternative pathway downstream of the ATR mediated DNA damage signaling pathway involved in the generation of this phenotype.

**Massive non-meiotic DSBs occur during oogenesis in *su(Hw)* mutants**

Our results suggest that DSBs activate DNA damage signaling pathways in *su(Hw)* mutants, resulting in MTOC disorganization and Gurken mislocalization. In order to further investigate whether DSBs in these mutants activate the ATR-mediated DNA damage pathway, we performed immunostaining in ovaries using specific antibodies against phosphorylated histone 2Av variant (γH2Av) as a marker for detection of DSBs. In the wild-type, DSBs were observed in dividing cystocytes, which later become nurse cells and pro-oocytes in region two of the germarium where homologous recombination takes place (Figure 2.6 A and B). These meiotic DSBs are produced by Spo11, an exonuclease encoded by the *mei-w68* gene, and the DNA breaks in the oocyte are repaired before developing egg chambers reach stage one (JANG *et al.* 2003; MCKIM and HAYASHI-HAGIHARA 1998; MEHROTRA and MCKIM 2006). In order to eliminate the background of meiotic DSBs, we generated *su(Hw)* and *mei-68* double mutant flies, and then detected non-meiotic DSBs with a γH2Av

antibody in ovaries. We found an excess of non-meiotic double strand breaks in nurse cells of this double mutant beginning at the germarium stage (Figure 2.6 C, D and E) and continuing until later egg chamber stages (Figure 2.6 F and G). This result strongly indicates that loss of Su(Hw) activity leads to formation of non-meiotic DSBs in the female germline cells.

**Su(Hw) does not play a major role in regulating global transposable element activity in the *Drosophila* germline**

It is well known that Su(Hw) strongly regulates transcription of the *gypsy* retrotransposon, and loss of the insulator activity reverses the phenotype of *gypsy* induced mutations at several different loci in *Drosophila* (HARRISON *et al.* 1993; PARKHURST and CORCES 1985; PARKHURST and CORCES 1986; PARKHURST *et al.* 1988). Our data, showing a dramatic accumulation of meiotic-independent DSBs in female germline cells of *su(Hw)* mutants, led us to ask in addition to *gypsy* whether other transposable elements (TEs) are overexpressed in the *su(Hw)* mutant, creating an excess of DSBs in the genome and activating the DNA damage checkpoints during oogenesis.

TEs are divided into two classes depending on the molecular structures and mobilization mechanisms. Class I elements are retrotransposons, which transpose through integration of the copied DNA from RNA intermediates produced by reverse transcription; and class II elements are DNA transposons that utilize the DNA excision mechanism to transfer the elements into a new

position in the genome (SLOTKIN and MARTIENSSEN 2007). To measure the activity of TEs, we performed real-time RT-PCR to quantify the transcripts of TEs produced in wild-type and *su(Hw)*$^{e04061}$ homozygous mutant ovaries. In both genotypes, egg chambers later than stage nine were manually removed to eliminate sources of potential interference during different developmental stages, such as a global misregulation of TEs caused by oogenesis defects but not Su(Hw) specific regulation. Ovarian total RNA from both genotypes was also extracted for real-time RT-PCR using specific primer sets for fifteen different TEs and *rp49* as an internal control. Our selection included germline and somatic specific transposons, and it also covered the TEs with long-terminal repeats (LTR) and non-LTR.

The expression patterns of fifteen transposons in the mutant were compared to the wild-type shown in a fold-change graph (Figure A8). Our data show consistent with previous studies that *gypsy* transcript levels are significantly reduced in *su(Hw)* mutants; however, different patterns of expression change were observed in other TEs. Besides *gypsy*, expression of four other TEs, Stalker, Copia, Jockey and I-element, have statistically significant changes in *su(Hw)* mutants (Figure 2.7). Loss of Su(Hw) had a slight effect on expression change of TEs, which is independent of tissue specificity and LTRs; therefore, Su(Hw) may not directly be involved in suppression of transposon activity during female germline development. This data suggests the cause of excess DSBs in mutants may correlate with other unknown factors.

**Abundant monomethylation of H4K20 accumulates in *su(Hw)* mutant ovaries**

We have shown that loss of Su(Hw) causes a dramatic accumulation of DSBs in nurse cells and that these DSBs are not induced by transposable element activity, suggesting Su(Hw) plays an important role in maintaining genome stability in germline cells in a TE independent manner. On the other hand, mounting evidence suggests that monomethylation of histone 4 lysine 20 (H4K20me1), mediated by the PR-Set7/ SET8 methyltransferase, has an important role in maintaining genome stability (BECK *et al.* 2012; JORGENSEN *et al.* 2013; WU and RICE 2011). For example, in mammalian cells, removal of *pr-set7* results in DNA damage and S-phase arrest; conversely, constant expression of PR-Set7 causes accumulation of H4K20me1 at replication origins and results in re-replication (JORGENSEN *et al.* 2007; TARDAT *et al.* 2010). Additionally, highly proliferating tissues in *Drosophila*, such as wing discs and salivary glands, are smaller in size and contain fewer cells in *pr-set7* mutants due to improper cell division during development. Finally, in *Drosophila* S2 cells, depletion of *pr-set7* affects chromosome compaction in higher-order chromatin organization and triggers the DNA damage response (KARACHENTSEV *et al.* 2007; KARACHENTSEV *et al.* 2005; SAKAGUCHI *et al.* 2012; SAKAGUCHI and STEWARD 2007). Together, this evidence suggests that misregulation of *pr-set7* and H4K20me1 affect genome stability and cell cycle progression.

To test whether Su(Hw) and H4K20me1 function in the same pathway that leads to DSBs and activation of DNA damage responses in *su(Hw)* mutants, we performed western blotting in ovaries of wild-type and mutants using a H4K20me1 antibody. Our results show that the amount of H4K20me1 significantly increased in *su(Hw)* mutant ovaries (Figure 2.8), revealing that lack of Su(Hw) may relate to abnormal chromosome packing and chromatin organization in a global manner. Moreover, elevated amounts of H4K20me1 may indicate inappropriate re-replication occurs, causing DSBs, disrupting genome stability, and eventually leading to oogenesis failure.

## ***Discussion***

### Activation of the DNA damage signaling pathway results in female germline developmental defects in *su(Hw)* mutants

This study has revealed a new role of Su(Hw) in regulating *Drosophila* female germline development through maintenance of genome integrity. We have shown that loss of Su(Hw) results in massive DSBs in germline cells and turns on the ATR mediated DNA damage signaling pathway leading to cessation of oocyte development at mid-oogenesis (Figure 2.9).

Cytoskeleton disorganization, morphogen mislocalization and irregular numbers of nurse cells were found in *su(Hw)* mutant egg chambers. These phenotypes are usually observed in DNA repair mutants or piRNA pathway mutants (GONZALEZ-REYES *et al.* 1997; KLATTENHOFF *et al.* 2007; MORRIS and LEHMANN 1999). Our results show that mutations of the checkpoint gate keeper, *ATR/ mei-41*, partially rescued oogenesis in *su(Hw)* mutants; whereas, *Chk2/mnk* mutation did not. This result implies that the ATR/Chk2 DNA damage pathway may not be the only activated signaling pathway in response to DSBs resulting from loss of Su(Hw). It is known that both ATR and telangiectasia-mutated (ATM) kinases are involved in DNA damage and DNA repair responses. Both kinases are able to phosphorylate H2Av in response to DSBs, and the cross talk between these two pathways function in meiotic checkpoints in both mammals and flies (JOYCE *et al.* 2011; SANCAR *et al.* 2004). Although the detailed mechanism of how ATR and ATM coordinate and perform the function during in *Drosophila*

oogenesis still remains unclear, we cannot rule out the possibility that ATM is responsible for the DNA damage response triggered by DSBs upon loss of Su(Hw).

**Abnormal endoreplication may be the cause of excessive DSBs in nurse cells of *su(Hw)* mutants**

The recognition of γH2Av has become a standard assay for DSB detection. Up to date, the known intrinsic causes of DSBs in female germline development are meiotic recombination, retrotransposon mobilization and endoreplication (HONG *et al.* 2007; KLATTENHOFF *et al.* 2007; LAKE *et al.* 2013; LILLY and SPRADLING 1996; MEHROTRA *et al.* 2008). We have proven the accumulation of DSBs in *su(Hw)* mutant results from neither meiotic recombination (Figure 2.6) nor retrotransposon mobilization (Figure 2.7); hence, we speculate that excessive DSBs in *su(Hw)* mutants may result from abnormal endoreplication in nurse cells.

In *Drosophila* ovaries, endoreplication is a specialized event that produces polyploid nurse cells that supply nutrients for oocyte development, and it takes place within a limited time during oogenesis, passing only through Gap (G) and DNA synthesis (S) phases but not the mitosis (M) phase. During endoreplication, the euchromatin regions are first duplicated. Afterwards, some heterochromatic sequences are duplicated during late S phase, possibly losing the opportunity for replication in each endoreplication cycle, and this loss of replication is called

underreplication. The damaged DNA has been found locate at the junction between replicated euchromatin and underreplicated heterochromatin regions (HAMMOND and LAIRD 1985; LILLY and SPRADLING 1996). During replication, Su(Hw) has the ability to function as a boundary that prevents heterochromatin from spreading into replicating sequences and ensures successful DNA replication (LU and TOWER 1997). In addition, Su(Hw) is capable of altering chromatin accessibility by recruiting histone acetyltransferase and the chromatin remodeling complexes, thereby creating a platform for replication firing (LU and TOWER 1997; VOROBYEVA *et al.* 2013). In our study, both massive DSB accumulation and significantly increased H4K20me1 in the *su(Hw)* mutant suggest DSBs may correlate with abnormal endoreplication in nurse cells because of unbalanced replication between heterochromatin and euchromatin regions upon loss of Su(Hw). Considering, we propose Su(Hw) may be involved in maintaining genome stability by properly organizing chromatin during DNA replication amid female germline development.

Abnormal DNA damage and unrepaired DNA lesions also cause genome instability (CHAPMAN *et al.* 2012). We still cannot rule out the possibility that loss of Su(Hw) may slow down DNA repair through an unclear mechanism resulting in DSB accumulation. One way to correct the DSBs is homologous recombination (HR) repair, and Su(Hw) influences the DSB repair frequency in germline cells by altering chromatin conformation. Lankenau et al., suggested that chromatin bound Su(Hw) tightens the chromatin conformation; whereas, loss of Su(Hw)

reduces the conformational constraints of chromatin fibers and enhances recombinational repair frequency. The repair frequency is enhanced due to a gain of mobility of the 3'-hydroxy breakage end while it searches for homology (LANKENAU *et al.* 2000). On the other hand, in somatic cells, Su(Hw) functions to promote DNA pairing during embryogenesis (BOSCO 2012; FRITSCH *et al.* 2006). Altogether, these observations imply that Su(Hw) may influence homologous pairing by directing higher-order chromatin organization in a tissue specific manner, but the detailed mechanism requires resolution. Whether the accumulation of γH2Av foci in the *su(Hw)* mutant is derived from the change of repair frequency through chromatin organization remains unknown. Our study opens an exciting new avenue to understand the function of chromatin insulator proteins in DNA replication and DNA repair through alteration of chromatin structure in eukaryotic cells.

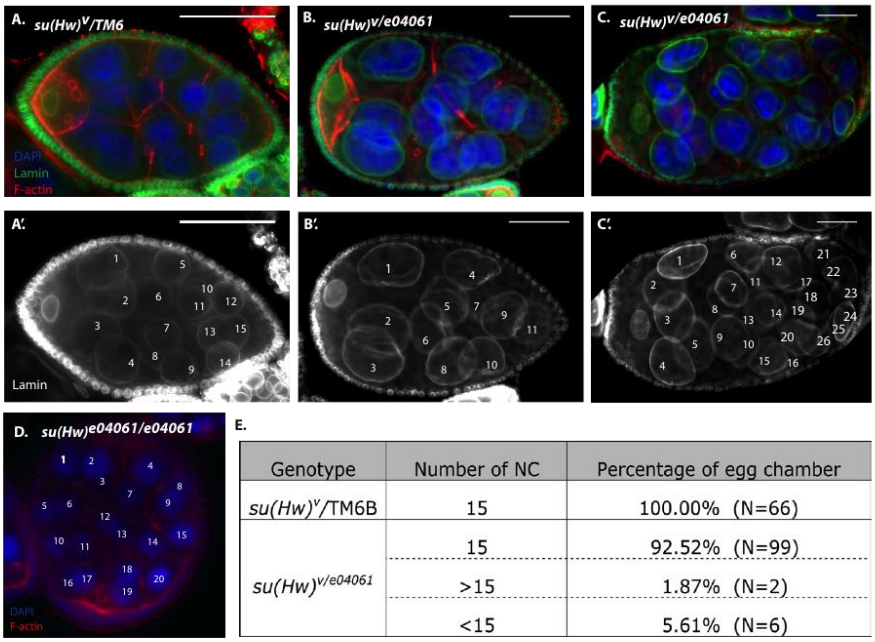


E.

| Genotype | Number of NC | Percentage of egg chamber |
|---|---|---|
| *su(Hw)*$^{v}$/TM6B | 15 | 100.00% (N=66) |
| *su(Hw)*$^{v/e04061}$ | 15 | 92.52% (N=99) |
| | >15 | 1.87% (N=2) |
| | <15 | 5.61% (N=6) |

**Figure 2.1. An abnormal number of nurse cells in egg chambers of *su(Hw)* mutants.**

Wild-type and mutant egg chambers were stained with Lamin antibody in green and phalloidin in red. A-A': fifteen nurse cells in one wild-type egg chamber. B-B': an example of *su(Hw)*$^{v/e04061}$ egg chamber with less than fifteen nurse cells. C-C': a *su(Hw)*$^{v/e04061}$ mutant egg chamber with more than fifteen nurse cells. D: more than fifteen nurse cells in a *su(Hw)*$^{e04061/e04061}$ egg chamber. E. In total, 66 *su(Hw)* $^{v}$*/TM6* and 107 *su(Hw)* $^{e04061/v}$ individual egg chambers were observed and percentages of egg chamber with equal, more and less than fifteen cells were shown in the table.

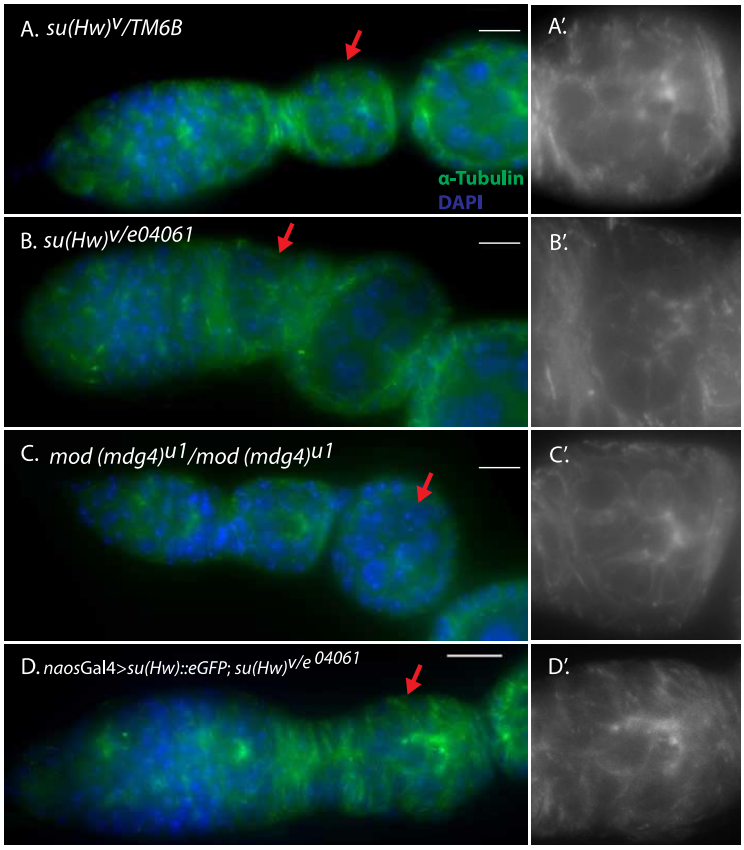


**Figure 2.2. The impaired MTOC formation in *su(Hw)* mutants.**

The microtubule is labeled with α-tubulin antibody in green. A-D: The different genotype egg chambers at the germarium stage were shown and stage one egg chambers (red arrows) were magnified. A'-D': Magnified stage one egg chambers showed a bright and condensed MTOC at the anterior in both wild-type (A') and *mod(mdg4)*$^{u1}$ mutants (C'), but not in the *su(Hw)* mutant (B). The expression of germline Su(Hw)::eGFP rescued the MTOC organization (D). Scale bars are 10 μm.

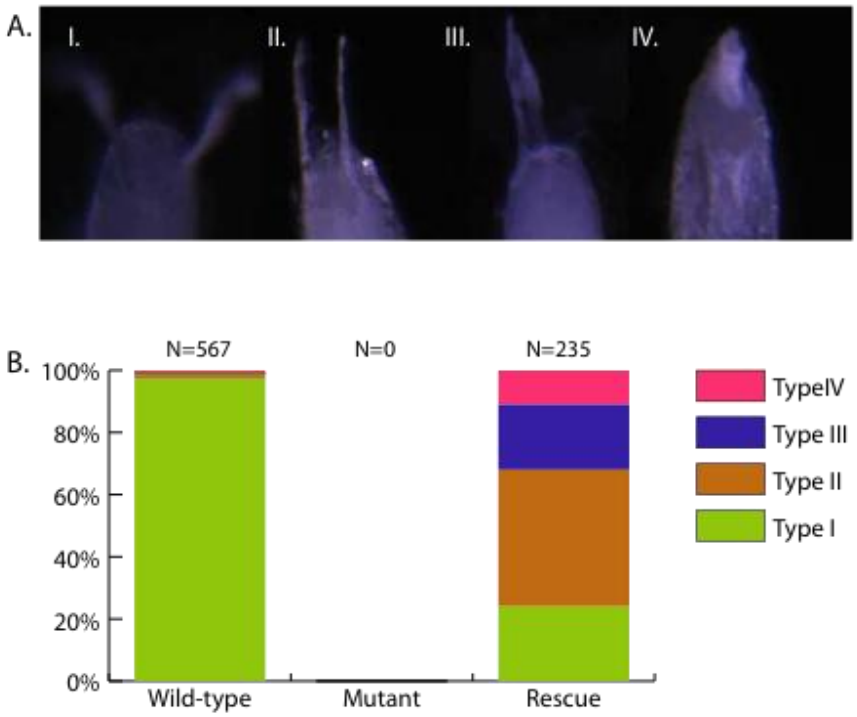


**Figure 2.3. Expression of Su(Hw) in germline cells rescues female fertility but only partially rescues embryo development.**

The same number of virgin female flies of the wild-type and rescued flies (only rescued flies expressing Nanos-Gal4 driven Su(Hw)::eGFP) were crossed with wild-type male flies for three days and eggs were collected. Different dorsal-ventral phenotypes of embryos were categorized as I to IV (A) and the percentage of each type of embryos was counted as shown in the stacked column graph (B). Wild-type female flies produced 97% type I, 2% type II and 1% type IV embryos; however, rescued flies produced only 24% type I (two normal appendages), 44% type II (two abnormal appendages), 21% type III (one appendage), and 11% type IV (no appendage). Sterile *su(Hw)* mutant females were used as a negative control.

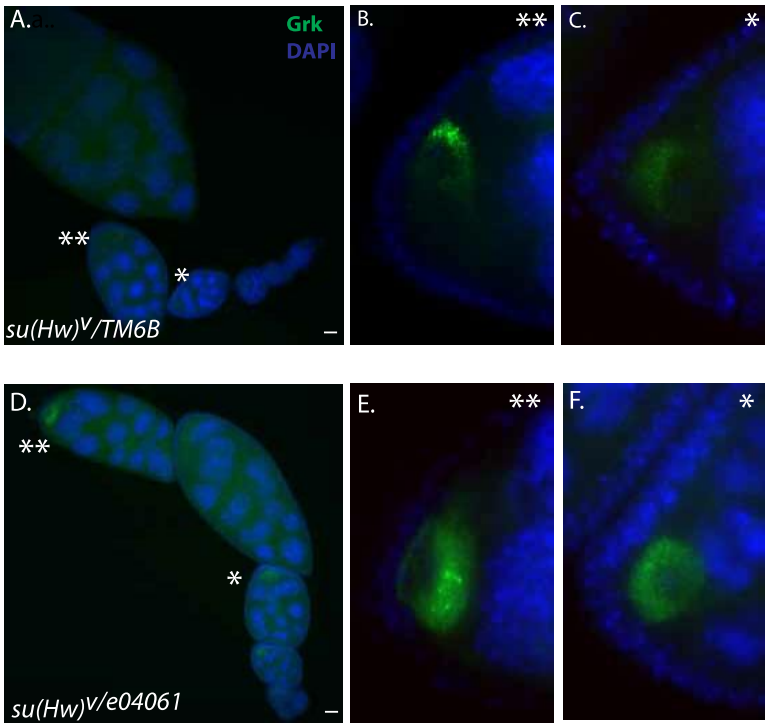


**Figure 2.4. Mislocated Gurken protein in *su(Hw)* mutant egg chambers.**

The Grk protein was labeled in green and its location was monitored at stage six (*) and nine (**). A-C: In wild-type, Grk locates at the posterior of oocyte at stage six (C) and translocates to the dorsal-anterior corner at stage nine (B). D-F: Instead of locating at dorsal-anterior corner, Grk mislocates to the anterior of oocyte at stage nine in the *su(Hw)* mutant.

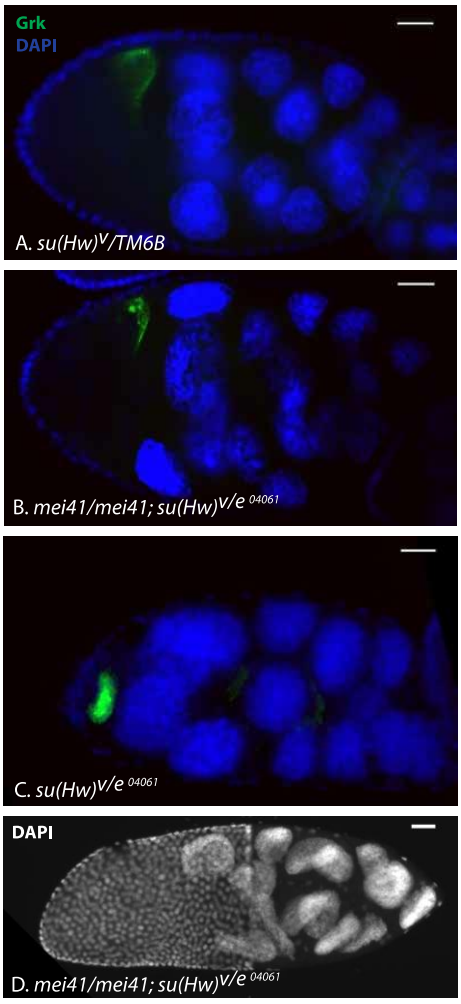


**Figure 2.5. Oogenesis progresses further in the *su(Hw)* mutant while ATR is mutated.**

A-C: Grk was labeled in green and the signal was detected in different genotype egg chambers at stage nine. D. The stage ten egg chamber was detected in *mei-41* and the *su(Hw)* double mutant with DAPI staining. The scale bar is equivalent to 20 μM.

**Figure 2.6. The accumulation of non-meiotic DNA double strand breaks in *su(Hw)* mutants.**

The DSB foci were also visualized using immunoflorescence staining with γH2Av antibody in red at the early germarium and later stage egg chambers. Orb was used as a marker to locate the oocyte. A. In wild-type, the DSBs were detected in region 2 of germarium (A') and a few foci in nurse cells at stage one (A''). B. Accumulated DSB foci were observed in the mutant germarium (B') and the cropped stage one egg chamber was shown in B''. C-C'' and E-E'': *mei-w68* mutant showed the clearance of DSBs in region 2 but DSBs in nurse cells at stage one were still observed. D-D'': Strong DSB foci accumulated in the nurse cells at stage one. The scale bar is 10 μm in A-E and 5 μm in A''-E''. F-G: The DSB foci were detected throughout the oogenesis, and the γH2Av signal was relatively stronger in *su(Hw)* mutants (G'') compared to wild-type (F'').

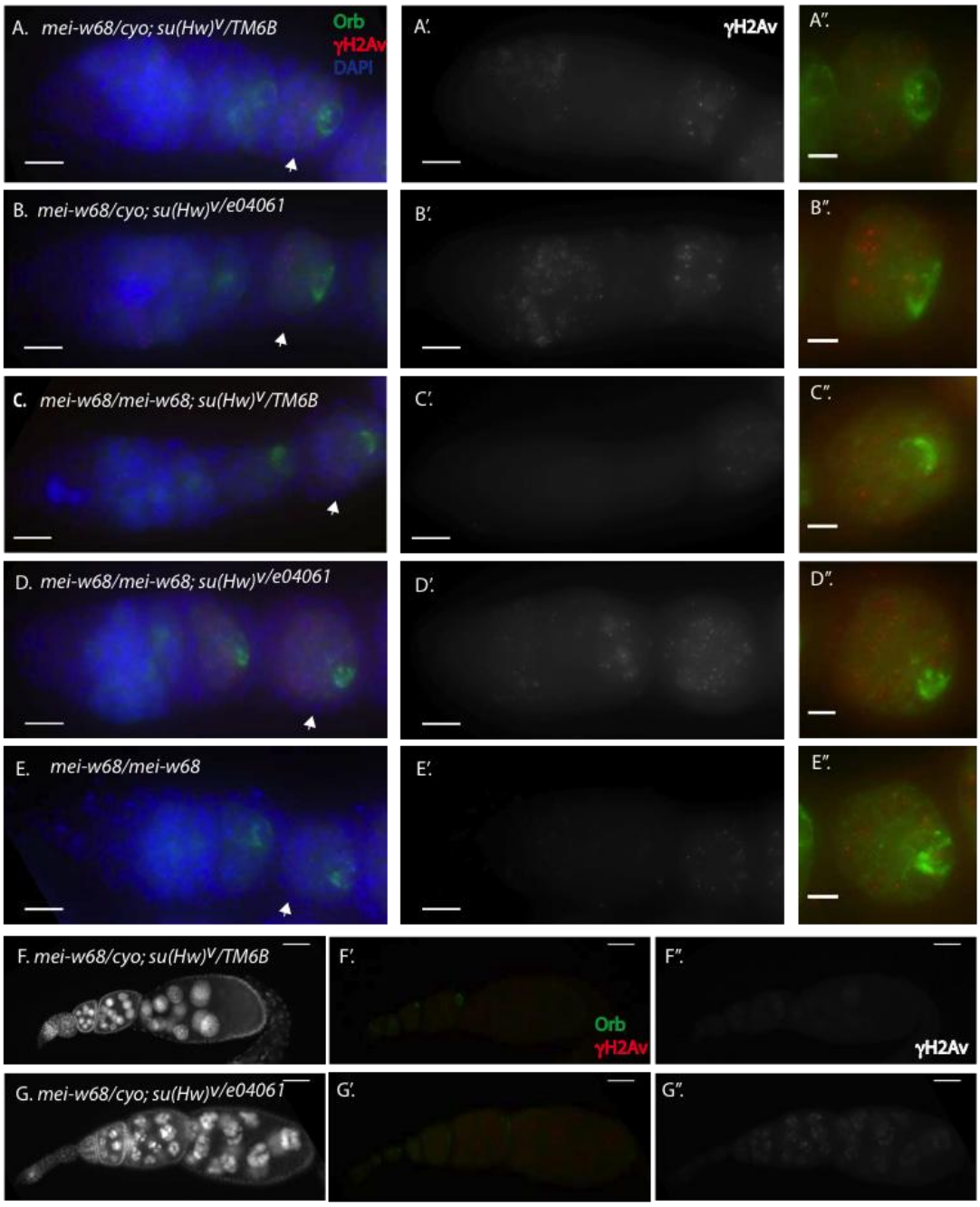
A. mei-w68/cyo; su(Hw)V/TM6B
Orb
γH2Av
DAPI
A′.
γH2Av
A″.
B. mei-w68/cyo; su(Hw)V/e04061
B′.
B″.
C. mei-w68/mei-w68; su(Hw)V/TM6B
C′.
C″.
D. mei-w68/mei-w68; su(Hw)V/e04061
D′.
D″.
E. mei-w68/mei-w68
E′.
E″.
F. mei-w68/cyo; su(Hw)V/TM6B
F′.
Orb
γH2Av
F″.
γH2Av
G. mei-w68/cyo; su(Hw)V/e04061
G′.
G″.

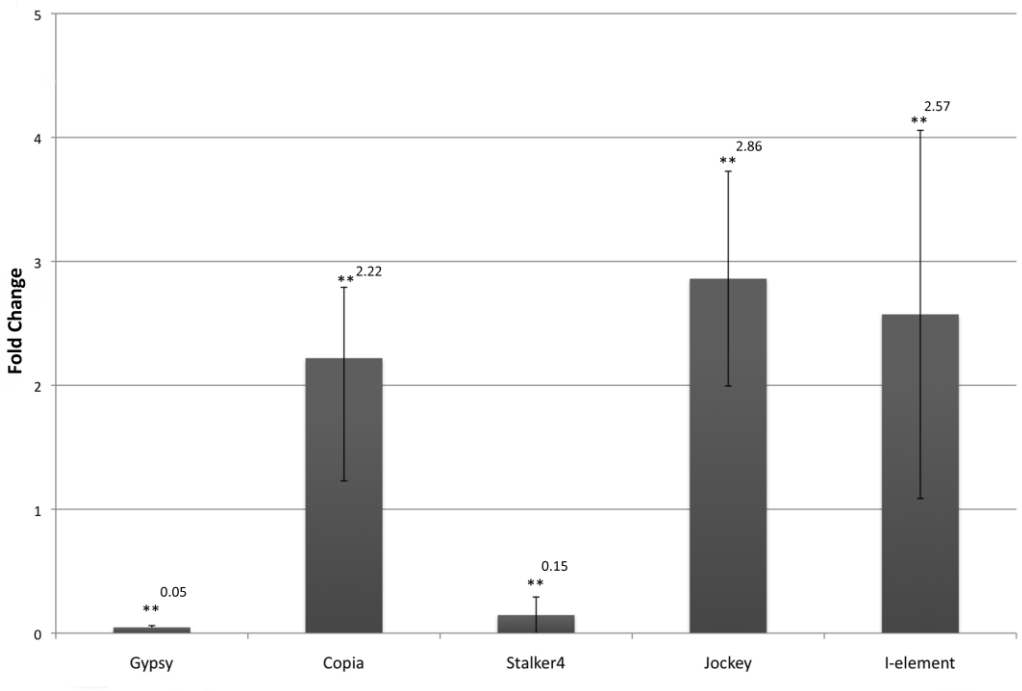


**Figure 2.7. No major expression changes of transposable elements in the *su(Hw)* mutant.**

Transcript levels of TEs were quantified by real-time PCR and were normalized to rp49. Fold change values represent the relative expression of mRNA in ovaries from su(Hw)$^{e04061}$ homozygotes compared with ovaries from su(Hw)$^{e04061}$ heterozygotes. The late egg chambers of each sample are removed. Two asterisks indicate $P < 0.001$.

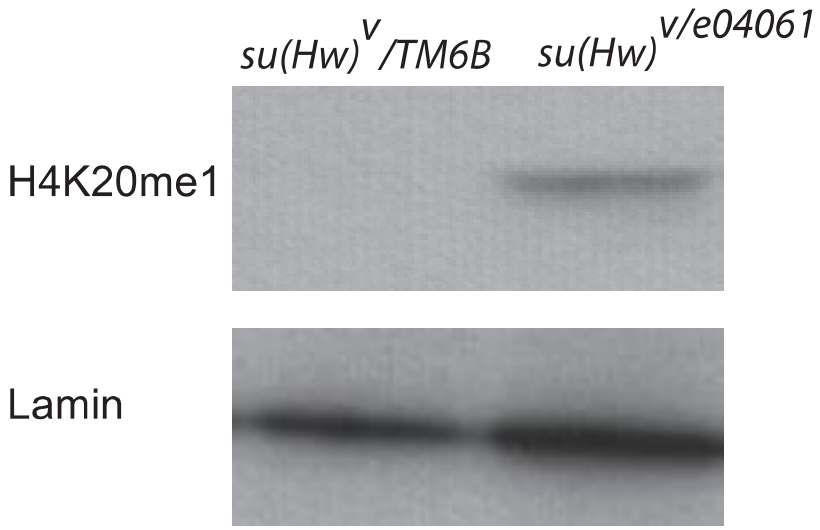


**Figure 2.8. Dramatically increased H4K20me1 in *su(Hw)* mutants.**

Western blot analysis of H4K20me1 in wild-type and *su(Hw)* mutant ovary extracts. Using Lamin as the loading control, significantly increased H4K20me1 was detected in mutants compared to wild-type.

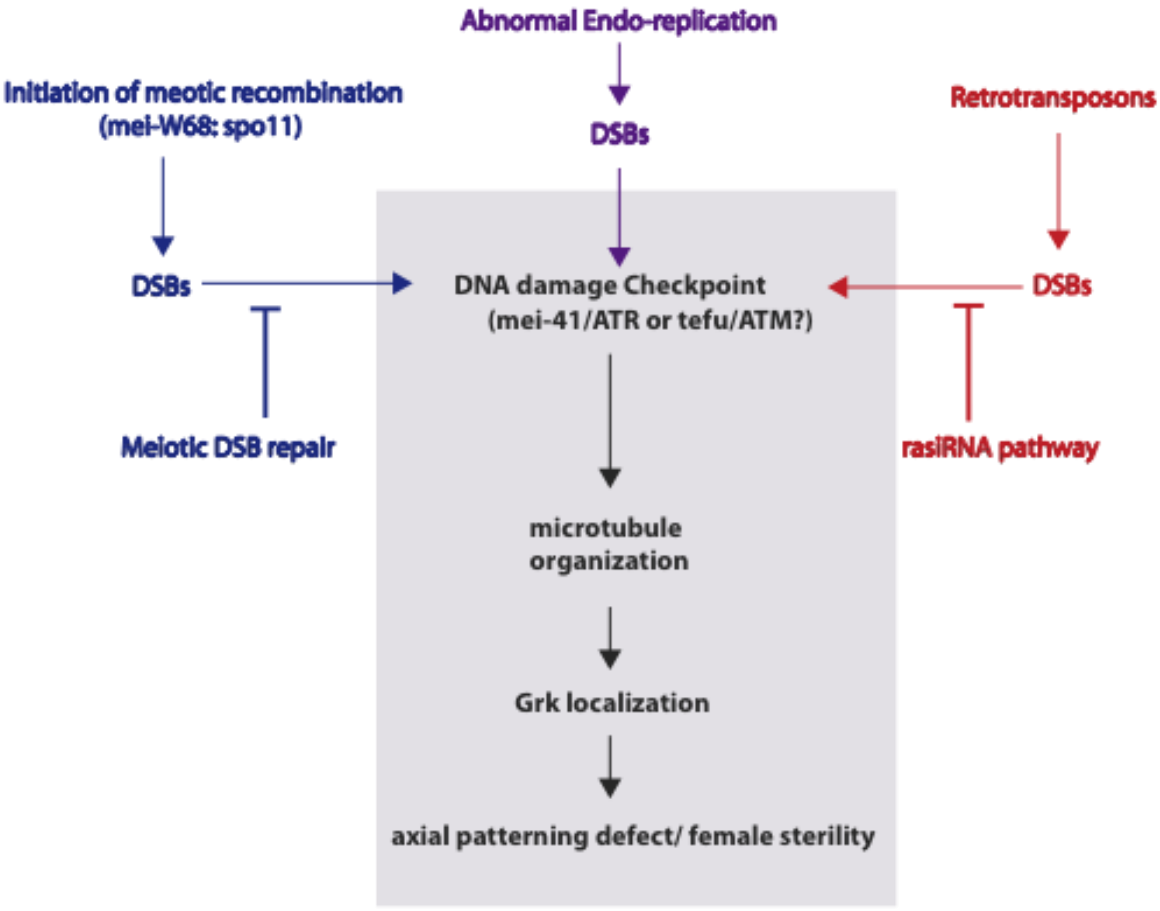


**Figure 2.9. Summary**

# CHAPTER III.

# Functional regulation of Su(Hw) in cells.

## ***Abstract***

During *Drosophila* oogenesis, cystocytes undergo mitotic cell division with incomplete cytokinesis, producing a specialized ring canal structure. The ring canal is a remaining structure from incomplete closure of a contractile ring; however, a similar structure in normal mitosis, called the midbody, functions as a transient intercellular bridge that facilitates transportation of vesicles and mitotic regulators. Upon completion of mitosis, this ring closes, causing the dissociation of two daughter cells from each other which completes cytokinesis. Immunoflorescence staining in S2 cells made a novel discovery that Su(Hw) locates at the midbody from telophase through cytokinesis. Other insulator proteins, Mod(mdg4)-67.2 and BEAF, co-localize with Su(Hw) at the midbody but CP190 does not. Investigations discovered that SUMO co-localized with insulator proteins during mitosis at several different subcellular locations, including the midbody, centrosomes, and insulator bodies as well as on chromatin. Yeast-two hybrid and immunoprecipitation data revealed that the interaction between Su(Hw) and SUMO may be facilitated through other proteins that participate in this complex. To understand how Su(Hw) is regulated by post-translational modifications, different forms of Su(Hw) containing mutations at the SUMO interacting domains, the SUMOylation sites, or the phosphorylation sites were generated and expressed in cells. Surprisingly, we found the protein stability of Su(Hw) is affected by different modifications. Altogether, our model proposes that both phosphorylation and SUMOylation may play an important role in regulating the proteolysis and subcellular localization of Su(Hw). Further study is needed to determine the detailed mechanism of regulation.

## ***Introduction***

During mitosis, two daughter cells obtain equal genomic material following chromosome segregation. The final step of mitosis, cytokinesis, is an essential process that ensures proper formation of the two duplicated cells. Inbetween the two dividing cells, anti-parallel bundles of microtubules form during anaphase and are called the midzone or central spindles. Later during telophase, the midzone compresses as the plasma membrane contracts to form the cleavage furrow which leaves the two daughter cells connected with an intracellular bridge that facilitates transportation of vesicles and mitotic regulators. The midbody (MB) is an organelle located within this bridge and contains a dense organization of microtubule interacting proteins derived from the midzone. The MB, also called Flemming body, was first described by Walther Flemming in 1891. For the past few decades, the MB has been known to serve as a platform for abscission. Through proteomic analysis, numerous proteins that are involved in different regulation pathways and that contribute to abscission were indentified in the MB (SKOP *et al.* 2004). The known pathways that regulate the abscission mechanism include vesicle trafficking, microtubule organization, membrane scission and ubiquitination. Following cytokinetic abscission, the two daughter cells separate completely and the post-mitotic MB either remains in one of the daughter cells or is released from both cells. The released MBs either undergo degradation or are taken up by other cells (CHEN *et al.* 2013; EGGERT *et al.* 2006; HU *et al.* 2012). Normal dividing mitotic cells and differentiating cells derived from the asymmetric cell division of stem cells have a unique feature of either releasing their MBs or have increased autophagic activity to degrade retained MBs; however, cancer stem cells and normal stem cells accumulate a high level of MBs (ETTINGER *et al.* 2011; KUO *et al.* 2011; SCHINK and

STENMARK 2011). These discoveries indicate that the MB plays an important role in determining cell fate. Beyond its cytokinetic function, MBs have a non-cytokinetic role in regulating polarity specification in chicken spinal cords, fly neurons and follicle cells within fly ovaries (MORAIS-DE-SA and SUNKEL 2013; POLLAROLO *et al.* 2011; WILCOCK *et al.* 2007). Although the MB was discovered a century ago, its precise function is still poorly understood.

Proteomic analysis and immunofluorescence staining have identified the mammalian chromatin insulator CTCF as a midbody protein. CTCF functions as a nuclear protein during interphase but has a different distribution during cell division. From metaphase to anaphase, CTCF translocates from the nucleus to the centrosome. Later, CTCF moves to the MB during telophase and returns to the nucleus while mitosis ends (SKOP *et al.* 2004; ZHANG *et al.* 2004). It is still unclear how the specific time and location of CTCF affect the cell cycle progression. In *Drosophila*, CP190 was first identified as a centrosomal microtubule associated protein (OEGEMA *et al.* 1995) and the CP190 association with the centrosome and microtubules is important for early embryogenesis. Although CP190 is required for viability in flies, it plays no role in mitosis in cultured S2 cells (CHODAGAM *et al.* 2005; PAI *et al.* 2004). Another insulator protein BEAF has been shown to play a role in regulating chromosome organization during the cell cycle. BEAF binding sites are strongly associated with cell cycle and chromosome segregation related genes, and depletion of BEAF causes chromosome segregation defects, an increased population of 4N cells, and eventually causes cell growth arrest (EMBERLY *et al.* 2008a). Though there has been progress in describing the

roles of CTCF, CP190 and BEAF within the cell cycle, the role of Su(Hw) within the cell cycle has not been described as of yet.

Su(Hw) locates on polytene chromosomes and in insulator bodies (SCHOBORG *et al.* 2013; SPANA *et al.* 1988), and our investigations found that Su(Hw) locates at the midbody as well. Our discovery encouraged us to investigate the regulation of Su(Hw) subcellular localization. Post-translational modifications (PTM) play important roles in regulating protein properties and functions. One of the PTMs, SUMOylation (small ubiqitin-related modifier modification), has been linked to alteration of protein-protein interactions and protein subcellular localization, both of which affect protein function. SUMOylation is a process of serial enzyme reactions that attach SUMO to its substrates. Initially, SUMO is synthesized as an inactive precursor and becomes mature once cleaved by a SUMO-specific isopeptidase (called ULP1 in invertebrates and SENPs in mammals) that exposes diglycines at the C-terminus. After SUMO activating E1 enzymes recognize the exposed diglycines of SUMO, SUMO subsequently transfers to the SUMO-conjugating E2 enzyme. Finally, E3 ligase conjugates SUMO to the lysine residues of the substrates by forming a covalent isopeptide bond. SUMO substrates often have lysine residues in the classic consensus SUMOylation sites (**ψ-**K-X-D/E, **ψ** is a large hydrophobic residue) or non-consensus sites. In addition to the covalent bond, SUMO also interacts with target proteins through non-covalent binding at its SUMO interacting motif (SIM), a short sequence with hydrophobic residues (V/I-X-V/I-V/I or inverted). The SUMO-SIM interaction behaves as a protein glue that not only enhances the intermolecular interaction of the proteins in the complex, but also modifies intramolecular interactions

within an individual protein (GAREAU and LIMA 2010). This feature reinforces the finding that the SUMOylation enzyme often targets a group of proteins that are functionally or physically linked to the same biological pathway or location within cells.

Recent studies have suggested that substrates of SUMO are mostly nuclear proteins. Through nuclear protein modification, SUMO can alter chromatin structure during multiple cellular events including transcription, replication and DNA repair. For example, mammalian CTCF is a substrate of SUMO, and SUMOylation of CTCF facilitates the regulation of chromatin structure alteration (KITCHEN and SCHOENHERR 2010; MACPHERSON *et al.* 2009a). Both *Drosophila* Mod(mdg4)-67.2 and CP190 are substrates of SUMO (CAPELSON and CORCES 2006); however, a direct relationship between SUMO and Su(Hw) has not been characterized as of yet. SUMO conjugation of Mod(mdg4)-67.2 is prerequisite for integration of SUMO conjugated Mod(mdg4)-67.2 and Su(Hw) into insulator bodies, but integration is not required for insulator function (GOLOVNIN *et al.* 2012).

To understand whether SUMO participates in regulating the interacting partners of Su(Hw) and consequently its function as it shuffles between the chromatin, insulator bodies, and midbody, we used cellular and molecular techniques to verify the location of Su(Hw), SUMO and other insulator proteins at the midbody of S2 cells. In addition, biochemistry and yeast genetics methods were applied for characterizing the interaction between Su(Hw) and SUMO.

## ***Materials and methods***

### Site-directed mutagenesis

The mutations of *SUMO, su(Hw), and mod(mdg4)-67.2* were generated with PCR-based site directed mutagenesis (WANG and WILKINSON 2000). Specific primers containing point mutations or deletion sites were designed and used in PCR reactions with a wild-type gene plasmid as the template. The PCR mixture was treated with DpnI to remove the template plasmid and the reaction mixture was transformed into DH5$\alpha$ competent cells. The plasmids were purified from the transformants and sequenced. All primer sequences are listed in Table A.1.

### Cell culture and transfection

*Drosophila* Schneider line 2 cells (S2 cells) were grown in HyQ SFX-insect medium (HyClone) with penicillin-streptomycin antibiotics at 25$^{o}$C without $CO_2$. Cells were plated in each well of a six-well plate and expression vectors were transfected using lipofectin reagent (Invitrogen Life Technologies). Cells used in immunoprecipitation assays were transfected with pPAC-FLAG-SUMO, pPAC-FLAG-SUMO$^{GG}$ or pPAC-FLAG-SUMO$^{dGG}$ gifts from Dr. Albert Courey (University of California, Los Angeles). The stable lines with Su(Hw) mutations were generated by transfection with different mutated Su(Hw)::eGFP constructs and selected with hygromycin (300 μg/ml, Invitrogen) for three weeks. The expression of Su(Hw)::eGFP mutants were induced by copper sulfate (500 μM, Sigma) in the culture medium for 24 hours prior to the subsequent assay.

**Treatment of dsRNA and cell growth curve measurement**

The DNA template for double stranded RNA (dsRNA) was generated using PCR with a pair of primers containing a T7 promoter sequence and was amplified from a specific sequence of target genes (Table A.1.). The cDNA containing T7 promoter was transcribed into single stranded RNA (ssRNA) using the *in vitro* transcription kit (Promega, Ribomax Large Scale production system T7), and ssRNAs were annealed to form double stranded RNAi probes using the temperature gradient method (WORBY *et al.* 2001). Nine different dsRNAs targeting specific sequences of *su(Hw)* were tested (Figure A9. in Appendix). $1X10^6$ S2 cells were plated on a well plate and test groups were treated with 15 μg *su(Hw)* dsRNA daily(generated by the aforementioned *in vitro* transcription reaction) while control groups were treated with distilled water daily. Each group had duplicated samples and cell numbers were counted manually.

**Tandem affinity purification**

*su(Hw)* was amplified using primers (Table A.1) containing Nco I (5') and Mfe I (3') and cloned into pBSacTAP. Both the Su(Hw) expression vector and pBS-PURO vector were transfected into S2 cells, and the transfected cells were selected with puromycin (10μg/ml) for three weeks. To isolate single cell clones, cells were diluted in 1% SFX based soft agar and grown for two weeks until colonies formed on the agar. The individual colonies were collected separately and maintained as a single population. The exogenous Su(Hw) expression in each individual line was checked with western blotting and immunoflorescence staining (Figure A.10 in Appendix).

$2X10^9$ cells were spun down and the cell pellet was dounced in Buffer B (20 mM HEPES pH 7.9, 20 % glycerol, 200 mM KCl, 0.5 mM DTT, 0.5 mM EDTA, 1 % Protease Inhibitor Cocktail, 0.5 % NP40) for nuclear protein extraction. The nuclear extract was incubated with cross-linked IgG sepharose resin (GE Healthcare) for 2 hours at 4 °C. The proteins attached to beads were washed three times with Buffer B, four times with Buffer C (20 mM HEPES pH 7.9, 20 % glycerol, 200 mM KCl, 0.5 mM DTT, 0.5 mM EDTA, 0.1 % NP40) and then twice with TEV cleavage buffer (10 mM Tris-Cl pH 8, 150 mM NaCl, 0.1 % NP40, 0.5 mM DTT, 0.5 mM EDTA). After these washes, protein-bead complexes were incubated with TEV protease (Invitrogen) at 4°C overnight. The next day, the cleaved Su(Hw) protein complexes in the supernatant were transferred to the calmodulin binding buffer (10 mM Tris-Cl pH 8, 10 mM beta-mercaptoethanol, 150 mM NaCl, 1 mM Mg-acetate, 1 mM imidazole, 2 mM $CaCl_2$, 0.1 % NP40). The mixture was then incubated with the second calmodulin affinity resin (Stratagene) for 2 hours at 4°C. After the incubation, the resin was washed five times with calmodulin binding buffer and eluted using SDS sample buffer. The purification efficiency was checked during the entire purification process (Figure A.11 in Appendix).

**Immunoprecipitation and western blot**

The cell lysate was extracted with RIPA buffer containing protease inhibitor (Roche) and IAA (Acros Organics). The cell extract was incubated with 1:100 rabbit $\alpha$-Su(Hw) antibody for 2 hours and Protein A agarose beads were added (Pierce) in the lysate-antibody reaction. The mixture was incubated at 4°C overnight. For FLAG-IP, EZview$^{TM}$ red $\alpha$-FLAG M2 agarose (Sigma) was used. The antigen-antibody complexes were

washed with the wash buffer (10 μM PMSF, 1 mM DTT in PBS buffer) six times, and samples were boiled with SDS-sample buffer. The proteins were separated on SDS-PAGE. Different primary and secondary antibodies were used for western blotting as follows: 1:5000 rabbit α-Su(Hw), 1:5000 rat α-CP190, 1:1000 α-GFP (Invitrogen), 1:5000 α-Rabbit-HRP (Pierce) and 1:1000 α-Rat-HRP (Pierce).

**Yeast-two hybrid assay**

pGAD424 (prey) and pGBDU-C1 (bait) vectors were used for testing the protein-protein interactions in the yeast strain pJ-694A (JAMES *et al.* 1996). Both vectors carry the constitutive promoter, ADH1, controlling expression of bait and prey genes. The bait fusion protein was fused with Gal4 BD (DNA binding domain) and the prey was fused with Gal4 AD (activation domain). Prey and bait constructs were created using the Infusion PCR Cloning System method (Clontech) with specific primers in Table A.1.The bait fusion protein was expressed, and it localized at the promoter of the reporter gene in the yeast genome. The positive interaction between bait and prey activated the transcription of the histidine (His) reporter gene in this system. First, the bait construct was transformed into cells using the lithium acetate method (JAMES 2001), and cells were selected on plates lacking uracil (Ura). Next, the transformants were transformed using the prey construct and co-transformants were selected on plates without uracil and leucine. The assay was carried out by plating co-transformants on the selective plates lacking His, and only the cells expressing the His reporter gene survived. After 3-4 days incubation at 30°C, appearance of cell growth on the selective plates indicated positive interaction between bait and prey.

**Immunofluorescence microscopy**

Cells were dropped onto concanavalin A pre-treated coverslips and fixed with 4% para-formaldehyde for 10 min at room temperature. Next, cells were permeabilized with 0.2% Triton X-100 for 5 min and blocked with blocking solution (3% milk in 1XPBS) for 10 min at room temperature. Fixed cells were incubated with different combinations of diluted antibodies. The dilution factors of each primary antibody used in this study were as follows: 1:200 rabbit α-Su(Hw) antibody, 1:200 rat α-CP190 antibody, 1:200 rat α-Mod(Mdg4)-67.2, 1:150 mouse α-Tubulin- FITC conjugated antibody (Sigma), 1:100 mouse α-FLAG antibody (Sigma), 1:100 mouse α-BEAF antibody and 1:100 mouse α-PEANUT antibody (Developmetal Studies hybridoma bank), FITC-conjugated donkey anti-rabbit IgG antibody, Texas Red dye-conjugated donkey anti-rabbit IgG antibody, Texas Red dye-conjugated donkey anti-rat IgG antibody, FITC-conjugated donkey anti-rat IgG antibody and FITC-conjugated donkey anti-mouse IgG antibody (Jackson ImmunoResearch). DNA was stained with DAPI solution (Roche) for 30 sec, and the slides were mounted with mounting medium (Vector Laboratories). Slides were observed using a Lecia DM6000B widefield epifluorescence microscope equipped with a Hamamatsu ORCA-ER CCD camera and a HC PL FLUOTAR 20x /0.50NA objective. Image acquisition was performed using Simple PCI v6.6 (Hamamatsu Photonics).

## ***Results***

### Insulator proteins locate at the midbody

The chromatin insulator protein, Su(Hw), is a zinc finger DNA binding protein that interacts with other proteins within the nucleus to form complexes with DNA as well as to aform macrostructures known as insulator bodies. A growing list of evidence shows that Su(Hw) plays a role in transcriptional regulation and perhaps DNA replication (LU and TOWER 1997; VOROBYEVA *et al.* 2013). Eukaryotic genome transcription is highly active in interphase but repressed when the cell enters mitosis (GOTTESFELD and FORBES 1997). Whether Su(Hw) is required to associate with chromatin DNA during mitosis while transcription is suppressed remains unclear. To answer this question, we first monitored the localization of Su(Hw) in S2 cells during mitosis. We performed immunofluorescence staining and made a novel discovery of different subcellular localizations of Su(Hw). From prophase, Su(Hw) gradually dissociated from chromatin, moved to the spindle midzone, and finally returned to the DNA by the end of mitosis (Figure 3.1). From telophase to cytokinesis, Su(Hw) was co-localized with $\alpha$-tubulin at the intracellular bridge structure at the midzone (Figure 3.1) and disassembled from the intracellular bridge while the two daughter cells separated. To determine whether the bridge structure where Su(Hw) located is at the MB or not, we compared our Su(Hw) immunofluorescence image with one of the well-known MB associated proteins, Aurora B protein kinase, which is one component of the chromosomal passenger complex (CPC) that conducts cell division (RUCHAUD *et al.* 2007) (Figure 3.2-A and B). Analysis of the images suggests that Su(Hw) is a potential MB protein. To further confirm Su(Hw) is present at the MB, we checked co-localization of Su(Hw) and other MB markers, namely Peanut and SUMO (SHIH *et al.*

2002). Indeed, Su(Hw) localization overlapped with both Peanut and SUMO in the images (Figure 3.2-C and D). This discovery aroused a question of whether other insulator proteins also exist in the MB. We detected whether CP190, Mod(mdg4)-67.2 and BEAF insulator proteins were present at the midbody in S2 cells using immunofluorescence staining. Our result was consistent with previous studies showing that CP190, a centrosomal protein, does not enter this transient bridge structure during the late stage of mitosis (Figure 3.3-A). Further investigation also revealed that Mod(mdg4)-67.2 and BEAF are detected at the midbody (Figure 3.3-B and C). Our interests lie in why and how chromatin insulator proteins have different subcelluar localizations during cell cycle progression.

**Su(Hw) may not play an important role in cytokinesis**

BEAF plays an important role in chromosome segregation (EMBERLY *et al.* 2008a) and locates at the MB (Figure 3.3-C), and we asked whether another MB insulator protein, Su(Hw), also interferes with the cell cycle progression. We knocked down Su(Hw) expression with *su(Hw)* dsRNA in S2 cells and knock-down efficiency was checked with western blotting (Figure 3.4). Cell growth was monitored by manual cell counts for five days. The cell growth curve showed *su(Hw)* knock-down cells had no noticeable difference of growth rate from wild-type cells (Figure 3.4). This data indicates no major effect of losing Su(Hw) in the cell cycle progression. The function of insulator proteins in the midbody during cytokinesis remains unclear and open for further study.

**Co-localization of SUMO with insulator proteins in S2 cells**

CP190 and Mod(mdg4)-67.2 interact with SUMO and are substrates for SUMOylation (CAPELSON and CORCES 2006). Our study shows that SUMO colocalizes with Su(Hw) at the MB, and SUMO was also found interacting with Su(Hw) in the *Drosophila* protein interaction map (DPiM). Moreover, using SUMOsp software (REN *et al.* 2009), we identified that the N-terminus of Su(Hw) has two SUMO interacting motifs (SIMs) and four potential SUMOylation sites (Figure 3.8-A). These sites are highly conserved through ten *Drosophila* species. To investigate whether Su(Hw) interacts with SUMO, we transfected a FLAG-tagged SUMO expression vector into S2 cells and performed immunofluorescence staining to determine the subcelluar localization of these proteins. Results indicated Su(Hw), BEAF, CP190 and Mod(mdg4)-67.2 all co-localized with SUMO. Notably, SUMO is enriched at large foci (insulator bodies), where insulator proteins aggregate (Figure 3.5). This data strongly suggests a possible role of SUMO directing the interaction between different subclasses of insulator proteins.

**Enhanced association between insulator proteins and Su(Hw) in a SUMO-dependent manner**

We have established a Su(Hw) stable line constitutively expressing Su(Hw) with a tandem affinity purification (TAP) tag. This stable line was used for further examination to check how SUMO affects insulator protein interactions. We treated cell lysate with iodoacetamide (IAA), which is an isopeptidase inhibitor that suppresses SUMO de-conjugation. Tandem affinity purification of the IAA treated sample revealed

that even more Su(Hw), Mod(mdg4)-67.2, and CP190 (Figure 3.6-A) were present, a finding consistent with the observation in the immunofluorescence staining results (Figure 3.5). Furthermore, purification followed by silver staining showed these three proteins along with other unknown proteins associate with Su(Hw) (Figure 3.6-B).

In a reciprocal immunoprecipitation assay, we found Su(Hw) presents in FLAG-SUMO pull-downs. Particularly, in the IAA treated sample, a band of higher molecular weight than that of Su(Hw) was observed, (Figure 3.7-A) suggesting that the post-translational modification of Su(Hw) only occured when excess SUMO was present while de-SUMOylation was suppressed. Also, we used two other mutation forms of SUMO to show whether the interaction between SUMO and Su(Hw) is mediated by SUMOylation or SUMO interaction. The diglycines at the C-terminus of SUMO are required for the SUMO activating enzymes to recognize and activate SUMO proteins which must be properly activated by the SUMO activating enzymes in order to SUMOylate target proteins. FLAG-SUMO$^{GG}$ functions as an active form of SUMO while the other mutant, FLAG-SUMO$^{dGG}$, cannot be activated but is still able to associate with proteins through non-covalent interactions mediated by SIMs on the targets (SMITH *et al.* 2004). Su(Hw) was detected in both FLAG-SUMO$^{dGG}$ and FLAG-SUMO$^{GG}$ pull-downs, indicating that Su(Hw) was present in the complexes mediated by both the SUMO interacting motifs and SUMOylation sites (Figure 3.7-B). More Su(Hw) associated proteins are present in a SUMO-dependent manner, revealing a possible role of SUMO in regulating the Su(Hw) insulator protein complex formation and stability.

**Characterization of the interactions between SUMO and Su(Hw)**

SUMO regulates insulator proteins by conjugating Mod(mdg4)-67.2 and CP190 (GOLOVNIN *et al.* 2012). Our results showed insulator protein interactions were enhanced in a SUMO-dependent manner (Figure 3.6), and the subcellular localization of insulator proteins overlaped with SUMO (Figure 3.5). Also, Su(Hw) was detected in the SUMO complexes. These data indicate that assembly of the Su(Hw) insulator complex may occur under the control of SUMO regulation. It is possible that SUMO stabilizes the entire Su(Hw) insulator complex and this process is regulated by both covalent SUMOylation and noncovalent SUMO interaction. Although Capelson et al., (2006) suggested that Su(Hw) is not a substrate of SUMOylation *in vitro*, the connection between SUMO and Su(Hw) may be mediated by noncovalently bound SUMO interacting through SIMs in Su(Hw). We have identified two predicted SIMs in Su(Hw) (Figure 3.8-A) which may be responsible for this interaction.

To further dissect the interaction between SUMO and Su(Hw), we performed a yeast-two-hybrid assay. *su(Hw)* was cloned into pGBDU-C1 fused with a Gal4 DNA binding domain as a bait, and its corresponding prey were wild-type mod(mdg4)-67.2, mod(mdg4)-67.2 mSIM (mutated SUMO interacting motif: V 495,497,498 A), full-length SUMO, and a truncated form, $SUMO^{dGG}$. All the prey genes were cloned in pGAD424 and fused to a Gal4 activation domain. The reciprocal assay was also performed by swapping prey genes into bait genes and vice versa. All the mutant constructs were generated using the site-directed mutagenesis method (WANG and WILKINSON 2000).

The interaction between Su(Hw) and Mod(mdg4)-67.2 was already verified in yeast two-hybrid experiments (GHOSH *et al.* 2001) and was consequently used as a positive control. The results show that Su(Hw) interacted with Mod(mdg4)-67.2, consistent with previous findings. Also, Mod(mdg4)-67.2 interacted with SUMO as expected, and Mod(mdg4)-67.2 mSIM lost the interaction with $SUMO^{dGG}$, indicating Mod(mdg4)-67.3 495-VRVV-498 is a bona fide SIM. On the contrary, no interaction was identified between Su(Hw) with either SUMO or $SUMO^{dGG}$ in yeast cells (Table 3.1). All together, these results imply that the interactions between SUMO and Su(Hw) in the pull-down could be mediated by other proteins, such as Mod(mdg4)-67.2 in physiological conditions that do not exist in yeast cells.

**Loss of SUMO interaction with Su(Hw) may cause an unknown cleavage of Su(Hw)**

In order to understand how SUMO may regulate the biological function of Su(Hw), we generated different mutant constructs of Su(Hw) at predicted SUMOylation sites as well as at SIMs. These constructs were driven by metallothionein promoters and were transfected into S2 cells to establish stable transfectants. Using western blotting, we detected the expression of Su(Hw)-GFP fusion proteins with anti-GFP antibodies in the stable transfectants. Surprisingly, not only a full-length form of Su(Hw) but also a 10-20KDa shortened form were found in the cells expressing mutated Su(Hw). These mutations are *su(Hw) K140A* with a mutated SUMOylation site and *su(Hw) V150A* containing a disrupted SIM where VTVV is converted to ATAA. In addition to SUMO related mutations, *su(Hw) d100* is a mutation with a truncation of 144

base pairs from amino acid 155 to 202 (Figure 3.8-A) that is able to rescue insulator function while only partially recovering sterility in *su(Hw)* mutants (HARRISON *et al.* 1993). The deleted sequence is next to the predicted SUMO regulatory sequence, and its deletion may interfere with the regulation of SUMO on Su(Hw). The immunoblotting data from these three mutants indicate interference of SUMO regulation in Su(Hw) may cause cleavage or degradation of Su(Hw) and produce shortened Su(Hw). Nevertheless, the function of this shortened Su(Hw) is still unknown.

**Su(Hw) may be a substrate of Aurora Kinase, which promotes Su(Hw) phosphorylation and subsequent cleavage**

Interaction with SUMO alters the biological function of target proteins and affects downstream cellular events. This functionality switch is controlled by SUMO binding. We have shown that mutations at SUMO related sites of Su(Hw) lead to cleavage, but we sought how this switch works. SUMOylation and SUMO interaction can be positively or negatively regulated by substrate phosphorylation. We found in a phosphorylation site mapping database that the 65$^{th}$ serine (Ser 65) of Su(Hw) near the SUMO regulatory region is a phosphorylaton site in *Drosophila* Kc167 cells (BODENMILLER *et al.* 2007) and Ser 65 was also predicted as an Aurora kinase phosphorylation site using the GPS2.0, which predicts kinase-specific phosphorylation sites (XUE *et al.* 2008). Our data and the published data indirectly suggest that Aurora B and Su(Hw) may co-localize at the MB during telophase (Figure 3.1). Based on these predictions and data analyses, we speculate Su(Hw) may transiently interact with Aurora B and undergo phosphorylation during a specific stage of mitosis. To answer whether phosphorylation of Ser 65 of

Su(Hw) controls SUMO regulation on Su(Hw), we created a constitutively phosphorylated Ser 65 on *su(Hw)* by changing Ser to aspartic acid, which mimics a phosphorylated serine. This mutated Su(Hw) was transfected into S2 cells and western blotting data showed that this constitutively phosphorylated Ser 65 of Su(Hw) results in cleavage and shortening of Su(Hw) (Figure 3.8-B). The phosphorylated Su(Hw) undergoes proteolysis and generates a N-terminal fragment smaller than 20KDa plus a remaining C-terminal fragment. Taken together, Aurora B phosphorylation and SUMOylation may both play a role in regulating an unknown cleavage mechanism of Su(Hw).

## ***Discussion***

Numerous studies suggest that combination of post-translational modifications regulates protein stability (ULRICH 2012). For example, by forming a complex with IkBα, the transcription factor function of NFkB is inhibited. While IkBα is phosphorylated by IkB kinase (IKK) and undergoes degradation, dissociated NFkB is activated again. In this scenario, SUMOylation antagonizes phosphorylation of IkBα, thereby preventing degradation of IkBα (DESTERRO *et al.* 1998). A similar regulation mechanism may also apply to Su(Hw). Our working model proposes SUMOylation or SUMO interaction inhibits cleavage of Su(Hw). At specific stages of mitosis, Su(Hw) is phosphorylated by Aurora B triggering an unknown cleavage mechanism causing the N-terminal fragment of Su(Hw) to translocate to the MB where it performs an unknown function (Figure 3.9).

In addition to the potential post-translational modifications of Su(Hw) described here, several open questions remain unanswered. First, the function of Su(Hw) in the MB is still unknown. Although no noticeable cell growth defect was detected in *su(Hw)* knock-down cells, it is still possible that the function of Su(Hw) at the MB is unnecessary in embryonic cells (S2 cells) but is required in other types of cells. Just as stem cells in mammals contain high concentrations of MBs for specialized biological functions (ETTINGER *et al.* 2011; KUO *et al.* 2011; SCHINK and STENMARK 2011; WILCOCK *et al.* 2007), MBs in *Drosophila* stem cells may be necessary for an unknown celluar function. Additionally, we observed that SUMO stabilizes insulator protein complex formation and concentrated SUMO signals were detected in the large insulator bodies containing BEAF and Su(Hw) (Figure 3.5 and 3.6). These data reveal the possibility that SUMO

directs the association between different subclasses of insulators. To uncover the importance of SUMO in regulating insulator interactions and further reorganizing the chromatin structure in response to different cellular events or developmental processes, it will be an interesting study in the future.

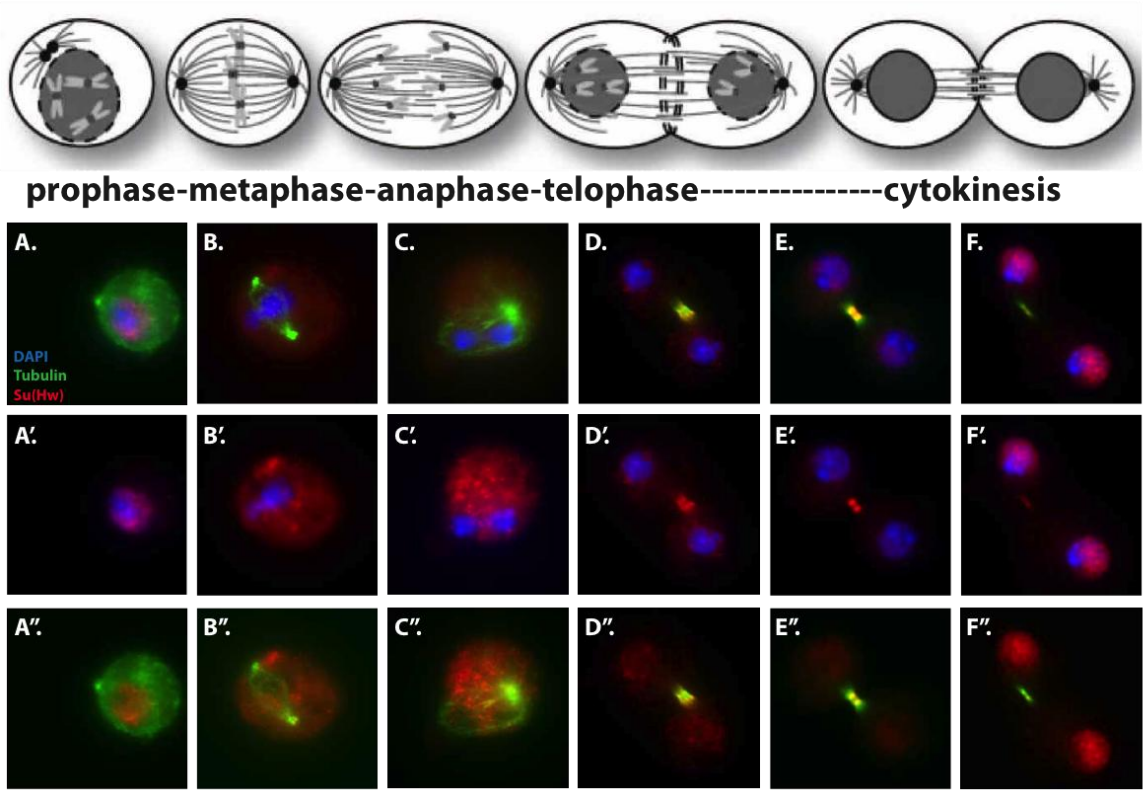


**Figure 3.1. Dynamic subcellular localization of Su(Hw) during mitosis.**

S2 cells were collected for immunofluorescence staining using α-Tubulin (green) and Su(Hw) (red) antibodies. Images of cells at different stages of the cell cycle were selected and labeled from prophase (A-A''), metaphase (B-B''), anaphase (C-C''), telophase (D-D'' and E-E'') and cytokinesis (F-F''). Upper carton panel is the picture from Vader et al. (VADER and LENS 2008).

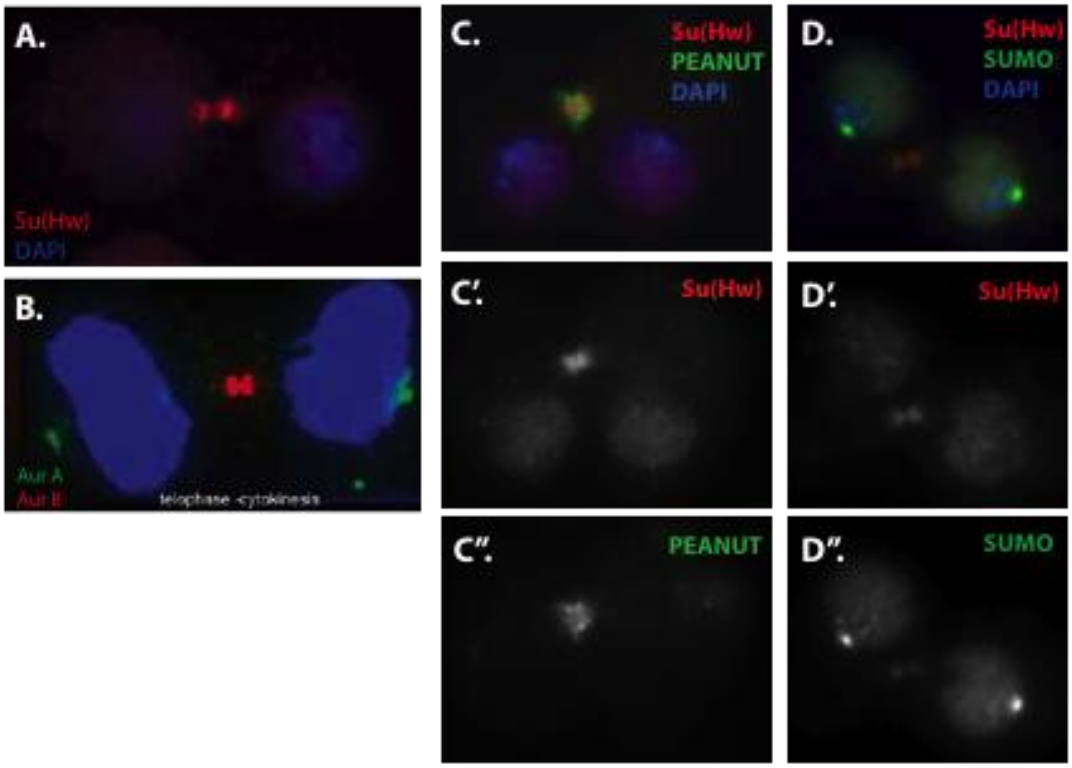


**Figure 3.2. Su(Hw) is a midbody protein.**

S2 cells were used for immunofluorescence and different antibodies were used as labeled in A and C-C''. Cells in panel D were transfected with FLAG-tagged SUMO and anti-FLAG antibody was used for SUMO detection. The panel B is an image modified from a reference paper (CARMENA *et al.* 2009).

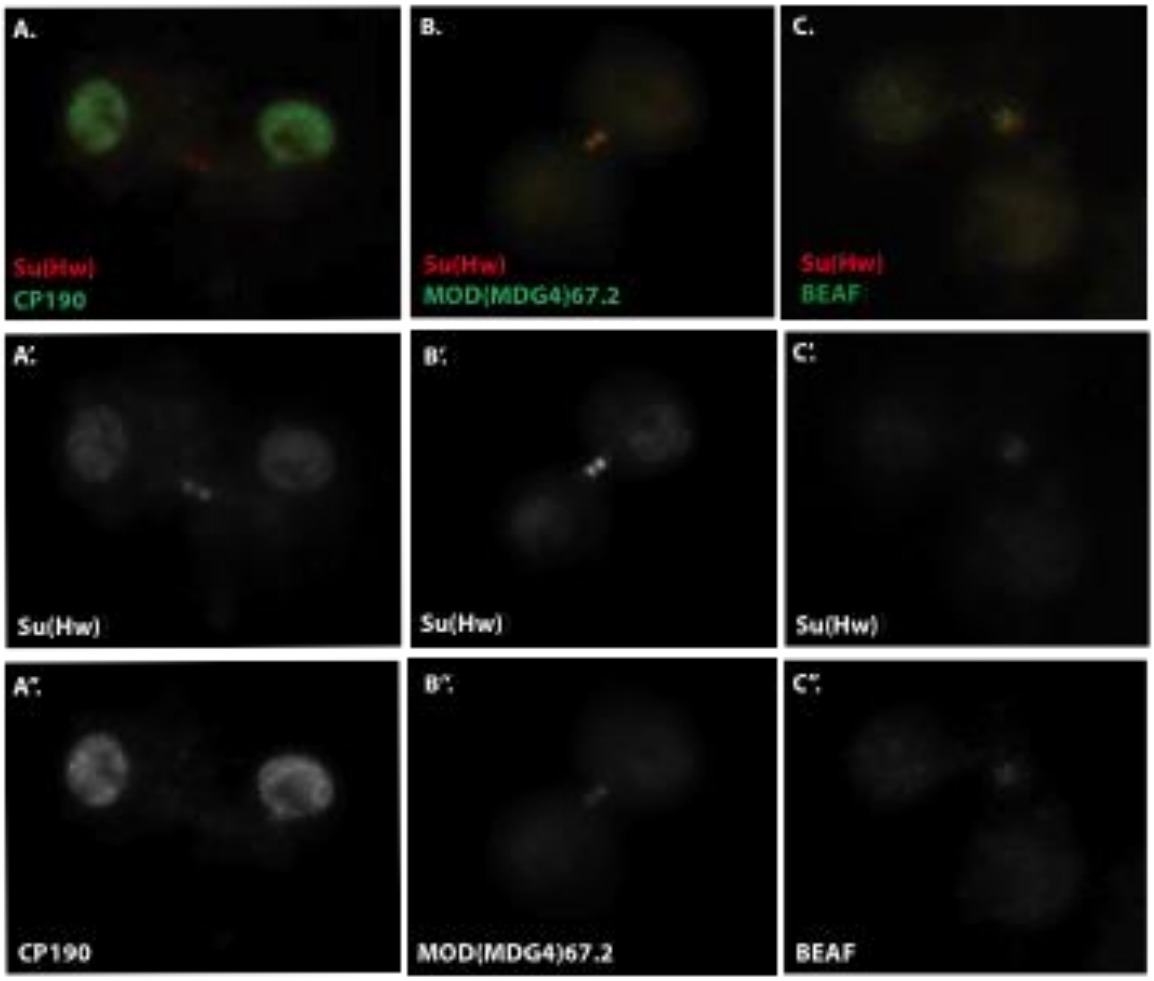


**Figure 3.3. Mod(mdg4)-67.2 and BEAF co-localize with Su(Hw) in the midbody.**

Immunofluorescence was performed in S2 cells with distinct antibody combinations as labeled and A-C shows the co-localization of two proteins. A'-C' and A''-C'' shows the staing of individul protein.

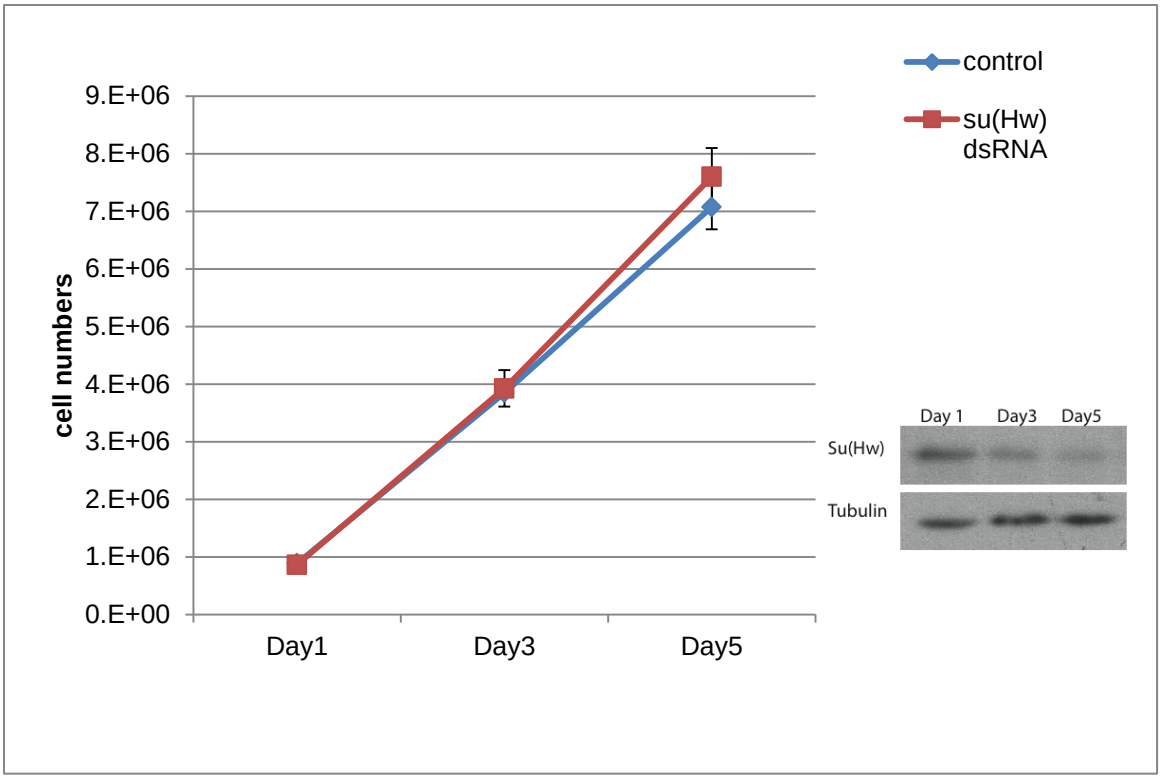


**Figure 3.4. Su(Hw) does not have a major effect on cell growth.**

$1X10^6$ S2 cells were plated in the six-well plate and treated with *su(Hw)* dsRNA daily. The cell growth was monitored by manual counts, and the Su(Hw) knock-down efficiency was checked using western blotting.

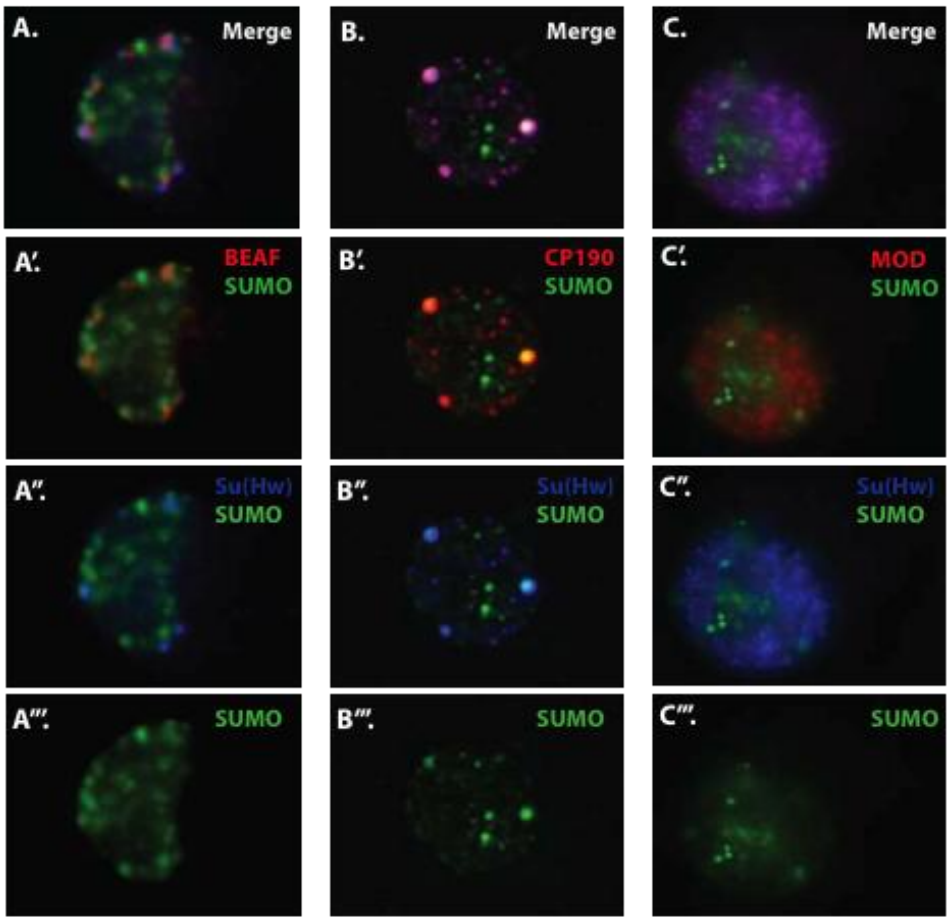


**Figure 3.5. Tagged SUMO co-localizes with insulator proteins in S2 cells.**

Cells transfected with FLAG-SUMO were collected 48 hours later and different antibody combinations were used for immunoflorescence staining to detect the co-localization of each insulator protein with SUMO labeled in each image. A-A''' shows co-localization of BEAF, Su(Hw) and SUMO; B-B''' represents the co-localization of CP190, Su(Hw) and SUMO, and C-C''' shows co-localization of Mod(mdg4)-67.2, Su(Hw) and SUMO.

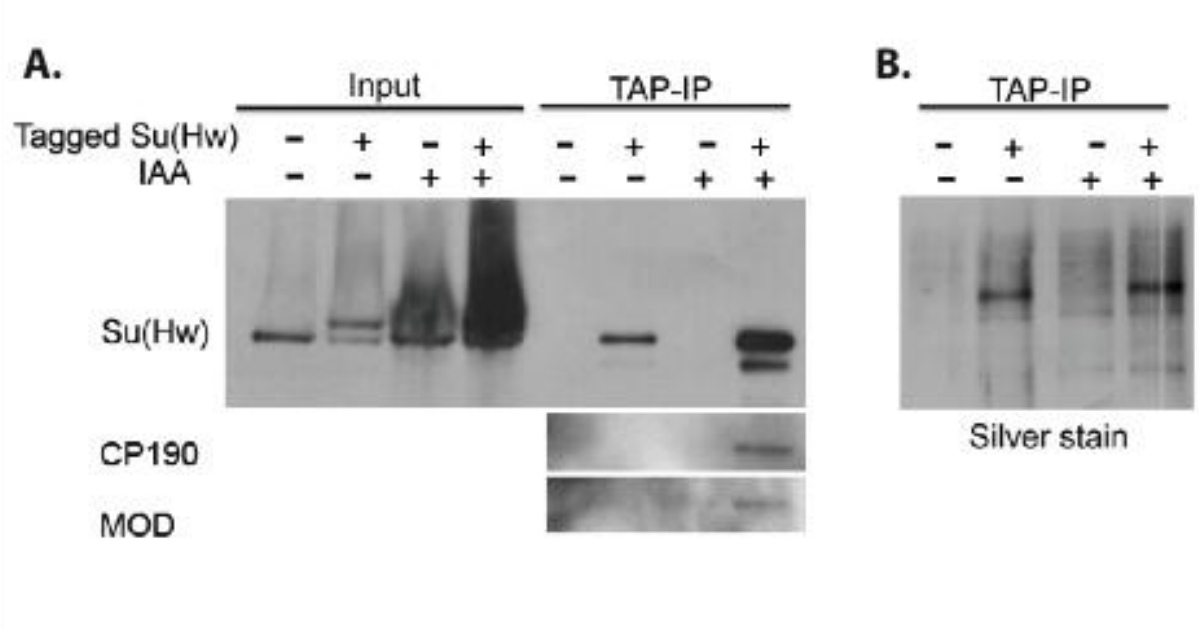


**Figure 3.6. More proteins bound to Su(Hw) when desumoylation is inhibited.**

Cell extracts from tagged Su(Hw)-expressing cells and control wild-type cells were treated with iodoacetamide (IAA) and purified by sequential immunoprecipitation using IgG beads and CAM beads. **A.** The western blot shows the Su(Hw) in input and insulator proteins in pull-down. B. Sliver staining was carried out using pull-down extract.

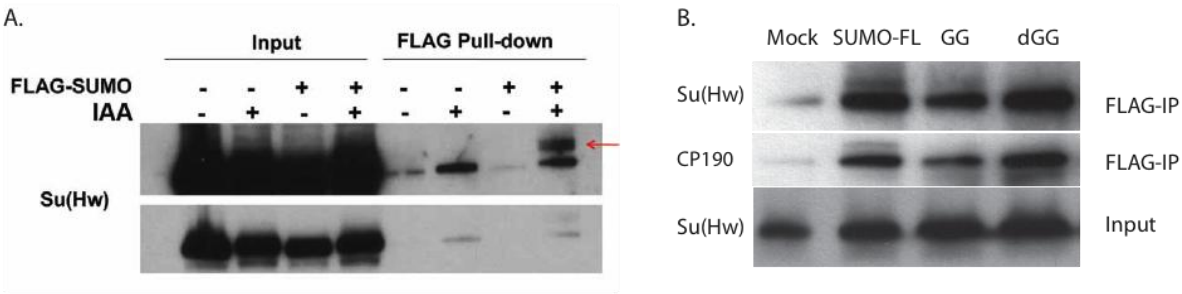


**Figure 3.7. Su(Hw) interacts with SUMO in S2 cells.**

FLAG-tagged SUMO$^{FL}$, SUMO$^{GG}$ and SUMO$^{dGG}$ were transfected into S2 cells and 48 hours after transfection, cells were harvested for protein extraction with the lysis buffer containing IAA. Immunoprecipitation of FLAG was then performed. A. Using western blot, Su(Hw) was detected in the cell extract (Input) on the left and SUMO protein complex (FLAG pull-down) on the right. Different exposure times of Su(Hw) are both shown here in the upper panel (longer exposure time) and bottom panel (shorter exposure time). B. FLAG pull-down was performed with different forms of FLAG-SUMO and insulator proteins were detected using western blotting (first two panels). The bottom panel showed the input of each IP reaction.

**Table 3.1. Yeast-two-hybrid assay results.**

| AD \ BD | SUMO-dGG | Mod(mdg4)-67.2 | Mod(mdg4)-67.2 mSIM | Su(Hw) | pGBDU-C1 |
|---|---|---|---|---|---|
| SUMO | NA | +++ | ++ | - | - |
| SUMO-dGG | NA | +++ | - | - | - |
| Su(Hw) | - | +++ | ++ | - | - |
| Su(Hw)-d100 | NA | +++ | + | - | NA |
| Su(Hw)-mSIM | NA | +++ | NA | NA | NA |
| Mod(mdg4)-67.2 | NA | NA | NA | +++ | NA |
| pGAD424 | NA | - | - | - | NA |

The number of "+" indicates the strength of interaction. "-" represents no interaction and "+" represents interaction. NA means "not available."

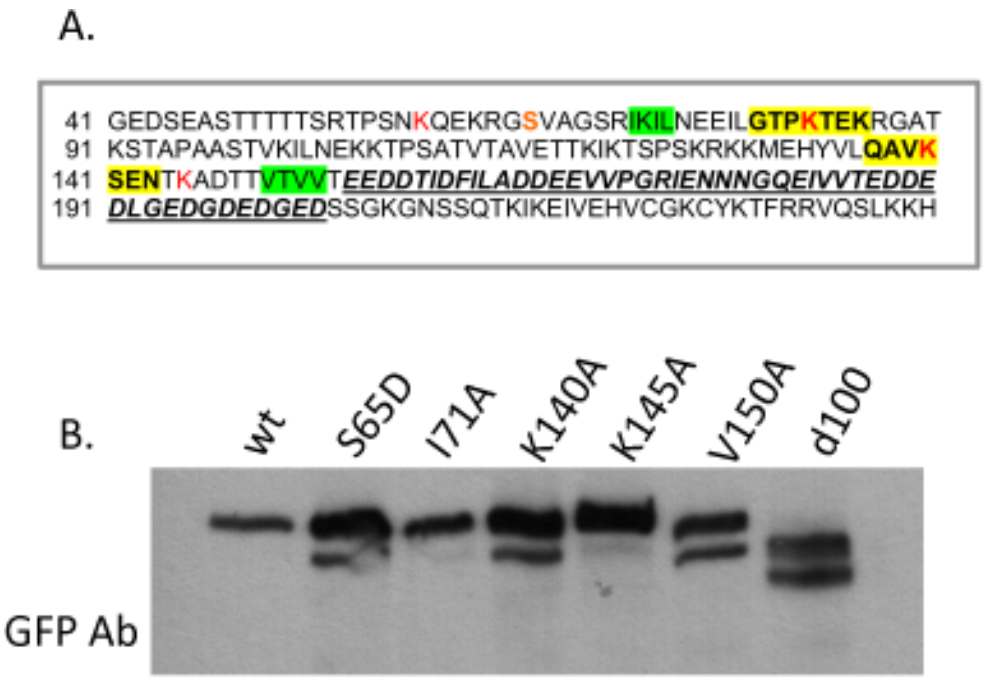


**Figure 3.8. Su(Hw) proteolysis may be regulated by SUMOylation and Phosphorylation.**

A. The amino acid sequence of Su(Hw) from amino acid 41 to 210. The lysines (K) in red are predicted SUMOylation sites. K140 (bold) is the classic consensus SUMOylation site (**ψ**KxD/E, **ψ** is a large hydrophobic residue) and highly conserved through 10 *Drosophila* strains. The two sequences IKIL and VTVV in green boxes are SUMO interaction motifs (consensus: **V/I-X-V/I-V/I)** and both are highly conserved. The amino acids underlined represent truncation regions in the d100 mutant. S65 in orange is a phosphorylation site.

B. Expression of wild-type and mutant Su(Hw)-GFP using western blotting with a GFP antibody.

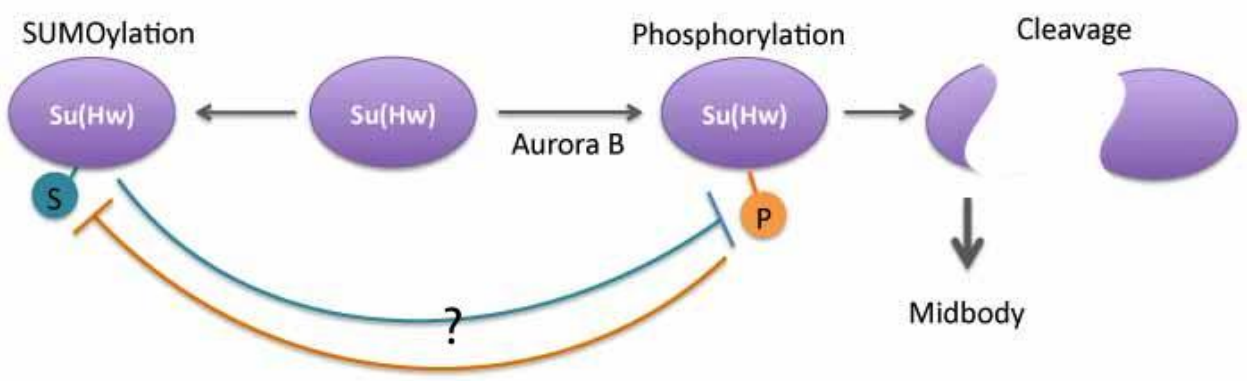


**Figure 3.9. The working model.**

A combination of post-translational modifications may regulate proteolysis of Su(Hw) and further influence subcellular localization and function of Su(Hw) in *Drosophila* cells.

# REFERENCES

ABDU, U., M. BRODSKY and T. SCHUPBACH, 2002 Activation of a meiotic checkpoint during Drosophila oogenesis regulates the translation of gurken through Chk2/Mnk. Current Biology **12:** 1645-1651.

ARAVIN, A. A., M. LAGOS-QUINTANA, A. YALCIN, M. ZAVOLAN, D. MARKS *et al.*, 2003 The small RNA profile during Drosophila melanogaster development. Dev Cell **5:** 337-350.

BANIAHMAD, A., C. STEINER, A. C. KOHNE and R. RENKAWITZ, 1990 Modular Structure of a Chicken Lysozyme Silencer - Involvement of an Unusual Thyroid-Hormone Receptor-Binding Site. Cell **61:** 505-514.

BASTOCK, R., and D. ST JOHNSTON, 2008 Drosophila oogenesis. Curr Biol **18:** R1082-1087.

BATE, M., and A. MARTINEZ ARIAS, 1993a *The development of Drosophila melanogaster*. Cold Spring Harbor Laboratory, Cold Spring Harbor, N.Y.

BATE, M., and A. MARTINEZ ARIAS, 1993b *The development of Drosophila melanogaster*. Cold Spring Harbor Laboratory Press, Plainview, N.Y.

BAXLEY, R. M., A. A. SOSHNEV, D. E. KORYAKOV, I. F. ZHIMULEV and P. K. GEYER, 2011 The role of the Suppressor of Hairy-wing insulator protein in Drosophila oogenesis. Dev Biol **356:** 398-410.

BECK, D. B., H. ODA, S. S. SHEN and D. REINBERG, 2012 PR-Set7 and H4K20me1: at the crossroads of genome integrity, cell cycle, chromosome condensation, and transcription. Genes & Development **26:** 325-337.

BELL, A. C., and G. FELSENFELD, 2000 Methylation of a CTCF-dependent boundary controls imprinted expression of the Igf2 gene. Nature **405:** 482-485.

BELL, A. C., A. G. WEST and G. FELSENFELD, 1999 The protein CTCF is required for the enhancer blocking activity of vertebrate insulators. Cell **98:** 387-396.

BERLETH, T., M. BURRI, G. THOMA, D. BOPP, S. RICHSTEIN *et al.*, 1988 The Role of Localization of Bicoid Rna in Organizing the Anterior Pattern of the Drosophila Embryo. Embo Journal **7:** 1749-1756.

BLACK, J. C., and J. R. WHETSTINE, 2011 Chromatin landscape Methylation beyond transcription. Epigenetics **6:** 13-19.

BODENMILLER, B., J. MALMSTROM, B. GERRITS, D. CAMPBELL, H. LAM *et al.*, 2007 PhosphoPep-a phosphoproteome resource for systems biology research in Drosophila Kc167 cells. Molecular Systems Biology **3**.

BOSCO, G., 2012 Chromosome Pairing: A Hidden Treasure No More. Plos Genetics **8**.

BRASSET, E., and C. VAURY, 2005 Insulators are fundamental components of the eukaryotic genomes. Heredity **94:** 571-576.

BRENNECKE, J., A. A. ARAVIN, A. STARK, M. DUS, M. KELLIS *et al.*, 2007 Discrete small RNA-generating loci as master regulators of transposon activity in Drosophila. Cell **128:** 1089-1103.

BRIDGES, C. B., and K. S. BREHME, 1944 *The mutants of Drosophila melanogaster*, Washington, D.C.,.

BRODSKY, M. H., B. T. WEINERT, G. TSANG, Y. S. RONG, N. M. MCGINNIS *et al.*, 2004 Drosophila melanogaster MNK/Chk2 and p53 regulate multiple DNA repair and apoptotic pathways following DNA damage. Mol Cell Biol **24:** 1219-1231.

BUSHEY, A. M., E. RAMOS and V. G. CORCES, 2009a Three subclasses of a Drosophila insulator show distinct and cell type-specific genomic distributions. Genes & Development **23:** 1338-1350.

BUSHEY, A. M., E. RAMOS and V. G. CORCES, 2009b Three subclasses of a Drosophila insulator show distinct and cell type-specific genomic distributions. Genes Dev **23:** 1338-1350.

BUSZCZAK, M., and L. COOLEY, 2000 Eggs to die for: cell death during Drosophila oogenesis. Cell Death Differ **7:** 1071-1074.

BUTCHER, R. D., S. CHODAGAM, R. BASTO, J. G. WAKEFIELD, D. S. HENDERSON *et al.*, 2004 The Drosophila centrosome-associated protein CP190 is essential for viability but not for cell division. Journal of Cell Science **117:** 1191-1199.

CAPELSON, M., and V. G. CORCES, 2005 The ubiquitin ligase dTopors directs the nuclear organization of a chromatin insulator. Mol Cell **20:** 105-116.

CAPELSON, M., and V. G. CORCES, 2006 SUMO conjugation attenuates the activity of the gypsy chromatin insulator. Embo J **25:** 1906-1914.

CARMENA, M., S. RUCHAUD and W. C. EARNSHAW, 2009 Making the Auroras glow: regulation of Aurora A and B kinase function by interacting proteins. Curr Opin Cell Biol **21:** 796-805.

CARRIERE, L., S. GRAZIANI, O. ALIBERT, Y. GHAVI-HELM, F. BOUSSOUAR *et al.*, 2012 Genomic binding of Pol III transcription machinery and relationship with TFIIS transcription factor distribution in mouse embryonic stem cells. Nucleic Acids Res **40:** 270-283.

CHA, B. J., B. S. KOPPETSCH and W. E. THEURKAUF, 2001 In vivo analysis of Drosophila bicoid mRNA localization reveals a novel microtubule-dependent axis specification pathway. Cell **106:** 35-46.

CHA, B. J., L. R. SERBUS, B. S. KOPPETSCH and W. E. THEURKAUF, 2002 Kinesin I-dependent cortical exclusion restricts pole plasm to the oocyte posterior. Nature Cell Biology **4:** 592-598.

CHAPMAN, J. R., M. R. G. TAYLOR and S. J. BOULTON, 2012 Playing the End Game: DNA Double-Strand Break Repair Pathway Choice. Molecular Cell **47:** 497-510.

CHEN, C. T., A. W. ETTINGER, W. B. HUTTNER and S. J. DOXSEY, 2013 Resurrecting remnants: the lives of post-mitotic midbodies. Trends in Cell Biology **23:** 118-128.

CHERNUKHIN, I., S. SHAMSUDDIN, S. Y. KANG, R. BERGSTROM, Y. W. KWON *et al.*, 2007 CTCF interacts with and recruits the largest subunit of RNA polymerase II to CTCF target sites genome-wide. Mol Cell Biol **27:** 1631-1648.

CHODAGAM, S., A. ROYOU, W. WHITFIELD, R. KARESS and J. W. RAFF, 2005 The centrosomal protein CP190 regulates myosin function during early Drosophila development. Curr Biol **15:** 1308-1313.

CLEGG, N. J., S. D. FINDLEY, A. P. MAHOWALD and H. RUOHOLA-BAKER, 2001 maelstrom is required to position the MTOC in stage 2-6 Drosophila oocytes. Development Genes and Evolution **211:** 44-48.

CLEGG, N. J., D. M. FROST, M. K. LARKIN, L. SUBRAHMANYAN, Z. BRYANT *et al.*, 1997 maelstrom is required for an early step in the establishment of Drosophila oocyte polarity: posterior localization of grk mRNA. Development **124:** 4661-4671.

COOK, H. A., B. S. KOPPETSCH, J. WU and W. E. THEURKAUF, 2004 The Drosophila SDE3 homolog armitage is required for oskar mRNA silencing and embryonic axis specification. Cell **116:** 817-829.

COOLEY, L., 1998 Drosophila ring canal growth requires Src and Tec kinases. Cell **93:** 913-915.

DE CUEVAS, M., and A. C. SPRADLING, 1998 Morphogenesis of the Drosophila fusome and its implications for oocyte specification. Development **125:** 2781-2789.
DELGADO, M. D., I. V. CHERNUKHIN, A. BIGAS, E. M. KLENOVA and J. LEON, 1999 Differential expression and phosphorylation of CTCF, a c-myc transcriptional regulator, during differentiation of human myeloid cells. Febs Letters **444:** 5-10.
DESTERRO, J. M., M. S. RODRIGUEZ and R. T. HAY, 1998 SUMO-1 modification of IkappaBalpha inhibits NF-kappaB activation. Mol Cell **2:** 233-239.
DING, D., S. M. PARKHURST and H. D. LIPSHITZ, 1993 Different genetic requirements for anterior RNA localization revealed by the distribution of Adducin-like transcripts during Drosophila oogenesis. Proc Natl Acad Sci U S A **90:** 2512-2516.
DJAGAEVA, I., S. DORONKIN and S. K. BECKENDORF, 2005 Src64 is involved in fusome development and karyosome formation during Drosophila oogenesis. Dev Biol **284:** 143-156.
DODSON, G. S., D. J. GUARNIERI and M. A. SIMON, 1998 Src64 is required for ovarian ring canal morphogenesis during Drosophila oogenesis. Development **125:** 2883-2892.
DONZE, D., C. R. ADAMS, J. RINE and R. T. KAMAKAKA, 1999 The boundaries of the silenced HMR domain in Saccharomyces cerevisiae. Genes & Development **13:** 698-708.
EGGERT, U. S., T. J. MITCHISON and C. M. FIELD, 2006 Animal cytokinesis: from parts list to mechanisms. Annual Review of Biochemistry **75:** 543-566.
EMBERLY, E., R. BLATTES, B. SCHUETTENGRUBER, M. HENNION, N. JIANG *et al.*, 2008a BEAF regulates cell-cycle genes through the controlled deposition of H3K9 methylation marks into its conserved dual-core binding sites. PLoS Biol **6:** 2896-2910.
EMBERLY, E., R. BLATTES, B. SCHUETTENGRUBER, M. HENNION, N. JIANG *et al.*, 2008b BEAF Regulates Cell-Cycle Genes through the Controlled Deposition of H3K9 Methylation Marks into Its Conserved Dual-Core Binding Sites. Plos Biology **6:** 2896-2910.
EPHRUSSI, A., L. K. DICKINSON and R. LEHMANN, 1991 Oskar Organizes the Germ Plasm and Directs Localization of the Posterior Determinant Nanos. Cell **66:** 37-50.
EPSTEIN, A. M., C. R. BAUER, A. HO, G. BOSCO and D. C. ZARNESCU, 2009 Drosophila Fragile X protein controls cellular proliferation by regulating cbl levels in the ovary. Dev Biol **330:** 83-92.
ETTINGER, A. W., M. WILSCH-BRAUNINGER, A. M. MARZESCO, M. BICKLE, A. LOHMANN *et al.*, 2011 Proliferating versus differentiating stem and cancer cells exhibit distinct midbody-release behaviour. Nat Commun **2:** 503.
FAY, A., Z. MISULOVIN, J. LI, C. A. SCHAAF, M. GAUSE *et al.*, 2011 Cohesin Selectively Binds and Regulates Genes with Paused RNA Polymerase. Current Biology **21:** 1624-1634.
FESCHOTTE, C., 2008 Transposable elements and the evolution of regulatory networks. Nat Rev Genet **9:** 397-405.
FILIPPOVA, G. N., 2008 Genetics and epigenetics of the multifunctional protein CTCF. Curr Top Dev Biol **80:** 337-360.
FILIPPOVA, G. N., S. FAGERLIE, E. M. KLENOVA, C. MYERS, Y. DEHNER *et al.*, 1996 An exceptionally conserved transcriptional repressor, CTCF, employs different combinations of zinc fingers to bind diverged promoter sequences of avian and mammalian c-myc oncogenes. Molecular and Cellular Biology **16:** 2802-2813.
FILIPPOVA, G. N., C. P. THIENES, B. H. PENN, D. H. CHO, Y. J. HU *et al.*, 2001 CTCF-binding sites flank CTG/CAG repeats and form a methylation-sensitive insulator at the DM1 locus. Nature Genetics **28:** 335-343.

FRITSCH, C., G. PLOEGER and D. J. ARNDT-JOVIN, 2006 Drosophila under the lens: imaging from chromosomes to whole embryos. Chromosome Research **14:** 451-464.
GAREAU, J. R., and C. D. LIMA, 2010 The SUMO pathway: emerging mechanisms that shape specificity, conjugation and recognition. Nat Rev Mol Cell Biol **11:** 861-871.
GASZNER, M., and G. FELSENFELD, 2006 Insulators: exploiting transcriptional and epigenetic mechanisms. Nat Rev Genet **7:** 703-713.
GASZNER, M., J. VAZQUEZ and P. SCHEDL, 1999 The Zw5 protein, a component of the scs chromatin domain boundary, is able to block enhancer-promoter interaction. Genes Dev **13:** 2098-2107.
GAUSE, M., P. MORCILLO and D. DORSETT, 2001 Insulation of enhancer-promoter communication by a gypsy transposon insert in the Drosophila cut gene: cooperation between suppressor of hairy-wing and modifier of mdg4 proteins. Mol Cell Biol **21:** 4807-4817.
GAUSE, M., C. A. SCHAAF and D. DORSETT, 2008 Cohesin and CTCF: cooperating to control chromosome conformation? Bioessays **30:** 715-718.
GEORGIEV, P., and M. KOZYCINA, 1996 Interaction between mutations in the suppressor of Hairy wing and modifier of mdg4 genes of Drosophila melanogaster affecting the phenotype of gypsy-induced mutations. Genetics **142:** 425-436.
GEORGIEV, P. G., and T. I. GERASIMOVA, 1989 Novel genes influencing the expression of the yellow locus and mdg4 (gypsy) in Drosophila melanogaster. Mol Gen Genet **220:** 121-126.
GERASIMOVA, T. I., and V. G. CORCES, 2001 Chromatin insulators and boundaries: effects on transcription and nuclear organization. Annu Rev Genet **35:** 193-208.
GERASIMOVA, T. I., D. A. GDULA, D. V. GERASIMOV, O. SIMONOVA and V. G. CORCES, 1995 A Drosophila Protein That Imparts Directionality on a Chromatin Insulator Is an Enhancer of Position-Effect Variegation. Cell **82:** 587-597.
GERASIMOVA, T. I., E. P. LEI, A. M. BUSHEY and V. G. CORCES, 2007 Coordinated control of dCTCF and gypsy chromatin insulators in Drosophila. Mol Cell **28:** 761-772.
GHABRIAL, A., R. P. RAY and T. SCHUPBACH, 1998 okra and spindle-B encode components of the RAD52 DNA repair pathway and affect meiosis and patterning in Drosophila oogenesis. Genes & Development **12:** 2711-2723.
GHABRIAL, A., and T. SCHUPBACH, 1999 Activation of a meiotic checkpoint regulates translation of Gurken during Drosophila oogenesis. Nature Cell Biology **1:** 354-357.
GHOSH, D., T. I. GERASIMOVA and V. G. CORCES, 2001 Interactions between the Su(Hw) and Mod(mdg4) proteins required for gypsy insulator function. EMBO J **20:** 2518-2527.
GOLOVNIN, A., A. MAZUR, M. KOPANTSEVA, M. KURSHAKOVA, P. V. GULAK *et al.*, 2007 Integrity of the Mod(mdg4)-67.2 BTB domain is critical to insulator function in Drosophila melanogaster. Mol Cell Biol **27:** 963-974.
GOLOVNIN, A., I. VOLKOV and P. GEORGIEV, 2012 SUMO conjugation is required for the assembly of Drosophila Su(Hw) and Mod(mdg4) into insulator bodies that facilitate insulator complex formation. J Cell Sci.
GONDOR, A., and R. OHLSSON, 2008 Chromatin insulators and cohesins. EMBO Rep **9:** 327-329.
GONZALEZ-REYES, A., H. ELLIOTT and D. ST JOHNSTON, 1997 Oocyte determination and the origin of polarity in Drosophila: the role of the spindle genes. Development **124:** 4927-4937.

GONZALEZREYES, A., H. ELLIOTT and D. STJOHNSTON, 1995 Polarization of Both Major Body Axes in Drosophila by Gurken-Torpedo Signaling. Nature **375:** 654-658.
GOTTESFELD, J. M., and D. J. FORBES, 1997 Mitotic repression of the transcriptional machinery. Trends in Biochemical Sciences **22:** 197-202.
GRIEDER, N. C., M. DE CUEVAS and A. C. SPRADLING, 2000 The fusome organizes the microtubule network during oocyte differentiation in Drosophila. Development **127:** 4253-4264.
GUILD, G. M., P. S. CONNELLY, M. K. SHAW and L. G. TILNEY, 1997 Actin filament cables in Drosophila nurse cells are composed of modules that slide passively past one another during dumping. J Cell Biol **138:** 783-797.
GURUDATTA, B. V., and V. G. CORCES, 2009 Chromatin insulators: lessons from the fly. Brief Funct Genomic Proteomic **8:** 276-282.
GUTZEIT, H. O., 1986 The role of microfilaments in cytoplasmic streaming in Drosophila follicles. Journal of Cell Science **80:** 159-169.
HAGLUND, K., I. P. NEZIS and H. STENMARK, 2011 Structure and functions of stable intercellular bridges formed by incomplete cytokinesis during development. Commun Integr Biol **4:** 1-9.
HAMMOND, M. P., and C. D. LAIRD, 1985 Chromosome Structure and DNA-Replication in Nurse and Follicle Cells of Drosophila-Melanogaster. Chromosoma **91:** 267-278.
HARRISON, D. A., D. A. GDULA, R. S. COYNE and V. G. CORCES, 1993 A leucine zipper domain of the suppressor of Hairy-wing protein mediates its repressive effect on enhancer function. Genes Dev **7:** 1966-1978.
HARRISON, D. A., M. A. MORTIN and V. G. CORCES, 1992 The RNA polymerase II 15-kilodalton subunit is essential for viability in Drosophila melanogaster. Mol Cell Biol **12:** 928-935.
HILGERS, V., S. B. LEMKE and M. LEVINE, 2012 ELAV mediates 3' UTR extension in the Drosophila nervous system. Genes Dev **26:** 2259-2264.
HONG, A., K. NARBONNE-REVEAU, J. RIESGO-ESCOVAR, H. Q. FU, M. I. ALADJEM *et al.*, 2007 The cyclin-dependent kinase inhibitor Dacapo promotes replication licensing during Drosophila endocycles. Embo Journal **26:** 2071-2082.
HU, C. K., M. COUGHLIN and T. J. MITCHISON, 2012 Midbody assembly and its regulation during cytokinesis. Mol Biol Cell **23:** 1024-1034.
HULSKAMP, M., C. PFEIFLE and D. TAUTZ, 1990 A morphogenetic gradient of hunchback protein organizes the expression of the gap genes Kruppel and knirps in the early Drosophila embryo. Nature **346:** 577-580.
HUYNH, J. R., and D. ST JOHNSTON, 2004 The origin of asymmetry: early polarisation of the Drosophila germline cyst and oocyte. Curr Biol **14:** R438-449.
IRISH, V., R. LEHMANN and M. AKAM, 1989 The Drosophila Posterior-Group Gene Nanos Functions by Repressing Hunchback Activity. Nature **338:** 646-648.
JAMES, P., 2001 Yeast two-hybrid vectors and strains. Methods Mol Biol **177:** 41-84.
JAMES, P., J. HALLADAY and E. A. CRAIG, 1996 Genomic libraries and a host strain designed for highly efficient two-hybrid selection in yeast. Genetics **144:** 1425-1436.
JANG, J. K., D. E. SHERIZEN, R. BHAGAT, E. A. MANHEIM and K. S. MCKIM, 2003 Relationship of DNA double-strand breaks to synapsis in Drosophila. Journal of Cell Science **116:** 3069-3077.
JEONG, K., and J. KIM-HA, 2003 Expression of Rbp9 during mid-oogenesis induces apoptosis in egg chambers. Mol Cells **16:** 392-396.

JIANG, N., E. EMBERLY, O. CUVIER and C. M. HART, 2009 Genome-Wide Mapping of Boundary Element-Associated Factor (BEAF) Binding Sites in Drosophila melanogaster Links BEAF to Transcription. Molecular and Cellular Biology **29:** 3556-3568.

JORGENSEN, S., I. ELVERS, M. B. TRELLE, T. MENZEL, M. ESKILDSEN *et al.*, 2007 The histone methyltransferase SET8 is required for S-phase progression. Journal of Cell Biology **179:** 1337-1345.

JORGENSEN, S., G. SCHOTTA and C. S. SORENSEN, 2013 Histone H4 Lysine 20 methylation: key player in epigenetic regulation of genomic integrity. Nucleic Acids Research **41:** 2797-2806.

JOYCE, E. F., M. PEDERSEN, S. TIONG, S. K. WHITE-BROWN, A. PAUL *et al.*, 2011 Drosophila ATM and ATR have distinct activities in the regulation of meiotic DNA damage and repair. Journal of Cell Biology **195:** 359-367.

KARACHENTSEV, D., M. DRUZHININA and R. STEWARD, 2007 Free and chromatin-associated mono-, di-, and trimethylation of histone H4-lysine 20 during development and cell cycle progression. Developmental Biology **304:** 46-52.

KARACHENTSEV, D., K. SARMA, D. REINBERG and R. STEWARD, 2005 PR-Set7-dependent methylation of histone H4 Lys 20 functions in repression of gene expression and is essential for mitosis. Genes & Development **19:** 431-435.

KATOKHIN, A. V., A. V. PINDIURIN, E. V. FEDOROVA and E. M. BARICHEVA, 2001 [Molecular genetic analysis of Thrithorax-like gene encoded transcriptional factor GAGA in Drosophila melanogaster]. Genetika **37:** 467-474.

KELLUM, R., and P. SCHEDL, 1991 A position-effect assay for boundaries of higher order chromosomal domains. Cell **64:** 941-950.

KELSO, R. J., A. M. HUDSON and L. COOLEY, 2002 Drosophila Kelch regulates actin organization via Src64-dependent tyrosine phosphorylation. J Cell Biol **156:** 703-713.

KHURANA, J. S., and W. THEURKAUF, 2010 piRNAs, transposon silencing, and Drosophila germline development. Journal of Cell Biology **191:** 905-913.

KIM, J., B. SHEN, C. ROSEN and D. DORSETT, 1996 The DNA-binding and enhancer-blocking domains of the Drosophila suppressor of Hairy-wing protein. Mol Cell Biol **16:** 3381-3392.

KIM, Y. J., and B. S. BAKER, 1993 The Drosophila gene rbp9 encodes a protein that is a member of a conserved group of putative RNA binding proteins that are nervous system-specific in both flies and humans. J Neurosci **13:** 1045-1056.

KIM-HA, J., J. L. SMITH and P. M. MACDONALD, 1991 oskar mRNA is localized to the posterior pole of the Drosophila oocyte. Cell **66:** 23-35.

KITCHEN, N. S., and C. J. SCHOENHERR, 2010 Sumoylation modulates a domain in CTCF that activates transcription and decondenses chromatin. J Cell Biochem **111:** 665-675.

KLATTENHOFF, C., D. P. BRATU, N. MCGINNIS-SCHULTZ, B. S. KOPPETSCH, H. A. COOK *et al.*, 2007 Drosophila rasiRNA pathway mutations disrupt embryonic axis specification through activation of an ATR/Chk2 DNA damage response. Developmental Cell **12:** 45-55.

KLATTENHOFF, C., H. XI, C. LI, S. LEE, J. XU *et al.*, 2009 The Drosophila HP1 homolog Rhino is required for transposon silencing and piRNA production by dual-strand clusters. Cell **138:** 1137-1149.

KLENOVA, E. M., R. H. NICOLAS, H. F. PATERSON, A. F. CARNE, C. M. HEATH *et al.*, 1993 Ctcf, a Conserved Nuclear Factor Required for Optimal Transcriptional Activity of the

Chicken C-Myc Gene, Is an 11-Zn-Finger Protein Differentially Expressed in Multiple Forms. Molecular and Cellular Biology **13:** 7612-7624.

KLUG, W. S., D. BODENSTEIN and R. C. KING, 1968 Oogenesis in the suppressor of hairy-wing mutant of Drosophila melanogaster. I. Phenotypic characterization and transplantation experiments. J Exp Zool **167:** 151-156.

KLUG, W. S., R. C. KING and J. M. WATTIAUX, 1970 Oogenesis in the suppressor of hairy-wing mutant of Drosophila melanogaster. II. Nucleolar morphology and in vitro studies of RNA protein synthesis. J Exp Zool **174:** 125-140.

KORNBERG, R. D., and Y. L. LORCH, 1999 Twenty-five years of the nucleosome, fundamental particle of the eukaryote chromosome. Cell **98:** 285-294.

KUGLER, J. M., and P. LASKO, 2009 Localization, anchoring and translational control of oskar, gurken, bicoid and nanos mRNA during Drosophila oogenesis. Fly (Austin) **3:** 15-28.

KUO, T. C., C. T. CHEN, D. BARON, T. T. ONDER, S. LOEWER *et al.*, 2011 Midbody accumulation through evasion of autophagy contributes to cellular reprogramming and tumorigenicity. Nat Cell Biol **13:** 1214-1223.

LABRADOR, M., and V. G. CORCES, 2002 Setting the boundaries of chromatin domains and nuclear organization. Cell **111:** 151-154.

LAKE, C. M., J. K. HOLSCLAW, S. P. BELLENDIR, J. SEKELSKY and R. S. HAWLEY, 2013 The Development of a Monoclonal Antibody Recognizing the Drosophila melanogaster Phosphorylated Histone H2A Variant (gamma-H2AV). G3-Genes Genomes Genetics **3:** 1539-1543.

LALL, S., 1998 Transcript localisation and nuclear polarity during the early development of drosophila melanogaster, pp. 148 leaves, [138 leaves of plates]. University of Oxford, 1998.

LANKENAU, D. H., M. V. PELUSO and S. LANKENAU, 2000 The Su(Hw) chromatin insulator protein alters double-strand break repair frequencies in the Drosophila germ line. Chromosoma **109:** 148-160.

LAROCQUE, J. R., B. JAKLEVIC, T. T. SU and J. SEKELSKY, 2007 Drosophila ATR in double-strand break repair. Genetics **175:** 1023-1033.

LEATHERMAN, J. L., and S. DINARDO, 2010 Germline self-renewal requires cyst stem cells and stat regulates niche adhesion in Drosophila testes. Nat Cell Biol **12:** 806-811.

LEE, B. K., and V. R. IYER, 2012 Genome-wide Studies of CCCTC-binding Factor (CTCF) and Cohesin Provide Insight into Chromatin Structure and Regulation. Journal of Biological Chemistry **287:** 30906-30913.

LILLY, M. A., and A. C. SPRADLING, 1996 The Drosophila endocycle is controlled by cyclin E and lacks a checkpoint ensuring S-phase completion. Genes & Development **10:** 2514-2526.

LIN, H., L. YUE and A. C. SPRADLING, 1994 The Drosophila fusome, a germline-specific organelle, contains membrane skeletal proteins and functions in cyst formation. Development **120:** 947-956.

LIN, H. F., and A. C. SPRADLING, 1995 Fusome Asymmetry and Oocyte Determination in Drosophila. Developmental Genetics **16:** 6-12.

LOBANENKOV, V. V., V. V. ADLER, E. M. KLENOVA, R. H. NICOLAS and G. H. GOODWIN, 1990 Ccctc-Binding Factor (Ctcf) - a Novel Sequence-Specific DNA-Binding Protein Which Interacts with the 5'-Flanking Sequence of the Chicken C-Myc Gene. Gene Regulation and Aids : Transcriptional Activation, Retroviruses, and Pathogenesis **7:** 45-68.

LU, L., and J. TOWER, 1997 A transcriptional insulator element, the su(Hw) binding site, protects a chromosomal DNA replication origin from position effects. Molecular and Cellular Biology **17:** 2202-2206.
MACPHERSON, M. J., L. G. BEATTY, W. ZHOU, M. DU and P. D. SADOWSKI, 2009a The CTCF insulator protein is posttranslationally modified by SUMO. Mol Cell Biol **29:** 714-725.
MACPHERSON, M. J., L. G. BEATTY, W. J. ZHOU, M. J. DU and P. D. SADOWSKI, 2009b The CTCF Insulator Protein Is Posttranslationally Modified by SUMO. Molecular and Cellular Biology **29:** 714-725.
MARSMAN, J., and J. A. HORSFIELD, 2012 Long distance relationships: enhancer-promoter communication and dynamic gene transcription. Biochim Biophys Acta **1819:** 1217-1227.
MATA, J., S. CURADO, A. EPHRUSSI and P. RORTH, 2000 Tribbles coordinates mitosis and morphogenesis in Drosophila by regulating string/CDC25 proteolysis. Cell **101:** 511-522.
MCKIM, K. S., and A. HAYASHI-HAGIHARA, 1998 mei-W68 in Drosophila melanogaster encodes a Spo11 homolog: evidence that the mechanism for initiating meiotic recombination is conserved. Genes Dev **12:** 2932-2942.
MEHROTRA, S., S. B. MAQBOOL, A. KOLPAKAS, K. MURNEN and B. R. CALVI, 2008 Endocycling cells do not apoptose in response to DNA rereplication genotoxic stress. Genes & Development **22:** 3158-3171.
MEHROTRA, S., and K. S. MCKIM, 2006 Temporal analysis of meiotic DNA double-strand break formation and repair in Drosophila females. Plos Genetics **2:** 1883-1897.
MISTELI, T., 2007 Beyond the sequence: cellular organization of genome function. Cell **128:** 787-800.
MODOLELL, J., W. BENDER and M. MESELSON, 1983 Drosophila melanogaster mutations suppressible by the suppressor of Hairy-wing are insertions of a 7.3-kilobase mobile element. Proc Natl Acad Sci U S A **80:** 1678-1682.
MOHAN, M., M. BARTKUHN, M. HEROLD, A. PHILIPPEN, N. HEINL *et al.*, 2007 The Drosophila insulator proteins CTCF and CP190 link enhancer blocking to body patterning. EMBO J **26:** 4203-4214.
MOON, H., G. FILIPPOVA, D. LOUKINOV, E. PUGACHEVA, Q. CHEN *et al.*, 2005 CTCF is conserved from Drosophila to humans and confers enhancer blocking of the Fab-8 insulator. EMBO Rep **6:** 165-170.
MOQTADERI, Z., J. WANG, D. RAHA, R. J. WHITE, M. SNYDER *et al.*, 2010 Genomic binding profiles of functionally distinct RNA polymerase III transcription complexes in human cells. Nat Struct Mol Biol **17:** 635-640.
MORAIS-DE-SA, E., and C. SUNKEL, 2013 Adherens junctions determine the apical position of the midbody during follicular epithelial cell division. EMBO Rep **14:** 696-703.
MORRIS, J., and R. LEHMANN, 1999 Drosophila oogenesis: versatile spn doctors. Curr Biol **9:** R55-58.
MOSHKOVICH, N., P. NISHA, P. J. BOYLE, B. A. THOMPSON, R. K. DALE *et al.*, 2011 RNAi-independent role for Argonaute2 in CTCF/CP190 chromatin insulator function. Genes Dev **25:** 1686-1701.
NEUMAN-SILBERBERG, F. S., and T. SCHUPBACH, 1993 The Drosophila dorsoventral patterning gene gurken produces a dorsally localized RNA and encodes a TGF alpha-like protein. Cell **75:** 165-174.

NEUMANSILBERBERG, F. S., and T. SCHUPBACH, 1993 The Drosophila Dorsoventral Patterning Gene Gurken Produces a Dorsally Localized Rna and Encodes a Tgf-Alpha-Like Protein. Cell **75:** 165-174.

OEGEMA, K., W. G. WHITFIELD and B. ALBERTS, 1995 The cell cycle-dependent localization of the CP190 centrosomal protein is determined by the coordinate action of two separable domains. J Cell Biol **131:** 1261-1273.

OHLSSON, R., V. LOBANENKOV and E. KLENOVA, 2010 Does CTCF mediate between nuclear organization and gene expression? Bioessays **32:** 37-50.

OHTSUKI, S., and M. LEVINE, 1998 GAGA mediates the enhancer blocking activity of the eve promoter in the Drosophila embryo. Genes Dev **12:** 3325-3330.

ONG, C. T., and V. G. CORCES, 2011 Enhancer function: new insights into the regulation of tissue-specific gene expression. Nat Rev Genet **12:** 283-293.

ONG, C. T., K. VAN BORTLE, E. RAMOS and V. G. CORCES, 2013 Poly(ADP-ribosyl)ation regulates insulator function and intrachromosomal interactions in Drosophila. Cell **155:** 148-159.

PAGE, S. L., and R. S. HAWLEY, 2001 c(3)G encodes a Drosophila synaptonemal complex protein. Genes Dev **15:** 3130-3143.

PAI, C. Y., E. P. LEI, D. GHOSH and V. G. CORCES, 2004 The centrosomal protein CP190 is a component of the gypsy chromatin insulator. Mol Cell **16:** 737-748.

PARELHO, V., S. HADJUR, M. SPIVAKOV, M. LELEU, S. SAUER *et al.*, 2008 Cohesins functionally associate with CTCF on mammalian chromosome arms. Cell **132:** 422-433.

PARK, S. J., E. S. YANG, J. KIM-HA and Y. J. KIM, 1998 Down regulation of extramacrochaetae mRNA by a Drosophila neural RNA binding protein Rbp9 which is homologous to human Hu proteins. Nucleic Acids Res **26:** 2989-2994.

PARKHURST, S. M., and V. G. CORCES, 1985 Forked, Gypsys, and Suppressors in Drosophila. Cell **41:** 429-437.

PARKHURST, S. M., and V. G. CORCES, 1986 Interactions among the Gypsy Transposable Element and the Yellow and the Suppressor of Hairy-Wing Loci in Drosophila-Melanogaster. Molecular and Cellular Biology **6:** 47-53.

PARKHURST, S. M., D. A. HARRISON, M. P. REMINGTON, C. SPANA, R. L. KELLEY *et al.*, 1988 The Drosophila Su(Hw) Gene, Which Controls the Phenotypic Effect of the Gypsy Transposable Element, Encodes a Putative DNA-Binding Protein. Genes & Development **2:** 1205-1215.

PETRELLA, L. N., T. SMITH-LEIKER and L. COOLEY, 2007 The Ovhts polyprotein is cleaved to produce fusome and ring canal proteins required for Drosophila oogenesis. Development **134:** 703-712.

PHILLIPS-CREMINS, J. E., and V. G. CORCES, 2013 Chromatin Insulators: Linking Genome Organization to Cellular Function. Molecular Cell **50:** 461-474.

POKRYWKA, N. J., and E. C. STEPHENSON, 1995 Microtubules are a general component of mRNA localization systems in Drosophila oocytes. Dev Biol **167:** 363-370.

POLLAROLO, G., J. G. SCHULZ, S. MUNCK and C. G. DOTTI, 2011 Cytokinesis remnants define first neuronal asymmetry in vivo. Nat Neurosci **14:** 1525-1533.

PRITCHETT, T. L., E. A. TANNER and K. MCCALL, 2009 Cracking open cell death in the Drosophila ovary. Apoptosis **14:** 969-979.

RAAB, J. R., J. CHIU, J. ZHU, S. KATZMAN, S. KURUKUTI *et al.*, 2012 Human tRNA genes function as chromatin insulators. EMBO J **31:** 330-350.

RAMOS, E., D. GHOSH, E. BAXTER and V. G. CORCES, 2006 Genomic organization of gypsy chromatin insulators in Drosophila melanogaster. Genetics **172:** 2337-2349.
REN, J., X. GAO, C. JIN, M. ZHU, X. WANG *et al.*, 2009 Systematic study of protein sumoylation: Development of a site-specific predictor of SUMOsp 2.0. Proteomics **9:** 3409-3412.
RIECHMANN, V., and A. EPHRUSSI, 2001 Axis formation during Drosophila oogenesis. Current Opinion in Genetics & Development **11:** 374-383.
ROBINSON, D. N., K. CANT and L. COOLEY, 1994 Morphogenesis of Drosophila ovarian ring canals. Development **120:** 2015-2025.
ROBINSON, D. N., and L. COOLEY, 1997 Drosophila kelch is an oligomeric ring canal actin organizer. Journal of Cell Biology **138:** 799-810.
RORTH, P., 1998 Gal4 in the Drosophila female germline. Mech Dev **78:** 113-118.
ROTH, S., and J. A. LYNCH, 2009 Symmetry breaking during Drosophila oogenesis. Cold Spring Harb Perspect Biol **1:** a001891.
ROTH, S., F. S. NEUMAN-SILBERBERG, G. BARCELO and T. SCHUPBACH, 1995 cornichon and the EGF receptor signaling process are necessary for both anterior-posterior and dorsal-ventral pattern formation in Drosophila. Cell **81:** 967-978.
ROY, S., M. K. GILBERT and C. M. HART, 2007 Characterization of BEAF mutations isolated by homologous recombination in Drosophila. Genetics **176:** 801-813.
RUBIO, E. D., D. J. REISS, P. L. WELCSH, C. M. DISTECHE, G. N. FILIPPOVA *et al.*, 2008 CTCF physically links cohesin to chromatin. Proc Natl Acad Sci U S A **105:** 8309-8314.
RUCHAUD, S., M. CARMENA and W. C. EARNSHAW, 2007 Chromosomal passengers: conducting cell division. Nat Rev Mol Cell Biol **8:** 798-812.
SAKAGUCHI, A., E. JOYCE, T. AOKI, P. SCHEDL and R. STEWARD, 2012 The Histone H4 Lysine 20 Monomethyl Mark, Set by PR-Set7 and Stabilized by L(3)mbt, Is Necessary for Proper Interphase Chromatin Organization. PLoS One **7**.
SAKAGUCHI, A., and R. STEWARD, 2007 Aberrant monomethylation of histone H4 lysine 20 activates the DNA damage checkpoint in Drosophila melanogaster. Journal of Cell Biology **176:** 155-162.
SANCAR, A., L. A. LINDSEY-BOLTZ, K. UNSAL-KACMAZ and S. LINN, 2004 Molecular mechanisms of mammalian DNA repair and the DNA damage checkpoints. Annual Review of Biochemistry **73:** 39-85.
SATO, K., K. M. NISHIDA, A. SHIBUYA, M. C. SIOMI and H. SIOMI, 2011a Maelstrom coordinates microtubule organization during Drosophila oogenesis through interaction with components of the MTOC. Genes Dev **25:** 2361-2373.
SATO, K., K. M. NISHIDA, A. SHIBUYA, M. C. SIOMI and H. SIOMI, 2011b Maelstrom coordinates microtubule organization during Drosophila oogenesis through interaction with components of the MTOC. Genes & Development **25:** 2361-2373.
SCHINK, K. O., and H. STENMARK, 2011 Cell differentiation: midbody remnants - junk or fate factors? Curr Biol **21:** R958-960.
SCHNORRER, F., K. BOHMANN and C. NUSSLEIN-VOLHARD, 2000 The molecular motor dynein is involved in targeting Swallow and bicoid RNA to the anterior pole of Drosophila oocytes. Nature Cell Biology **2:** 185-190.
SCHOBORG, T., R. RICKELS, J. BARRIOS and M. LABRADOR, 2013 Chromatin insulator bodies are nuclear structures that form in response to osmotic stress and cell death. J Cell Biol **202:** 261-276.

SCHOBORG, T. A., and M. LABRADOR, 2010 The phylogenetic distribution of non-CTCF insulator proteins is limited to insects and reveals that BEAF-32 is Drosophila lineage specific. J Mol Evol **70:** 74-84.

SCHUPBACH, T., 1987 Germ Line and Soma Cooperate during Oogenesis to Establish the Dorsoventral Pattern of Eggshell and Embryo in Drosophila-Melanogaster. Cell **49:** 699-707.

SHIH, H. P., K. G. HALES, J. R. PRINGLE and M. PEIFER, 2002 Identification of septin-interacting proteins and characterization of the Smt3/SUMO-conjugation system in Drosophila. Journal of Cell Science **115:** 1259-1271.

SHUKLA, S., E. KAVAK, M. GREGORY, M. IMASHIMIZU, B. SHUTINOSKI *et al.*, 2011 CTCF-promoted RNA polymerase II pausing links DNA methylation to splicing. Nature **479:** 74-U99.

SIENSKI, G., D. DONERTAS and J. BRENNECKE, 2012 Transcriptional Silencing of Transposons by Piwi and Maelstrom and Its Impact on Chromatin State and Gene Expression. Cell **151:** 964-980.

SKOP, A. R., H. LIU, J. YATES, 3RD, B. J. MEYER and R. HEALD, 2004 Dissection of the mammalian midbody proteome reveals conserved cytokinesis mechanisms. Science **305:** 61-66.

SLOTKIN, R. K., and R. MARTIENSSEN, 2007 Transposable elements and the epigenetic regulation of the genome. Nat Rev Genet **8:** 272-285.

SMITH, M., V. BHASKAR, J. FERNANDEZ and A. J. COUREY, 2004 Drosophila Ulp1, a nuclear pore-associated SUMO protease, prevents accumulation of cytoplasmic SUMO conjugates. J Biol Chem **279:** 43805-43814.

SOKOL, N. S., and L. COOLEY, 2003 Drosophila filamin is required for follicle cell motility during oogenesis. Dev Biol **260:** 260-272.

SOLLER, M., M. LI and I. U. HAUSSMANN, 2010 Determinants of ELAV gene-specific regulation. Biochem Soc Trans **38:** 1122-1124.

SOSHNEV, A. A., R. M. BAXLEY, J. R. MANAK, K. TAN and P. K. GEYER, 2013 The insulator protein Suppressor of Hairy wing is an essential transcriptional repressor in the Drosophila ovary. Development.

SOSHNEV, A. A., B. HE, R. M. BAXLEY, N. JIANG, C. M. HART *et al.*, 2012 Genome-wide studies of the multi-zinc finger Drosophila Suppressor of Hairy-wing protein in the ovary. Nucleic Acids Res **40:** 5415-5431.

SPANA, C., D. A. HARRISON and V. G. CORCES, 1988 The Drosophila-Melanogaster-Suppressor of Hairy-Wing Protein Binds to Specific Sequences of the Gypsy Retrotransposon. Genes & Development **2:** 1414-1423.

STEINHAUER, J., and D. KALDERON, 2006 Microtubule polarity and axis formation in the Drosophila oocyte. Developmental Dynamics **235:** 1455-1468.

SUBRAMANIAN, A., P. TAMAYO, V. K. MOOTHA, S. MUKHERJEE, B. L. EBERT *et al.*, 2005 Gene set enrichment analysis: A knowledge-based approach for interpreting genome-wide expression profiles. Proceedings of the National Academy of Sciences of the United States of America **102:** 15545-15550.

SULLIVAN, W., M. ASHBURNER and R. S. HAWLEY, 2000 *Drosophila protocols*. Cold Spring Harbor Laboratory Press, Cold Spring Harbor, NY.

TARDAT, M., J. BRUSTEL, O. KIRSH, C. LEFEVBRE, M. CALLANAN *et al.*, 2010 The histone H4 Lys 20 methyltransferase PR-Set7 regulates replication origins in mammalian cells. Nature Cell Biology **12:** 1086-U1082.

TECHNAU, M., M. KNISPEL and S. ROTH, 2012 Molecular mechanisms of EGF signaling-dependent regulation of pipe, a gene crucial for dorsoventral axis formation in Drosophila. Development Genes and Evolution **222:** 1-17.
THEURKAUF, W. E., S. SMILEY, M. L. WONG and B. M. ALBERTS, 1992 Reorganization of the cytoskeleton during Drosophila oogenesis: implications for axis specification and intercellular transport. Development **115:** 923-936.
UDVARDY, A., E. MAINE and P. SCHEDL, 1985 The 87A7 chromomere. Identification of novel chromatin structures flanking the heat shock locus that may define the boundaries of higher order domains. J Mol Biol **185:** 341-358.
ULRICH, H. D., 2012 Ubiquitin, SUMO, and phosphate: how a trio of posttranslational modifiers governs protein fate. Mol Cell **47:** 335-337.
VADER, G., and S. M. LENS, 2008 The Aurora kinase family in cell division and cancer. Biochim Biophys Acta **1786:** 60-72.
VAN BEMMEL, J. G., L. PAGIE, U. BRAUNSCHWEIG, W. BRUGMAN, W. MEULEMAN *et al.*, 2010 The insulator protein SU(HW) fine-tunes nuclear lamina interactions of the Drosophila genome. PLoS One **5:** e15013.
VAN BORTLE, K., and V. G. CORCES, 2012a Nuclear Organization and Genome Function. Annual Review of Cell and Developmental Biology, Vol 28 **28:** 163-187.
VAN BORTLE, K., and V. G. CORCES, 2012b tDNA insulators and the emerging role of TFIIIC in genome organization. Transcription **3:** 277-284.
VAN DOREN, M., A. L. WILLIAMSON and R. LEHMANN, 1998 Regulation of zygotic gene expression in Drosophila primordial germ cells. Current Biology **8:** 243-246.
VOLPE, A. M., H. HOROWITZ, C. M. GRAFER, S. M. JACKSON and C. A. BERG, 2001 Drosophila rhino encodes a female-specific chromo-domain protein that affects chromosome structure and egg polarity. Genetics **159:** 1117-1134.
VOROBYEVA, N. E., M. U. MAZINA, A. K. GOLOVNIN, D. V. KOPYTOVA, D. Y. GURSKIY *et al.*, 2013 Insulator protein Su(Hw) recruits SAGA and Brahma complexes and constitutes part of Origin Recognition Complex-binding sites in the Drosophila genome. Nucleic Acids Research **41:** 5717-5730.
WALLACE, H. A., M. P. PLATA, H. J. KANG, M. ROSS and M. LABRADOR, 2010 Chromatin insulators specifically associate with different levels of higher-order chromatin organization in Drosophila. Chromosoma **119:** 177-194.
WALLACE, J. A., and G. FELSENFELD, 2007 We gather together: insulators and genome organization. Curr Opin Genet Dev **17:** 400-407.
WANG, H., M. T. MAURANO, H. Z. QU, K. E. VARLEY, J. GERTZ *et al.*, 2012 Widespread plasticity in CTCF occupancy linked to DNA methylation. Genome Research **22:** 1680-1688.
WANG, J., and M. F. WILKINSON, 2000 Site-directed mutagenesis of large (13-kb) plasmids in a single-PCR procedure. Biotechniques **29:** 976-978.
WENDT, K. S., K. YOSHIDA, T. ITOH, M. BANDO, B. KOCH *et al.*, 2008 Cohesin mediates transcriptional insulation by CCCTC-binding factor. Nature **451:** 796-801.
WEST, A. G., M. GASZNER and G. FELSENFELD, 2002 Insulators: many functions, many mechanisms. Genes Dev **16:** 271-288.
WILCOCK, A. C., J. R. SWEDLOW and K. G. STOREY, 2007 Mitotic spindle orientation distinguishes stem cell and terminal modes of neuron production in the early spinal cord. Development **134:** 1943-1954.

WU, S. M., and J. C. RICE, 2011 A new regulator of the cell cycle The PR-Set7 histone methyltransferase. Cell Cycle **10:** 68-72.
WU, Z. J., R. A. IRIZARRY, R. GENTLEMAN, F. MARTINEZ-MURILLO and F. SPENCER, 2004 A model-based background adjustment for oligonucleotide expression arrays. Journal of the American Statistical Association **99:** 909-917.
XUE, F., and L. COOLEY, 1993 kelch encodes a component of intercellular bridges in Drosophila egg chambers. Cell **72:** 681-693.
XUE, Y., J. REN, X. J. GAO, C. J. JIN, L. P. WEN *et al.*, 2008 GPS 2.0, a tool to predict kinase-specific phosphorylation sites in hierarchy. Molecular & Cellular Proteomics **7:** 1598-1608.
YANG, J., and V. G. CORCES, 2012 Insulators, long-range interactions, and genome function. Curr Opin Genet Dev **22:** 86-92.
YIN, H., and H. F. LIN, 2007 An epigenetic activation role of Piwi and a Piwi-associated piRNA in Drosophila melanogaster. Nature **450:** 304-U316.
YU, W. Q., V. GINJALA, V. PANT, I. CHERNUKHIN, J. WHITEHEAD *et al.*, 2004 Poly(ADP-ribosyl)ation regulates CTCF-dependent chromatin insulation. Nature Genetics **36:** 1105-1110.
YUE, L., and A. C. SPRADLING, 1992 hu-li tai shao, a gene required for ring canal formation during Drosophila oogenesis, encodes a homolog of adducin. Genes Dev **6:** 2443-2454.
ZENTNER, G. E., and S. HENIKOFF, 2013 Regulation of nucleosome dynamics by histone modifications. Nature Structural & Molecular Biology **20:** 259-266.
ZHANG, R., L. J. BURKE, J. E. J. RASKO, V. LOBANENKOV and R. RENKAWITZ, 2004 Dynamic association of the mammalian insulator protein CTCF with centrosomes and the midbody. Experimental Cell Research **294:** 86-93.
ZHAO, K., C. M. HART and U. K. LAEMMLI, 1995 Visualization of chromosomal domains with boundary element-associated factor BEAF-32. Cell **81:** 879-889.

# APPENDIX

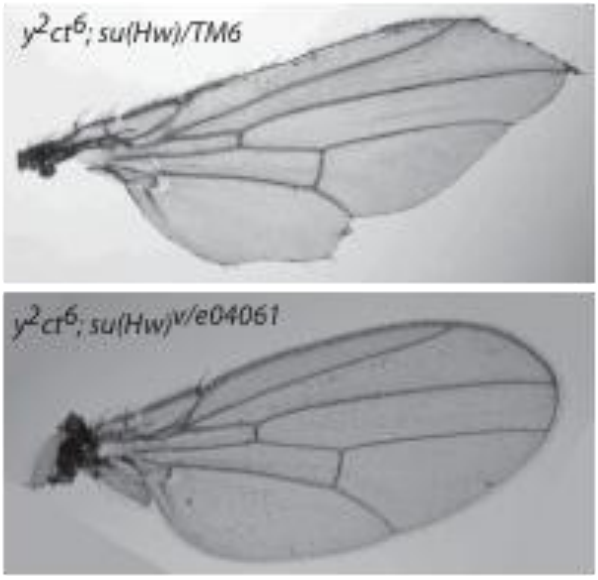


**Figure A1. Insulator activity assay.**

A phenotypic marker, $ct^6$, results from an insertion of the *gypsy* retrotransposon between the wing margin enhancer and the *cut* gene promoter, showing a jagged shape of wing edge (GAUSE *et al.* 2001). Here, $y^2ct^6$*; su(Hw)*$^+$ shows jagged wings, indicating functional insulator activity, yet the $y^2ct^6$*; su(Hw)*$^{v/e04061}$ does not.

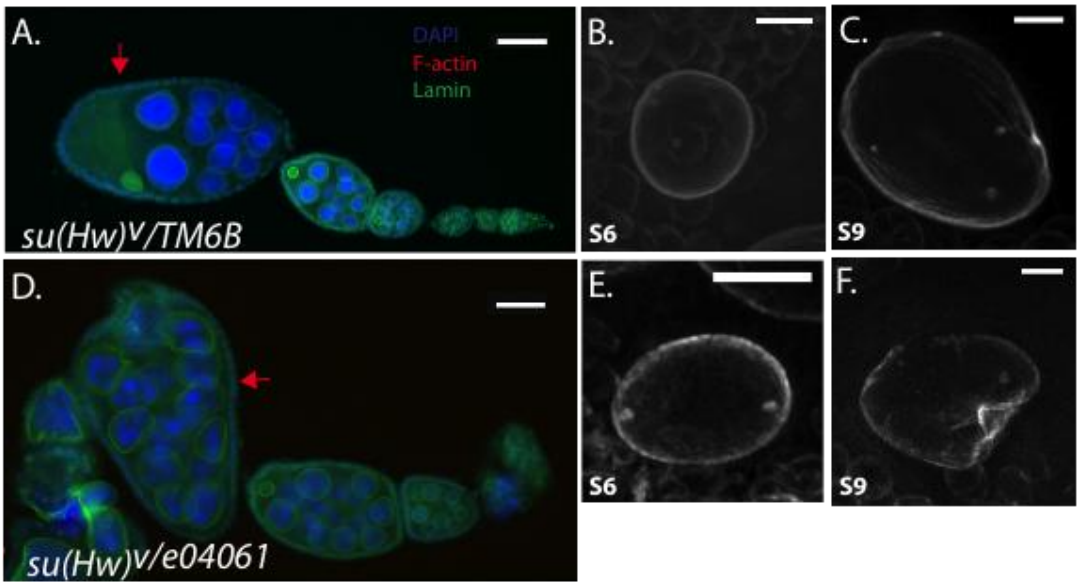


**Figure A2. Degenerated egg chambers during mid-oogenesis in *su(Hw)* mutants.**

The green-staining lamin shows the disrupted nurse cell nuclear lamin at stage nine in mutants but not wild-type (A). Arrows point to the stage nine egg chambers. The oocytes of stage six and nine were cropped for better resolution, and wild-type oocytes are shown in B and C and mutants in E and F. The scale bars are 50 μm in A and D, and 5 μm in B, C, E and F.

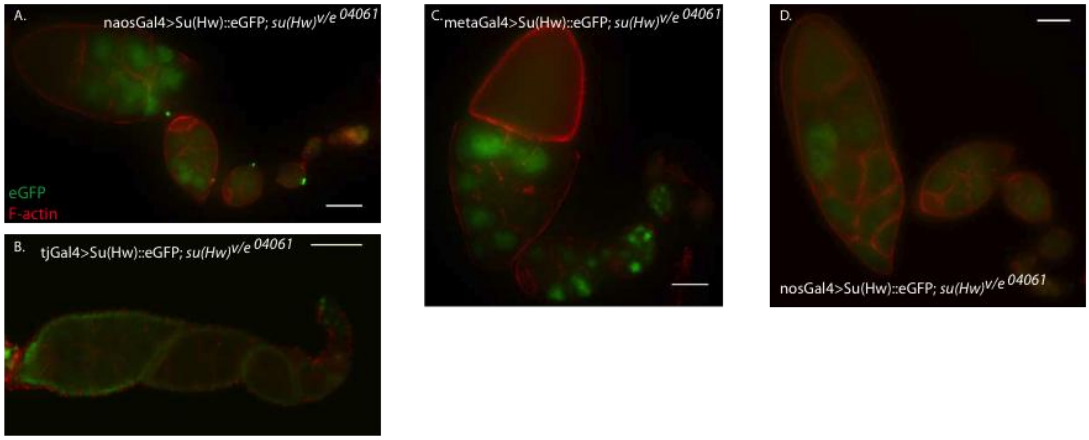


**Figure A3. Su(GFP)::GFP expression driven by various GAL4 drivers.**

The egg chambers were stained with GFP antibody in green and F-actin in red. Each image was labeled with its genotype, and the scale bar is equivalent to 50 μm.

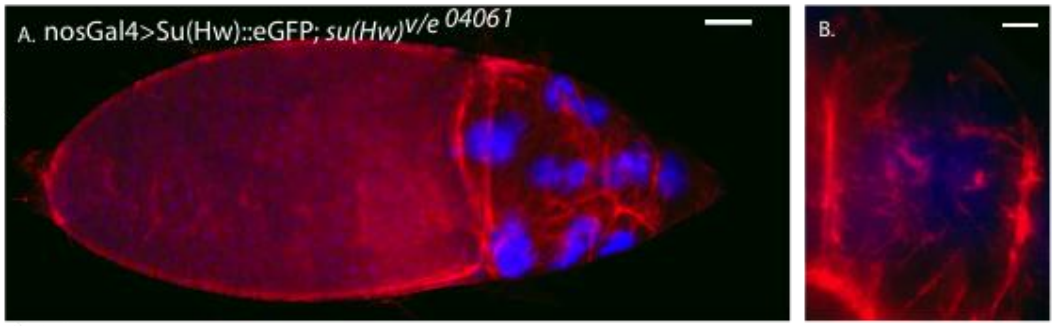


**Figure A4. Nurse cell dumping ocurrs while Su(Hw) is expressed in germline cells.**

*nos*Gal4 rescued ovaries were stained red for F-actin using phalloidin conjugated with TexRed at stage 10B (A). A zoom-in image was shown in (B). The scale bar is equal to 50 μm in A and 10 μm in B.

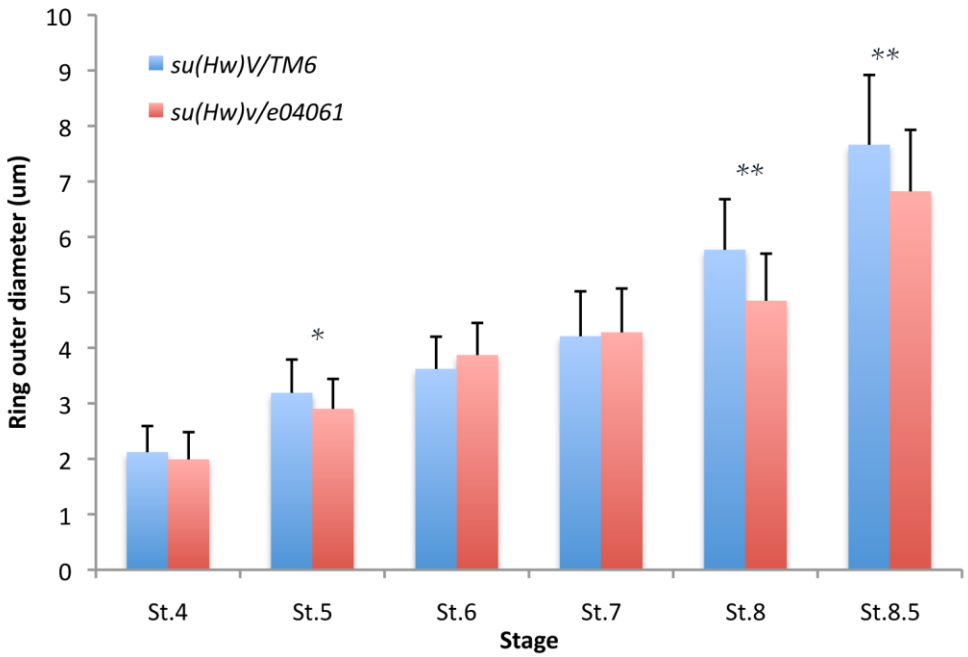


**Figure A5. The outer diameter of ring canals are different between wild-type and su(Hw) mutants.**

The outer ring diameter was measured in egg chambers of both genotypes and the bar chart shows the average outer ring diameter at each stage as labeled with colors. Single asterisks indicate $P < 0.05$ and double asterisks indicate $P < 0.001$.

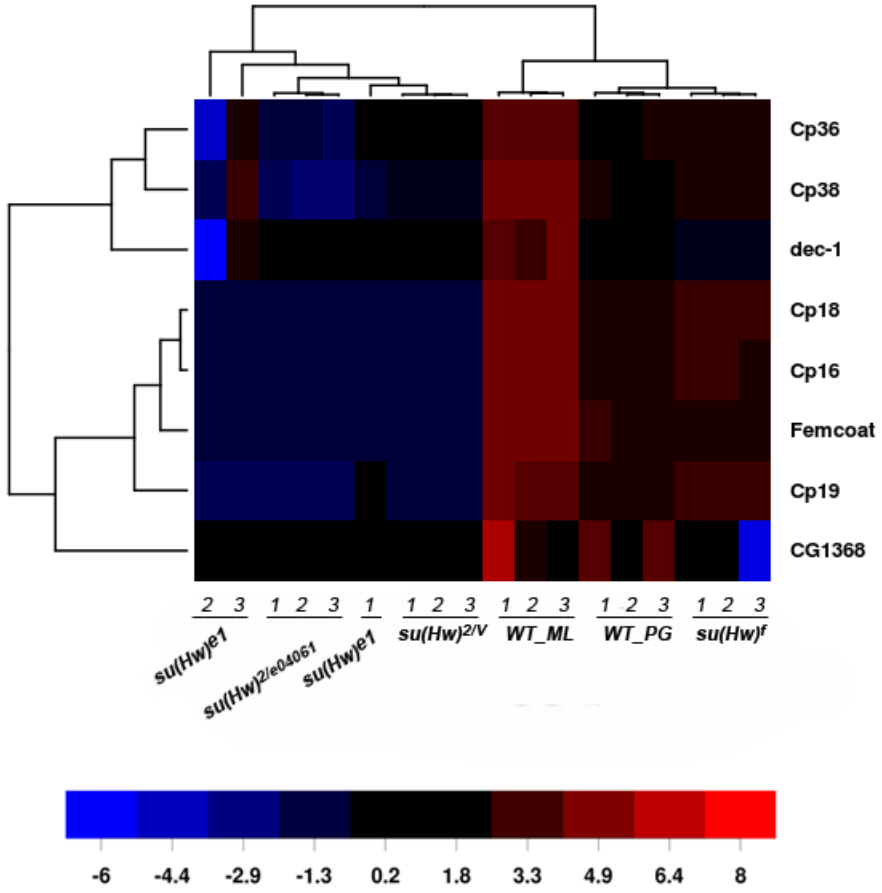


**Figure A6. The microarray heatmaps.**

**A6-A. The heatmap of structural constituent of chorion.**

The array data from different *su(Hw)* mutants was analyzed using the gene set enrichment analysis **(**GSEA) and flies were clustered based on genes in "structural constituent of chorion". Each mutant has three repeats.

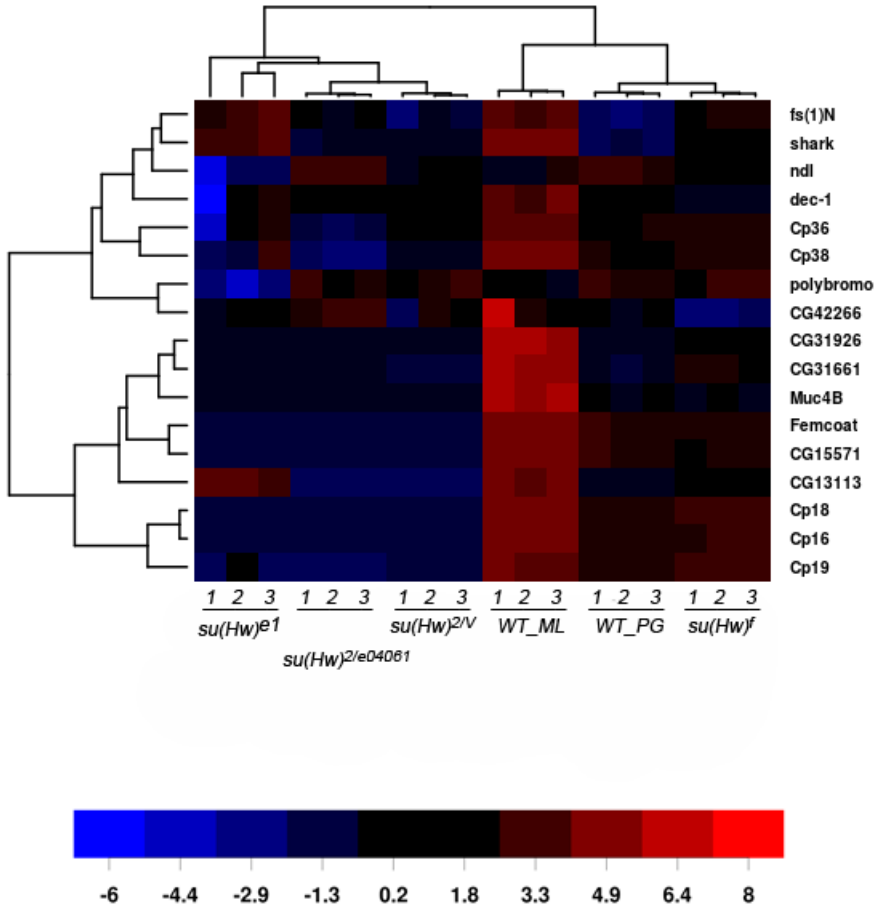


**A6-B. The heatmap of multi-cellular organism development**

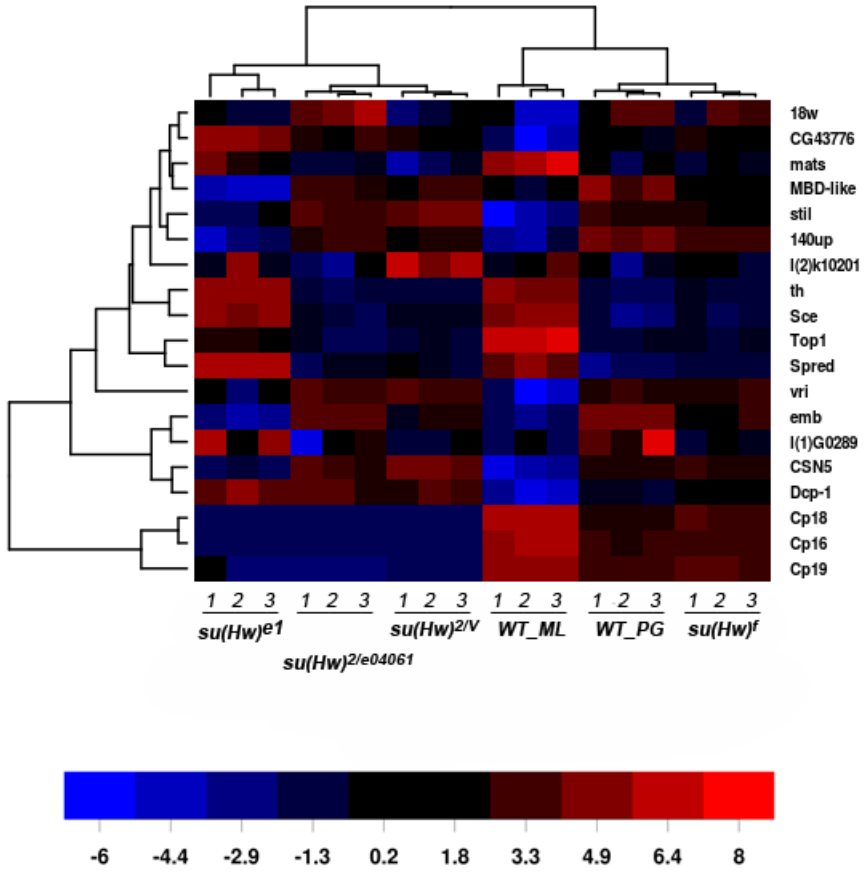


**A6-C. The heatmap of eggshell chorion assembly.**

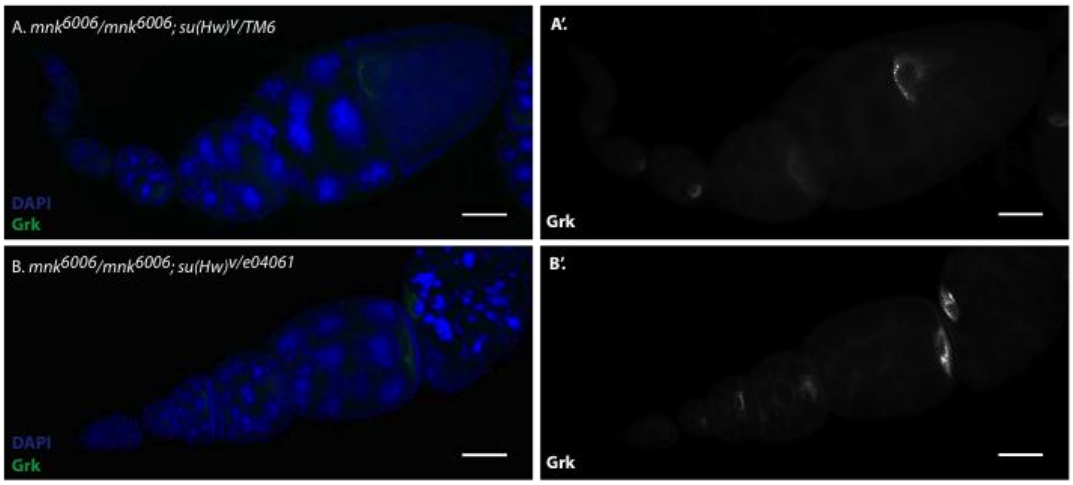


**Figure A7. Loss of Chk2 does not rescue oogenesis defects in *su(Hw)* mutants.**

Gurken was labeled in green and the signal was detected in different genotype egg chambers with DAPI staining (A and B). The Gurken only signal is shown in *mnk*$^{6006}$ homozygotes and the *mnk*$^{6006}$ ; *su(Hw)* double mutants.

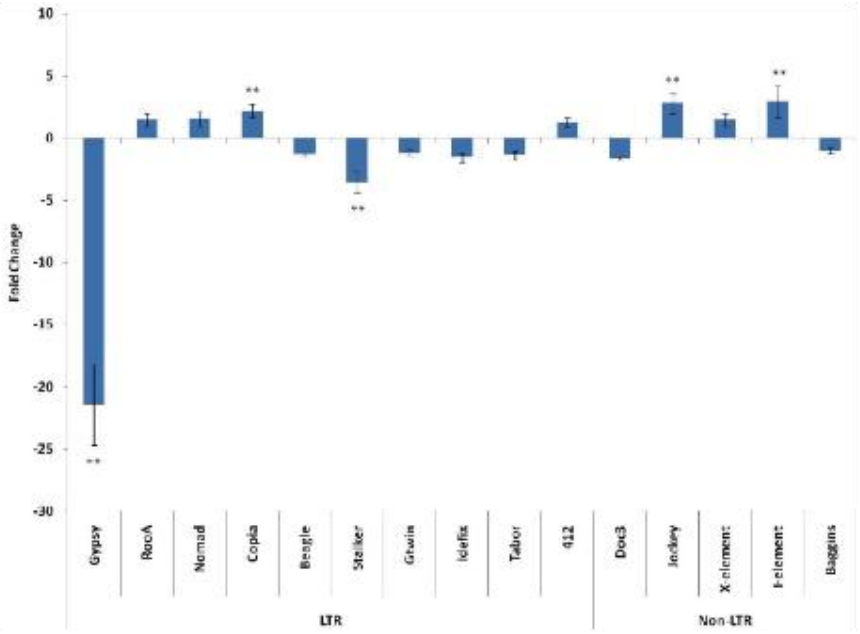


**Figure A8. The fold change of transcript levels of TEs in *su(Hw)*$^{e04061}$ compared to wild-type.**

Transcript levels of TEs were quantified by real-time PCR and were normalized to rp49. Fold change values represent the relative expression of mRNA in ovaries from *su(Hw)*$^{e04061}$ homozygotes compared with ovaries from *su(Hw)*$^{e04061}$ heterozygotes. The late egg chambers of each sample are removed. Two asterisks indicate $P < 0.001$.

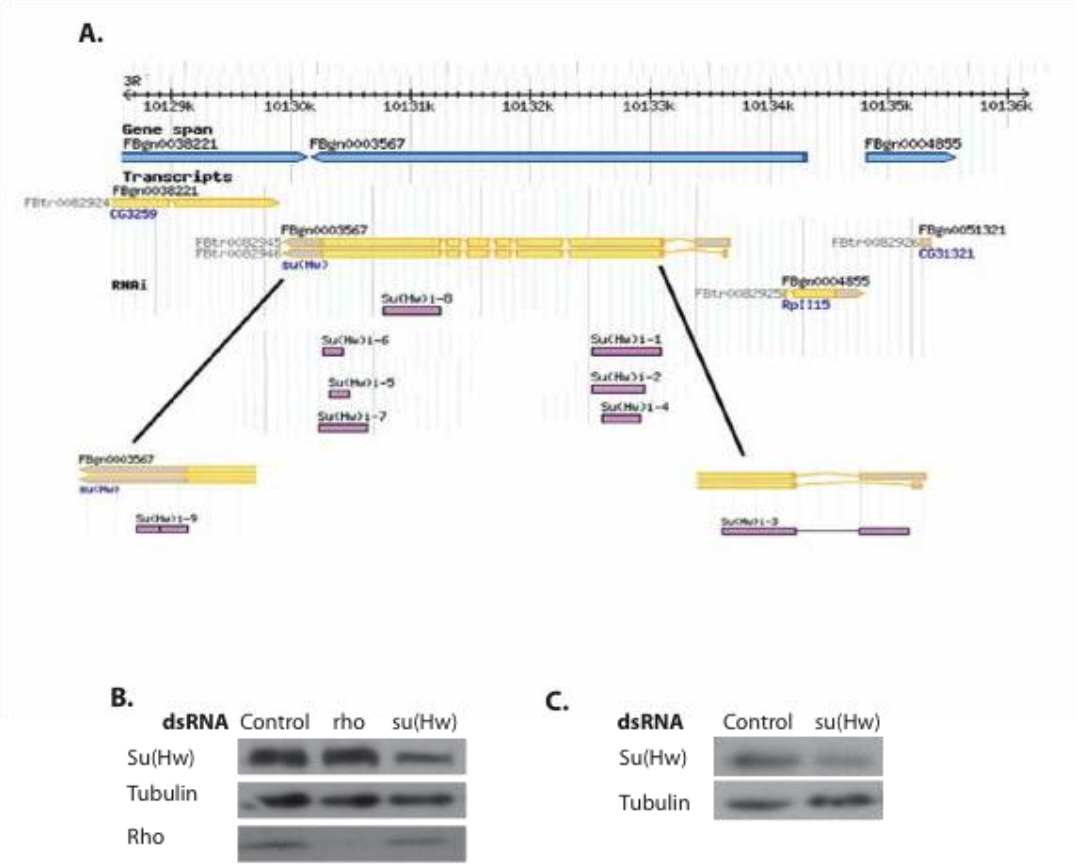


**Figure A9. Knock-down efficiency of *su(Hw)* dsRNA in S2 cells.**

**A.** The Su(Hw) RNAi probes 1-9 were designed using the E-RNAi website. **B.** The dsRNAs werre produced by *in vitro* transcription using DNA templates generated by PCR. Cells were treated with 15 µg *su(Hw)* dsRNA probe, and the knock-down efficiency of Su(Hw) was measured using western blotting with a anti-Su(Hw) antibody. Rho1 is a positive control for dsRNA treatment and tubulin as internal control. **C.** Cells were treated with 15 µg *su(Hw)* dsRNA probe 8 and the knock-down efficiency of Su(Hw) was analyzed using western blotting.

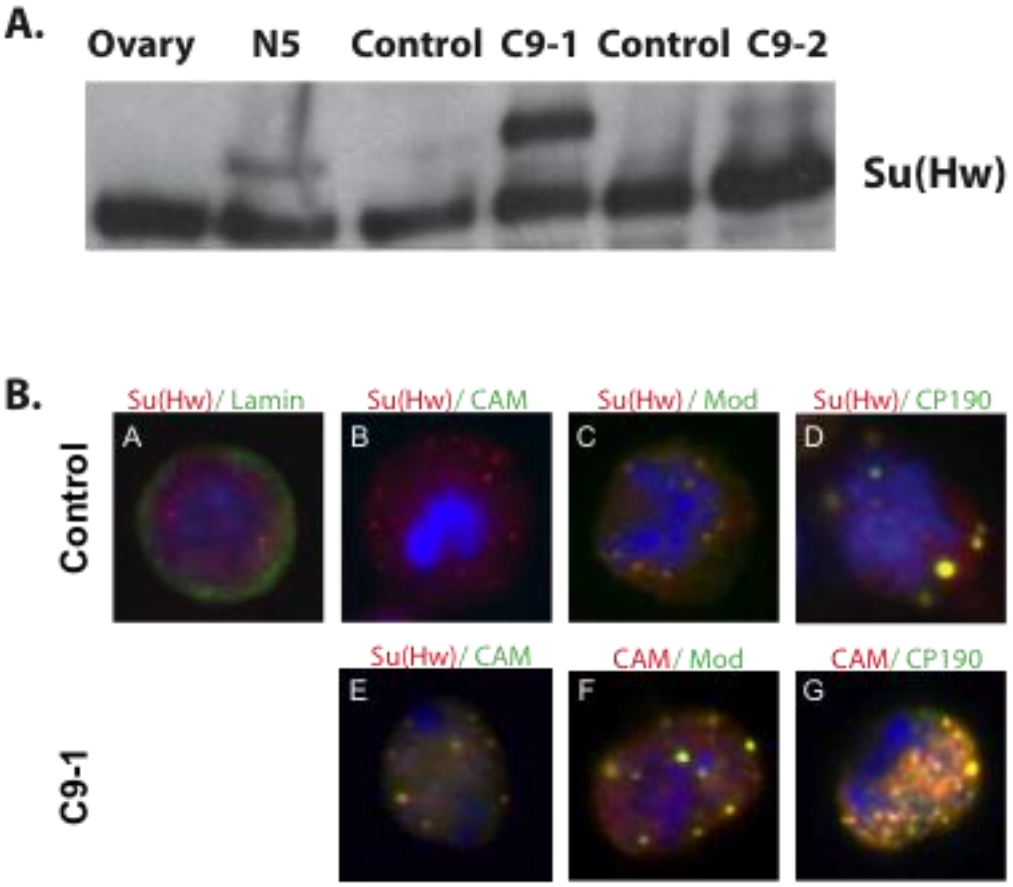


**Figure A10. Establishment of tagged Su(Hw) overexpression lines.**

**A.** Su(Hw) expression in control cells and stable lines (N5, C9-1 and C9-2) was checked with Su(Hw) antibody. 50 µg of ovarian protein from Oregon R flies was used as a positive control. **B.** C9-1 with the highest expression of tagged Su(Hw) was used for immunoflorescence staining and checked for co-localization with Mod(mdg4)67.2 and CP190. CAM antibody was used to detect tagged Su(Hw).

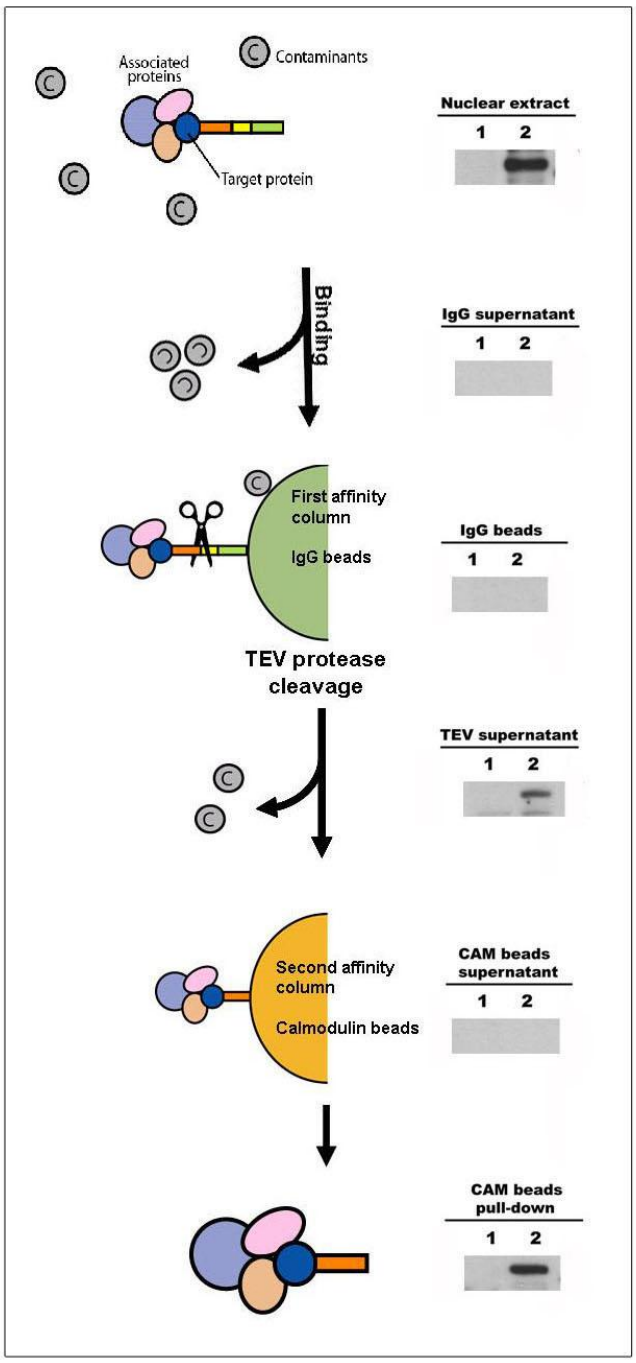


**Figure A11. Tandem affinity purification.**

The cartoon shows the entire procedure, and the western blot images on the side show the existence of tagged Su(Hw) in each step. Lane 1: control cells and 2: C9-1 cells with tagged Su(Hw) expression.

**Table A1. The primer list.**

All the primer sets were used in this study and were for different experments.

| Primer name | Sequence (5→3) | Experiment |
|---|---|---|
| Eco RI-DB-Su(Hw) F-infusion | AGACTACGCTGAATTCATGAGTGCCTCCAAGGAG | Y2H |
| Bam Hi-DB-Su(Hw) R-infusion | GCAGGTCGACGGATCCTCAAGCTTTCTCTTGTTCGC | Y2H |
| EcoRI-DB-Mod F infusion | AGACTACGCTGAATTCATGGCGGACGACGAGCAA | Y2H |
| BamHI-DB-Mod R: infusion | GCAGGTCGACGGATCCTCACTTCTTCTTGTTCTGCA | Y2H |
| EcoRI-DB-Sumo F | ATACGAATTCATGTCTGACGAAAAGAAGGGAGG | Y2H |
| BamHI-DB-Sumo R | TACTGGATCCTTATGGAGCGCCACCAGTCT | Y2H |
| Src64B-F | CATTCTGCTGATGGAGCTGT | RT-PCR |
| Src64B-R | CCGGGAAGTAGTGATTCGTT | RT-PCR |
| Rp49-F | TGTCCTTCCAGCTTCAAGATGACCATC | RT-PCR |
| Rp49-R | CTTGGGCTTGCGCCATTTGTG | RT-PCR |
| Gypsy-F | TGGAAGCACCGCAAATCAAG | RT-PCR |
| Gypsy-R | TCCAGGCCACATACTCGTC | RT-PCR |
| Jockey-F | GCAGCACGGTACTCCTGAG | RT-PCR |
| Jockey-R | CAGGGTGCCAGACTCTGTC | RT-PCR |
| Doc3-F | CTTCATGACCTTCATGCAAG | RT-PCR |
| Doc3-R | GCCATTAGCGTTCCAGGTA | RT-PCR |
| Nomad-F | CAACGCCTCTCCAGTGTAC | RT-PCR |
| Nomad-R | GAGAAGGGTTTACGGACTGT | RT-PCR |
| X-element-F | CCTTCGGCTACAGAACCTAG | RT-PCR |
| X-element-R | GCAGCTTGATGACTGGTACTG | RT-PCR |
| RooA-F | CAGAAGATGTTAACTCCAATTT | RT-PCR |
| RooA-R | TCAATGAGTGTAGCTGTTTCG | RT-PCR |
| Baggins-F | GGACTGTGTACCGATCGTG | RT-PCR |
| Baggins-R | GTGTTCAGCCAGTGCAGTG | RT-PCR |

**Table A1. Continued.**

| Primer name | Sequence (5→3) | Experiment |
|---|---|---|
| Beagle-F | CTGACCATCAGCCTTTGAC | RT-PCR |
| Beagle-R | CAGAGCGTCGGCTACAGTA | RT-PCR |
| Stalker-F | GTAGCAGACGCACTCTCAC | RT-PCR |
| Stalker-R | CCTAGGCAATAGTTCCTTG | RT-PCR |
| Gtwin-F | ATGAAGTCACTCGGCAACCT | RT-PCR |
| Gtwin-F | ACGCTTGGTAAAAGTATGCAATTG | RT-PCR |
| Tabor-F | GGACCGACAACAAAGAAACATG | RT-PCR |
| Tabor-R | GAGAACTTTCGATACCTGAG | RT-PCR |
| 412-F | CCGTGTGATGGAATAATCGG | RT-PCR |
| 412-R | GGACAACTTGGGATCTTGCT | RT-PCR |
| Idefix-F | GTACGGTACTGATCAACTG | RT-PCR |
| Idefix-R | GAATACTACTTTCACGTAGATTC | RT-PCR |
| Copia-F | CCCTATTTGAAGCCGTGAGA | RT-PCR |
| Copia-R | GACATGAGGGGTTGTTTGCT | RT-PCR |
| I-Element-F | GCTCTTTCACCTCAACCATC | RT-PCR |
| I-Element-R | GCTAGCCAATGTAGTCTCGT | RT-PCR |
| Su(Hw)K140A F: | CACTATGTACTTCAGGCTGTGGCATCAGAAAATACCAAGGCGGAC | SDM |
| Su(Hw)K140A R: | GTCCGCCTTGGTATTTTCTGATGCCACAGCCTGAAGTACATAGTG | SDM |
| Su(Hw)K145A F | CTGTGAAATCAGAAAATACCGCGGCGGACACCACGGTTAC | SDM |
| Su(Hw)K145A R | GTAACCGTGGTGTCCGCCGCGGTATTTTCTGATTTCACAG | SDM |
| Su(Hw)V150,152,153A F | CAAGGCGGACACCACGGCTACCGCGGCCACCGAAGAAGATGACACC | SDM |
| Su(Hw)V150,152,153A R | GGTGTCATCTTCTTCGGTGGCCGCGGTAGCCGTGGTGTCCGCCTTG | SDM |
| Su(Hw)d100 F | GACACCACGGTTACCGTGGTCACCTCCTCAGGCAAGGGCAACTCTAGC | SDM |
| Su(Hw)d100 R | GCTAGAGTTGCCCTTGCCTGAGGAGGTGACCACGGTAACCGTGGTGTC | SDM |
| Sumo-GG F | CAGCAGCAGACTGGTGGCTAAGAGCTCGAGGATCCGTC | SDM |
| Sumo-GG R | GTCGTCGTCTGACCACCGATTCTCGAGCTCCTAGGCAG | SDM |
| Su(Hw)I71,73&L74A F | GCAGTGTCGCTGGATCGCGCGCCAAAGCAGCCAATGAAGAAATACTGGGCACTCC | SDM |
| Su(Hw)I71,73&L74A R | GGAGTGCCCAGTATTTCTTCATTGGCTGCTTTGGCGCGCGATCCAGCGACACTGC | SDM |

**Table A1. Continued.**

| Primer name | Sequence (5→3) | Experiment |
|---|---|---|
| Su(Hw)S65D F | CAACAAGCAGGAGAAGCGTGGCGATGTCGCTGGATCGCGCATCAAAA | SDM |
| Su(Hw)S65D R | TTTTGATGCGCGATCCAGCGACATCGCCACGCTTCTCCTGCTTGTTG | SDM |
| Sumo-dGG F | GGTTTACCAGCAGCAGACTTAAGGATCCGTCGACCTGC | SDM |
| Sumo-dGG R | GCAGGTCGACGGATCCTTAAGTCTGCTGCTGGTAAACC | SDM |
| Sumo-dGG in pPAC-FlagF | GGTTTACCAGCAGCAGACTTAAGAGCTCGAGGATCCGTC | SDM |
| Sumo-dGG in pPAC-FlagR | GACGGATCCTCGAGCTCTTAAGTCTGCTGCTGGTAAACC | SDM |
| Rho1 dsRNA probe-F | TAATACGACTCACTATAGG TTTGTTTTGTGTTTAGTTCGGC | dsRNA |
| Rho1 dsRNA probe-R | TAATACGACTCACTATAGG ATCAAGAACAACCAGAACATCG | dsRNA |
| Su(Hw) dsRNA probe1-F | ttaatacgactcactatagggaggATGAGTGCCTCCAAGGAGG | dsRNA |
| Su(Hw) dsRNA probe1-R | ttaatacgactcactatagggaggTCTCCTTGATCTTTGTCTGG | dsRNA |
| Su(Hw) dsRNA probe2-F | gcacttaatacgactcactatagggaggCCTCCAACAAGCAGGAGAAG | dsRNA |
| Su(Hw) dsRNA probe2-R | gcacttaatacgactcactatagggaggTGTCTGGCTAGAGTTGCCCT | dsRNA |
| Su(Hw) dsRNA probe3-F | gaataatacgactcactatagggATTATCGGAAATGCGGTCAA | dsRNA |
| Su(Hw) dsRNA probe3-R | gaataatacgactcactatagggCGGTAGCACTGGGTGTCTTT | dsRNA |
| Su(Hw) dsRNA probe4-F | taatacgactcactatagggGGATCGCGCATCAAAATACT | dsRNA |
| Su(Hw) dsRNA probe4-R | taatacgactcactatagggTCCTGGCCGTTGTTATTTTC | dsRNA |
| Su(Hw) dsRNA probe5-F | taatacgactcactatagggATGAAGAAGCGGTGTCGGT | dsRNA |
| Su(Hw) dsRNA probe5-R | taatacgactcactatagggCAAGCTTTCTCTTGTTCGCC | dsRNA |
| Su(Hw) dsRNA probe6-F | taatacgactcactatagggTGGGAGATGAGGATCAGGAC | dsRNA |
| Su(Hw) dsRNA probe6-R | taatacgactcactatagggTTATCCACAGCTTTCCCCAC | dsRNA |
| Su(Hw) dsRNA probe7-F | taatacgactcactatagggTGTGCGGTAATTGTACGCAT | dsRNA |
| Su(Hw) dsRNA probe7-R | taatacgactcactatagggAACTGTGGCCACGACCTAAC | dsRNA |
| Su(Hw) dsRNA probe8-F | taatacgactcactatagggCTACATGATTCTTCCAAATTATCT | dsRNA |
| Su(Hw) dsRNA probe8-R | taatacgactcactatagggAAACAACAACGGTCATCAATG | dsRNA |
| Su(Hw) dsRNA probe9-F | taatacgactcactatagggAAGCTTGATTTTCCAGCCCT | dsRNA |
| Su(Hw) dsRNA probe9-R | taatacgactcactatagggGAATATTCAAGCAACAGACGG | dsRNA |
| psu(Hw)-TAP F | ACTACCATGGATGAGTGCCTCCAAGGAGGGC | Cloning |
| psu(Hw)-TAP R | TGCCCAATTGAGCTTTCTCTTGTTCGCCTAC | Cloning |

# VITA

Shih-Jui Hsu was born in Taipei, Taiwan. In 2001, she graduated from National Chung Hsing University in Taichung with a Bachelor's in Science with a major in Zoology. Her undergraduate study stimulated her curiosity to explore science, propelling her to pursue graduate studies in the lab of Dr. Shun-Yuan Jiang at the National Defense Medical Center in Taiwan where she earned her Master's degree in 2003. After two years working as a research assistant with Dr. Hsieh at Academia Sinica in Taiwan, she decided to gain a completely new research experience in the U.S by enrolling in the graduate program of Biochemistry, Cellular, and Molecular Biology Department at the University of Tennessee-Knoxville in 2006. She began her PhD work in the lab of Dr. Mariano Labrador. While working as a graduate student, she enjoyed the many opportunities to teach lab courses and discussion sections, and was ultimately honored with the Outstanding Teaching Assistant Award in 2011 and the Kouns Excellence in Teaching Award in 2013.